Kaila Noland

University of Maryland, Baltimore | kaila.noland.954@gmail.com

Education

University of Maryland, Baltimore (UMB) Spring 2024
Doctor of Philosophy, PhD – Molecular Medicine
Cellular and Molecular Physiology and Pharmacology Track

Berea College 2014
Biology, B.A.
Concentration: Cellular, Molecular and Systems

Universidad Veritas – San José, Costa Rica 2013
International Studies Abroad (ISA): Spanish for Healthcare Professionals

University of Cincinnati, Clermont College 2011
Biology, A.A.

Research Experience

University of Maryland, Baltimore 2014 - 2024
Graduate Research Assistant Fall 2018 – Spring 2024
PI: Robert Bloch, Ph.D. | University of Maryland, Baltimore
My work in Dr. Bloch's laboratory focuses on elucidating the cellular, metabolic, and physiological effects of skeletal muscle-specific high expression of the protein mu-crystallin in mice.

- Attended 8 conferences
  - American Physiological Society, Annual Summit, Long Beach, CA 2023
  - Martin Frank Diversity Travel Awardee
  - Poster Presentation
- Experimental Biology, Annual Meeting, Philadelphia, PA. 2022.
  - Poster Presentation
- 44th Annual Graduate Research Conference (GRC), University of Maryland, Baltimore. 2022.
  - Oral Presentation
- American Association for the Advancement of Science (AAAS) Annual Conference. 2022.
- EMBO | EMBL Symposium: Metabolism Meets Epigenetics. 2021.
- Experimental Biology. Annual Meeting. 2021.
- 8th Annual Public Health Research at Maryland. 2021.
- American Association for the Advancement of Science (AAAS) Annual Meeting. Virtual, 2021.

Graduate Research Assistant Fall 2016 - Fall 2018
PI: Rosemary Jagus, Ph.D. | Institute of Marine and Environmental Technology (IMET)
Investigated interacting protein partners of the translational components belonging to the eukaryotic translation initiation factor 4E family (eIF4E) in the dinoflagellate species Amphidinium carterae.

- Awarded two student travel awards
- Attended 4 conferences
    - 9th Annual US Harmful Algal Bloom Conference, Baltimore, MD, 2017.
        - Poster Presentation
    - EMBO's Protein Synthesis and Translational Control Conference, Heidelberg, Germany, 2017.
        - Poster Presentation
    - RNA Biology (NIH), Bethesda, MD, 2017.
    - DelMarVa's Aquatic Resources & Ecosystems Research Symposium, Berlin, MD, 2017.
        - Poster Presentation

Graduate Research Assistant Spring 2015 - Spring 2016
PI: Zeev Rosenzweig, Ph.D. | University of Maryland, Baltimore County, Center for Sustainable Nanotechnology
Work focused on determining the uptake and toxicity of gold nanoparticles coated with ligands known as Synthetic Mimics of Antimicrobial Peptides (SMAMPs) in the model organism Danio rerio.

Rotation Student Spring 2015
PI: Celine Plachez, Ph.D. | The Hussman Institute for Autism
Rotation focused on learning techniques necessary for molecular investigation into the etiology of autism.

Rotation Student Spring 2015
PI: Sandra Mooney, Ph.D. | University of Maryland, Baltimore
Rotation sought to elucidate the potentially ameliorating effects of docosahexaenoic acid (DHA) for a rat model of fetal alcohol spectrum disorder (FASD).

Rotation Student Summer 2014
PI: Doug Frost, Ph.D. | University of Maryland, Baltimore
Rotation explored the effects of the atypical antipsychotic Olanzapine (used for treating mood disorders - primarily for schizophrenia and bipolar disorder) on the developing adolescent brain (rat model).

Summer Research Student Summer 2012
PI: Marc Rowley, Ph.D. | Berea College
In this research, electrophysiology was utilized to explore the mechanoreceptor response, and characterize the photoreceptors of the cercariae of Proterometra macrostoma.

Presented findings at Kentucky Academy of Sciences (KAS) Annual Meeting, Richmond, KY, 2012.

Awards

UMB – 1807 Art and Literary Journal

Selected for publication of poem entitled "Aching for Resonance" | 2021
https://www.umaryland.edu/arts/journal/autumn-2021/

Selected for publication of scientific poem entitled "Introspection – seeking for answers" | 2020
https://www.umaryland.edu/arts/journal/summer-2020/

Department of Energy's ORISE Institute

First Place in the Graduate Student category for Science Poetry | 2018

University of Maryland, Baltimore

Student Travel Fellowship – Fourth Quarter | 2017

"The purpose of these fellowships is to aid students who otherwise would be unable to attend meetings without incurring financial hardship."

University of Maryland, Center for Environmental Sciences (UMCES)

Marine Estuarine Environmental Sciences Student Enhancement Award | 2017

"This award is used to enhance student's graduate/PhD education and research for conference travel and expenses, publication costs or other items."

Berea College

Wilson Evans Tennis Award | 2014

"Each year, the Wilson Evans Award is presented to a member of the Berea College tennis team who has displayed the character, sportsmanship, and enthusiasm for tennis in a manner typical of Wilson Evans."

Class of 1942 Scholarship | 2014

"Scholarships are awarded annually to students in each classification at Berea College with superior academic achievement who have demonstrated character, financial need, and the capacity to persevere."

Douglas R. Keeter Memorial Award | 2014

"This award is given to an outstanding Biology major who also participates in a varsity sport as either an athlete, team manager, or trainer."

Carlisle Keller MacDonald Scholarship | 2013

"A faculty committee chooses the Macdonald Scholars from among candidates with academic achievement and clearly stated plans of international study that will enrich their Berea education."

New Horizons Grant Recipient | 2013

This Berea College sponsored grant provides support for students studying abroad in an approved summer program.

National Association of Intercollegiate Athletics (NAIA) Scholar Athlete | 2011-2014

This award recognizes student-athletes who have an academic standing of a 3.5 or higher cumulative GPA.

University of Cincinnati, Clermont College

Outstanding Biology Student Award | 2011

Student Conference on Diversity and Social Justice | 2011

Essay Finalist - Redefining the Hegemonic Struggle into an Equitable Educational System

First Place – Poster Competition - Winning the War Now What? Psychosexual Functioning of Childhood Cancer Survivors

Fellowships

President's Fellows Program and White Paper Project 2021 – 2022

"The President's Symposium and White Paper Project is an interprofessional initiative that engages faculty, staff, and students from all of the University of Maryland, Baltimore's (UMB) schools and academic programs in a yearlong conversation on a topic that is of interest and importance to the University and its community."

Topic: "The State of EDI at UMB: Leveraging Inclusive Leadership to Develop and Implement EDI-Informed Curriculum"

Olive Ruth Russell Fellowship 2014, 2018, 2020

"Olive Ruth Russell Fellowship was established in honor of Ms. Olive Ruth Russell by Mrs. Ruth Roettinger. The fellowship is presented to women with outstanding academic records who present a defined plan to pursue graduate study in any academic discipline."

Trainings

Simple Western User Meeting – Focus on Cell and Gene Therapy Applications

March 6, 2024

"In-person, one-day workshop to learn more about how to develop quantitative assays on Simple Western from start to finish"

- Assay Development, Troubleshooting and Advanced Quantitation Workshop

Tenth Annual Nationwide Children's Hospital/OSU Myology Course

Aug. 30 – Sept. 3, 2021

"Featuring faculty from Nationwide Children's Hospital, The Ohio State University and the NCH/OSU Muscle Group, this course is oriented toward MD and PhD trainees, with a goal of providing an up-to-date and expert survey of neuromuscular diseases."

Laboratory Track Trainings:

In Vivo Mouse Electrophysiology and Physiology - Dave Arnold, MD
Seahorse Lab – Kedryn Baskin, PhD
Electroporation of DNA into Mouse Muscles - Federica Accornero, PhD and Noah Weisleder, PhD
Quantitative immunofluorescence Analysis in Muscle (Nikon NIS Elements) - Tatyana Vetter, PhD

Presidential Student Leadership Institute (PSLI) 2020
Paths: Inclusive Leadership
Career Development
Integrative Health and Wellbeing

University of Cincinnati Racial Awareness Pilot Program (RAPP) 2011

Scientific Writing
iSpy Physiology – American Physiological Society 2021
iSpy Physiology is an online scientific blog created by the American Physiological Society (APS) that is geared to the general public in effort to address questions one may have about physiology and why that matters to individuals.
"The COVID '15': Staying Healthy and Informed During a Pandemic"
https://ispyphysiology.com/2021/12/10/the-covid-15-staying-healthy-and-informed-during-a-pandemic

University of Maryland, Baltimore Institutional Service
Student Health Insurance Plan (SHIP) Advisory Committee 2022 - 2023

University Health COVID-19 Advisory Group 2022 - 2023

Inaugural USGA Diversity, Equity, and Inclusion (DEI) Officer Search Committee 2021 - 2022
Student led committee comprised of student government individuals tasked with creating the criteria, description of position and developing the interview process for the inaugural student government executive board position of Chief Student DEI officer.

Equity Committee 2020 - 2022
The Equity Committee is a newly formed organization at UMB that seeks to be a student-run body devoted to strengthening efforts for equity, through anti-oppression and social justice at UMB and within the Baltimore community.

USGA Pennington Committee 2020 - 2022
The Pennington Committee connects students with volunteering opportunities in UMB and the surrounding neighborhood. The committee organizes at least one community outreach event per semester, finds community volunteering opportunities and actively seeks out charity fundraising efforts.

Disability Justice Group (DREAM) 2020 - 2021
"We aim to advance disability justice by raising awareness on the diversity of disability, along with the various cultural and systemic barriers faced by persons with disabilities."

UMB - Institutional Service Leadership Positions

University Strategic Planning Committee 2022
Co-Chair of Student Engagement, Learning and Success Committee

University Student Government Association (USGA) Vice-President 2021 - 2022

USGA Pennington Committee – Committee Chair 2021 - 2022

USGA General Senator 2020 - 2021

Mentoring

Women Scientists 2020 - Current
Women Scientists is a Facebook group "for all women and nonbinary individuals in Science and other STEM fields. The purpose is support, mentoring, and professional connections."
-Mentee: Suzanna Kafer, PhD Candidate
University of Colorado, Anschutz Program in Integrated Physiology

Montgomery County Public Schools (MCPS) Internship Program Summer 2021
High school student internship program in fields of career interests within the Baltimore area. Mentorship included identifying, planning, and executing a scientific experiment from hypothesis through data analysis
-Mentee: Lisa Lin – Montgomery County Public Schools, High School Senior

GPILS Big Sibling Program 2019 - Current
Mentor fellow students, including advice on lab rotation selection, finding access to resources, answering questions about adjusting to graduate school life and other general help.
-Mentees: Madeline Alizadeh – MD/PhD Candidate in Molecular Medicine
Award: PhD Scholar Award (2021)
Amir Mehrabani Tabari – PhD Candidate in Molecular Medicine

Summer Undergraduate Intern Program – (Living Marine Resources Cooperative Science Center (LMRCSC) Summer 2018
A nine-week internship program for undergraduate students to gain hands-on research related to marine and environmental sciences. This program is designed for students that are underrepresented in marine and environmental sciences.
-Mentee: Nylah McClain – B.S. Student at UMCES in Environmental Sciences

Outreach and Volunteering

The Baltimore Neighbors Network 2021

"The Baltimore Neighbors Network (an initiative of Healing City Baltimore) provides a virtual community of trained volunteers to offer hope, comfort and social solidarity." Weekly volunteering includes calling 10 Baltimore residents and provide support, assess their well-being and referral to community resources throughout the COVID-19 pandemic.

UMB – "Together We've Got This Covered" Campaign 2021

This campaign developed a video featuring students, for students at UMB to encourage continuance of proper face mask wearing in a variety of settings, offering words of encouragement and highlighting socially distanced activities that students can participate in while properly wearing masks. In addition to participating as a featured student, work involved being the student organizer.
https://www.youtube.com/watch?v=NcL0nP00QnA

UMB – USGA Pennington Committee 2020 - 2022

The Pennington Committee connects students with volunteering opportunities in UMB and the surrounding neighborhood. The committee organizes at least one community outreach event per semester, finds community volunteering opportunities and actively seeks out charity fundraising efforts.

UMB – GPILS Student Recruitment 2019 - 2022

GPILS-SAC Hope Lodge Volunteer Event 2019

Once a month, UMB students make and provide breakfast to the residents of the American Cancer Society's Hope Lodge (a program that provides a free home away from home for patients in cancer treatments and their caregivers).

American Red Cross 2018

Disaster Relief Services – Disaster Action Team (DAT) Responder

As a DAT Responder volunteers respond to local emergencies such as home fires to assess damages, provide information and supplies, provide financial assistance and other support as needed for affected individuals and families.

Institute for Marine and Environmental Technology Open House 2016 - 2018

Professional Societies

American Physiological Society (APS) 2021 - Current

American Association for the Advancement of Science (AAAS) 2021 - Current

Patent Application

Regulating Muscle Physiology and Energy Metabolism Using Crym 2021
Kinney, Christian J. Bloch, Robert, J. McLenithan, John. Noland, Kaila. O'Neill, Andrea. 2021. Regulating Muscle Physiology and Energy Metabolism Using Crym. US 2021-0379148. Filed: 05/12/2021. Published: 12/09/2021.

Publications

Noland, K., Aja, Susan, Bloch, R.J., Metabolic Consequences of Skeletal Muscle Specific High Expression of mu-Crystallin Following Low- and High-Fat Diet Interventions are Diet- and Sex-Specific, in preparation.

Noland, K., Leath, M., Lee, G., Oliver, J., Scott, J. The State of Equity Diversity and Inclusion at UMB: Leveraging Inclusive Leadership to Develop and Implement EDI-Informed Curriculum. 2022, https://www.umaryland.edu/ile/presidents-symposium--white-paper-project/past-white-papers/

Kinney, C.J., O'Neill, A., Noland, K., Huang, W., Muriel, J., Lukyanenko, V., Kane, M.A., Ward, C.W., Collier, A.F., Roche, J.A., McLenithan, J.C., Reed, P.W., Bloch, R.J., μ-Crystallin in Mouse Skeletal Muscle Promotes a Shift from Glycolytic toward Oxidative Metabolism, Current Research in Physiology, 2021, https://doi.org/10.1016/j.crphys.2021.02.003

Professional Presentations

Noland, K, Leath, M, Oliver, J, Lee, G, Scott, J. The State of Equity, Diversity and Inclusion at UMB: Leveraging Inclusive Leadership to Develop and Implement EDI-Informed Curriculum. The President's Symposium, Baltimore, MD. May 2, 2022. Oral Presentation (Live and Recorded).
https://www.youtube.com/watch?v=HpjwBmXnjYk

Noland, K, O'Neill, A., Pimparkar, U., Aja, S., Bloch, R.J. Physiological Changes in Response to Skeletal Muscle Specific High-Expression of mu-Crystallin Following High- and Low-Fat Diets. Experimental Biology, Philadelphia, PA. April 3, 2022. Poster Presentation.

Noland, K, O'Neill, A., Pimparkar, U., Aja, S., Bloch, RJ. Physiological Changes in Response to Skeletal Muscle Specific High-Expression of mu-crystallin Following High- and Low- Fat Diets. 44th Annual Graduate Research Conference, University of Maryland, Baltimore. March 4, 2022. Oral Presentation.

Noland, K, Liu, CL, Jagus, R. Dramatic Changes in Protein Synthetic Rate of Axenic Amphidinium Carterae in Response to Increasing Temperatures, Density of Culture, and Over the Diel Cycle. DelMarVa's Aquatic Resources & Ecosystems Research Symposium. November 25, 2017. Poster Presentation.

Noland, K, Liu, CL, Jagus, R. Dramatic Changes in Protein Synthetic Rate of Axenic Amphidinium Carterae in Response to Increasing Temperatures, Density of Culture, and Over the Diel Cycle. 9th Annual US Harmful Algal Bloom Conference. November 11-17, 2017. Poster Presentation.

Noland, K, Liu, CL, Jagus, R. eIF4E-1a Phosphorylation Accompanies the Striking Diel Changes in Protein Synthetic Rate of Axenic Amphidinium carterae. EMBL: Protein Synthesis and Translational Control Conference. Heidelberg, Germany. September 06-09, 2017. Poster Presentation.

Noland, K. Zheng, Z, Lienkamp, K, Boschert, D, Gunsolus, I, Haynes, C, Rosenzweig, Z. Role and Impact of Gold Nanoparticles Coated with Synthetic Mimics of Antimicrobial Peptides (SMAMPs) on Zebrafish (Danio rerio). All Hands Meeting for Center for Sustainable Nanotechnology. Baltimore, Maryland. Spring 2016. Poster Presentation.

Noland, K, Johnson, R, Rowley, M. Characterization of the Sensory Systems of the Cercaria of the Trematode, Proterometra macrostoma. Kentucky Academy of Science (KAS) Annual Meeting. Richmond, Kentucky. Fall 2012. Poster Presentation.

Noland, K. Winning the War Now What? Psychosexual Functioning of Childhood Cancer Survivors. Student Conference on Diversity and Social Justice. University of Cincinnati, Clermont College. Cincinnati, Ohio. Spring 2011. First Place in Poster Presentation.

Noland, K. Redefining the Hegemonic Struggle into an Equitable Educational System. Student Conference on Diversity and Social Justice. University of Cincinnati, Clermont College. Cincinnati, Ohio. Spring 2011. Table Talk leader and Finalist in Essay Competition.

Abstract

The prevalence of obesity continues to rise globally while traditional modalities such as dietary change, increase in physical activity, and behavioral therapy are often insufficient countermeasures. As such additional treatment modalities are increasingly necessary. Pharmacotherapeutics have been developed and are proven to be key agents to address impaired cellular and molecular processes in certain obese individuals, generally targeting modulation of leptin and its associated signaling pathways. An additional potential target are thyroid hormones as they are potent regulators of metabolism. It is known that the thyroid hormone binding protein, mu-crystallin, is expressed in high levels in approximately 20% of the human population, and since skeletal muscle is a major metabolic organ, we sought to determine the role that skeletal-muscle specific high-expression (SM-HE) of mu-crystallin plays in the modulation of murine whole-body metabolism. Our work uses a transgenic line of mice, *Crym*-tg, that have (SM-HE) of mu-crystallin comparable to levels seen in high-expressing humans. Our previous work documented minor physiological and functional phenotypic factors of male *Crym*-tg mice on standard chow (of note, we did not evaluate female mice), but that there was a small but significant shift (13.7%) towards fatty acid metabolism when compared to controls as measured via indirect calorimetry of CLAMS cages. We also documented a ~192-fold increase in intracellular T3 levels in the *tibialis anterior* of *Crym*-tg mice. These findings were also consistent on the transcriptomic and proteomic levels with an increase in expression of slower contractile and oxidative metabolism genes, with a decrease in glycolytic and fast contractile genes.

This body of work further characterizes the role of SM-HE of mu-crystallin in the context of the *Crym*-tg line. To do so, we evaluated both male and female *Crym*-tg mice following a low- or high-fat diet intervention with glucose tolerance and insulin tolerance testing, indirect calorimetry metabolic analysis, and transcriptomic and proteomic based measures. We posited that both male and female *Crym*-tg mice would demonstrate a protection in the traditional high-fat diet-induced obesity phenotype with minimal differences in the low-fat diet cohort. Interestingly, we found diet- and sex-specific differences across the cohorts in a variety of parameters including decreased lean mass in males on low-fat diet and in females on high-fat diet, sex- and diet-specific changes in gene expression relating to various cellular pathways including branched-chain amino acid catabolism, and fiber cross-sectional area. However, we could not attribute these changes to indirect calorimetry data. Noting that the indirect calorimetry did not account for the utilization of protein as an energy source, we shifted our focus to mu-crystallin's other known functional role as a ketimine reductase. These data, along with our findings of significant changes in expression of genes relating to branched-chain amino acid metabolism, lend credence that the alterations in lean mass and other parameters are likely primarily due to mu-crystallin's role as a ketimine reductase. Further work is needed to determine the role that sex-hormones contribute to the sexually dimorphic results we describe, especially since the mediation of thyroid hormones effects are known to be influenced by estrogen.

Cellular, Molecular and Metabolic Variation Resulting from Skeletal-Muscle Specific High-Expression of the Thyroid Hormone Binding Protein mu-Crystallin are Sex-Specific and Diet-Dependent

by

Kaila Noland

Dissertation submitted to the Faculty of the Graduate School of the

University of Maryland, Baltimore in partial fulfillment

of the requirements for the degree of

Doctor of Philosophy

2024

Dedication

To every educator that encouraged and helped me along my path, propelled me toward my goals, and believed I was more – and that I deserved more than my circumstances

Acknowledgements

Throughout my doctoral studies, I have been incredibly fortunate to have many amazing individuals supporting me and encouraging me along the way. I am forever grateful to have found, and to have received the continuous and unwavering support of my parents, Marc and Rachel Rowley. Without your love and support I would not have the tools necessary to persevere and continue to believe in myself throughout this daunting process. You met me where I was and encouraged me to truly strive for and go after my aspirations. You were there every step along the way to encourage me, give me a lending ear and the unconditional support I never knew, and I thank you for that. I am incredibly grateful for the encouragement and care from my grandparents, Teresa and Harry Rowley, accepting me from day one and providing me a space in your home whenever needed, your time, love, and endless support. Thank you to my grandfather Harold Hutchinson for being a steady supporter of my educational goals, always telling anyone who would listen how proud he is of me. Thank you to Aunt Beth and family, having you nearby and having you as a sounding board and kind, but also frank insights, have been refreshing and appreciated. Of course, the wonderful meals you have made and time with the puppies always helped too, but your acceptance and love are so much more than I could have imagined knowing and having in a family.

Thank you to Dr. David Fankhauser, if it were not for your Introduction to Biology courses, I do not know that I would have ever found my passion for cellular and molecular biology. Thank you to Berea College for the opportunity to complete my undergraduate studies. Without the tuition-free promise of Berea College I could not

financially afford to complete my bachelor's degree or have the opportunities that I experienced during my undergraduate studies. I appreciate the further financial support from Berea College in the form of the Olive Ruth Russell Fellowship during my graduate studies.

Andrea "Mama-drea" O'Neill, there will never be an adequate way to show my appreciation for all that you have done for me throughout my time in the Bloch lab. Your kindness, words of wisdom, support and teachings in the lab were so invaluable along the way. I would never have become the scientist I am today without you. Thank you for teaching me not only scientific techniques, new ways of evaluating data, thinking more critically about my research but also how to take a step back and take a moment. You truly have become a friend to me along the way and I will always cherish that.

Thank you to my committee and especially my mentor Dr. Robert Bloch. My committee has provided invaluable insight on the possibilities of where my project could go and areas that needed bolstered. Dr. Susan Aja is such a wealth of information and always ready to talk through my data, thank you as I would not have gotten through the CLAMS data without you. Dr. Bloch's lab has been an incredibly supportive environment that I so needed for this journey. Dr. Bloch has given me leeway on exploring my theories on my work but also a guiding hand when I have come with questions, ideas, and things I needed help understanding. I could not have asked for a better mentor to support me and allow me to develop into the scientist I am freely, within reason.

Thank you to all my friends along every portion of my journey. Victoria “Tori” Stephens, Joel and Kylie Deutscher and Morgan Sowder, I am so thankful that Berea College brought us together and for your enduring friendship and support throughout my graduate studies. You believed in me even when I was overwhelmed and uncertain of my path forward. Joel, tennis may have brought us together, but you have continued to be my fierce supporter and I thank you for pushing me to continue and to adapt and overcome. Tori, you taught me so much of what it means to be a friend and your kind words and silly nature were so needed along my way, thank you. And to Morgan, thank you for always being there. While we live so far apart, you were always ready for a call, FaceTime so we could cook together, and are always excited to plan trips to see one another, your support and friendship is a source of happiness and often anchored me in times when I needed it most.

Thank you to Melissa Richardson, you were the very first person I met in Baltimore, I would have never imagined the friendship and camaraderie we developed along the way. I am so thankful to have your support and to see your family grow. Dr. Saddef Haq, my other day one, throughout our time working on the same floor to your vital advice on career trajectory and possibilities, thank you.

Dr. Victoria Halperin-Kuhns, Eilley Barron, Dr. Ava Zapf-Rickards, you all have been incredibly helpful and a tremendous source of support and wisdom, people to bounce experiment ideas off and to help troubleshoot things along the way. I am so lucky that the Woodward lab was across the hall from me and brought us together.

Thank you to the fellow students that I have been friends with throughout my time in this program. Specifically, Alli Mancini, Aishwarya Iyer, Maria Traficante, Bern Monari and Yi Li. I have gotten to know each of you during various points during this long process, and you each have provided a near and dear friendship that has made this process so much more enjoyable. Our times of laughter, commiseration, studying together, and nights out or in, were a tremendous help in maintaining perseverance and resilience for this whole time.

Words of gratitude do not begin to fully encompass the level of appreciation I have Amanda Lawrence and Suzzi Kafer. Amanda, since our time at IMET you have become such a close friend and major source of support and assurances that I can make it through even with all the unforeseen experiences we both had throughout graduate school. You have not only stood by my choices but have made fun of me where appropriate and I can always count on you for honest feedback and a sounding board for all things academic and personal. Suzzi, who would have ever thought that we would meet the way we did! I never thought that COVID19 could create such a positive impact in my life when it was such a hard and devastating pandemic. During this time a wonderful group of women scientists came together for support and mentorship. I am so glad that our paths crossed and that we quickly went from mentor and mentee to a tight friendship. I have seen you developing into a wonderful scientist that will do so many great things, but you have in turn provided me with such a fresh perspective and encouragement even if you are far away.

Lastly, but most certainly not least, thank you to the love of my life, my fiancé Charmaine Wilson-Jones. While she is not a scientist by training, she has always strived to understand and support my work as well as the entire process of this doctoral journey. During long nights of writing and preparing presentations, she has willingly taken on more responsibilities so that I may focus, and that is such a tremendous help that I truly appreciate. Hearing her constant soundtrack and being summoned for impromptu dance parties have provided such a light and joy that I didn't know how much I needed and would not otherwise know. She is such a fierce believer in my capabilities even when I am having hard days and has always given me words of support and encouragement. She has never once doubted me, and I thank her for that unwavering support. Even after being around many other physiology graduate students during our most recent vacation, she is certain that peptide is a scientific word but that next time we need a vacation without science.

Thank you to everyone who has been so supportive along the way and while I may not have been able to thank everyone individually, know that your care and words of encouragement have not gone unnoticed. Thank you!

Table of Contents

List of Tables

List of Figures

List of Abbreviations

Acc1	Acetyl-CoA carboxylase
ACVRIIB	Activin Receptor Type-2B
AgRP	Agouti-related Peptide
AKT	Protein Kinase B
ATP	Adenosine Triphosphate
ATPase	Adenosine Triphosphatase
AUC	Area Under the Curve
BCAA	Branched Chain Amino Acid
BCAT	Branched Chain Amino Acid Transferase
BCKDH	Branched Chain Amino Acid a-keto Dehydrogenase
CSA	Cross Sectional Area
DBT	Dihydrolipoamide Branched Chain Transacylase E2
Bckdhb	Branched Chain Amino Acid a-keto Dehydrogenase beta subunit
BDNF	Brain Derived Neurotrophic Factor
BMI	Body Mass Index
Calm3	Calmodulin 3
CAMK	$Ca^{2+/}$Calmodulin-Dependent Protein Kinase
cDNA	Complementary Deoxyribonucleic Acid
Ckmt2	Mitochondrial Creatine Kinase 2
CLAMS	Comprehensive Laboratory Animal Monitoring System
Crym-KO	Mu-crystallin Knock-Out
Crym-tg	Mu-crystallin transgenic

CSA	Cross Sectional Area
DEG	Differentially Expressed Gene
Deptor	DEP-Domain Containing mTOR-Interacting Protein
DIO1-3	Deiodinase 1, 2, and 3
DIO	Diet Induced Obesity
DNA	Deoxyribonucleic Acid
EDTA	Ethylenediamine Tetraacetic Acid
EE	Energy Expenditure
Eif4ebp1	Eukaryotic Translation Initiation Factor 4E Binding Protein 1
EMSA	Electrophoretic Mobility Shift Assay
ERK	Extracellular Signal-Regulated Kinase
Esr1	Estrogen Receptor alpha
ETC	Electron Transport Chain
FADH2	Dihydroflavine-adenine Dinucleotide
FDA	Food and Drug Administration
FOXO	Forkhead O Transcription Factors
Foxo3	Forkhead O Transcription Factor 3
FSHD	Facioscapulohumeral Muscular Dystrophy
gDNA	genomic Deoxyribonucleic Acid
GIP	Glucose Dependent Insulinotropic Peptide
GLP1	Glucagon-like Peptide-1
GLUT1	Glucose Transporter 1
GLUT4	Glucose Transporter 4

GOI	Gene of Interest
GTeX	Genome-Tissue Expression Portal
GTT	Glucose Tolerance Test
GWAS	Genome Wide Association Studies
HFD	High-Fat Diet
HPT	Hypothalamus Pituitary Thyroid Axis
HRE	Hormone Response Element
IACUC	Institutional Animal Care and Use Committee
IP	Intraperitoneal
Irs2	Insulin Receptor Subunit 2
ITT	Insulin Tolerance Testing
JAK-STAT	Janus Kinase-Signal Transducer and Activator of Transcription
K_D	Dissociation Constant
K_A	Association Constant
KIC	alpha-ketoisocapraote
LC/MS.MS	Liquid Chromatography with Tandem Mass Spectrometry
LEP	Leptin gene
LEPR	Leptin Receptor
LFD	Low-Fat Diet
MCR4	Melanocortin 4 Receptor
MCT8/10	Monocarboxylate Transporter 8 and 10
Mgea5	Nuclear Cytoplasmic OGlcNAcase and Acetyltransferase
MHC	Myosin Heavy Chain

Mib1	Mib E3 Ubiquitin-Protein Ligase
mRNA	Messenger Ribonucleic Acid
mTOR	Mammalian Target of Rapamycin
mTORC1	Mammalian Target of Rapamycin Complex 1
Mut	Methylmalonyl-CoA Mutase
MYH	Gene for Myosin Heavy Chain
NADH	Nicotinamide Adenine Dinucleotide + Hydrogen
NADPH	Nicotinamide Adenine Dinucleotide Phosphate Hydrogen
NES	Normalized Expression Signal
NFK-β	Nuclear Factor Kappa-Light-Chain-Enhancer of Activated B Cells
Nfkbia	Nuclear Factor-Kappa-B-Inhibitor α
Nom1	Nucleolar protein with MIF4G Domain 1
NPY	Neuropeptide Y
NTRK2	Neurotrophic Receptor Tyrosine Kinase 2
NZO	New Zealand Obese
Obq3	Obesity QTL3
Obq4	Obestiy QTL4
PI3/AKT	Phosphatidylinositol 3-Kinase/Protein Kinase B
PI3K	Phosphatidylinositol 3-Kinase
Pi3kr1	Phosphoinostide-3-Kinase Regulatory Subunit 1
POMC	Propiomelanocortin
Ppara	Peroxisome Proliferator-Activated Receptor-α
Ppargc1a	Peroxisome Proliferator-Activated Receptor-γ Coactivator 1-α

PPARs	Peroxisome Proliferator-Activated Receptors
PPARy	Peroxisome Proliferator-Activated Receptor-γ
PPARy2	Peroxisome Proliferator-Activated Receptor-γ 2
PCSK1	Proprotein Convertase Subtilisin/Kexin Type 1
Psme4	Proteasomal Activity Subunit 4
QNMR	Quantitative Nuclear Magnetic Resonance
qRT-PCR	Real-Time Quantitative Reverse Transcription PCR
QTL	Quantitative Trait Loci
RER	Respiratory Exchange Ratio
rhAmp	Rnase H-Dependent PCR
RIPA	Radioimmunoprecipitation Assay Buffer
RNA	Ribonucleic Acid
RNA-seq	RNA Sequencing
ROS	Reactive Oxygen Species
rT3	Reverse Triiodothyronine
RXR	Retinoid X Receptor
SIM1	Single-minded Homolog 1
SM-HE	Skeletal Muscle Specific High Expression
SNP	Single Nucleotide Polymorphism
Stat5b	Signal Transducer and Activator of Transcription 5b
T2	3,5-Diiodo-L-Thyronine
T3	Triiodothyronine
T4	Thyroxine

TC10	Small GTP-Binding Protein TC10
TCA	Tricarboxylic Acid Cycle
TH	Thyroid Hormone
THR	Thyroid Hormone Receptor
THRA	Thyroid Hormone Receptor α
THRB	Thyroid Hormone Receptor
TLR4	Toll-Like Receptor 4
TNF- α	Tumor Necrosis Factor α
TRE	Thyroid Response Element
TRH	Thyrotropin-Releasing Hormone
TSH	Thyroid-Stimulating Hormone
Ube2d1	Ubiquitin Conjugation Enzyme E2 D1
VCO_2	Volume of Carbon Dioxide
VDAC	Voltage Dependent Anion Channel
VO_2	Volume of Oxygen
VO_2 Max	Maximal Volume of Oxygen
WT	Wildtype

Chapter 1 Introduction and Background

Skeletal Muscle

Skeletal muscle is the largest organ by mass in the human body, accounting for approximately 40% of total body weight[1]. Total skeletal muscle mass is influenced by many factors including physical activity[2-8], diet and nutrition[2,9-19], and hormones[20-30], among others[31-34]. Skeletal muscle is responsible for respiration, thermogenesis[35-37], and voluntary body movement. It is critical for metabolic homeostasis as it accounts for approximately 30% of basal metabolism[1,31,34,37-44], is involved in glucose homeostasis[42] and heat production, provides glutamine needed for the immune system[33,42], and is necessary for breathing and posture[39].

Structure of Skeletal Muscle

The structure of skeletal muscle consists of thousands of highly organized muscle fibers (individual cells that are long, thin, and multinucleated), connective tissue, nerves, and vascular tissue[45]. Skeletal muscle is bound by connective tissue and attached to bones via tendons (Figure 1.1). Muscle vary in overall size, function and architecture, but their basic structure remains the same[46]. Groups of individual muscle fibers, myofibrils, are bundled into fascicles. Each fiber within the fascicle is surrounded by the connective tissue endomysium. Fascicles are surrounded by perimysium and bundles of fascicles are surrounded by epimysium, as shown in Figure 1.1.

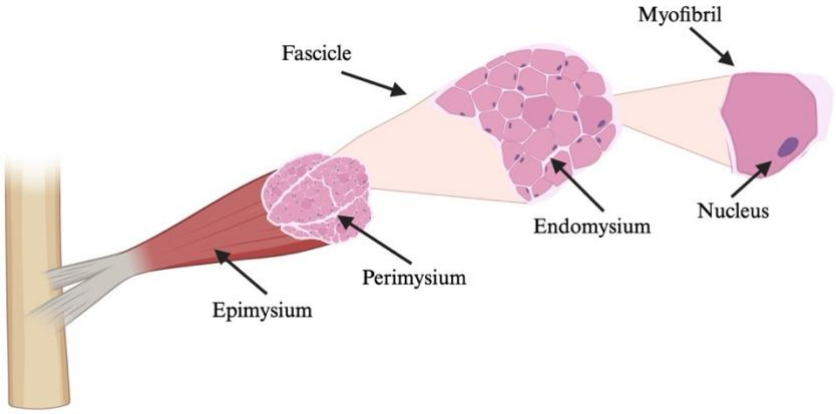

Figure 1.1. *Overview of the Structure of Skeletal Muscle.*
Skeletal muscle is attached to bone via tendons. Muscles are a collection of thousands of highly specialized myofibrils: long, thin, multinucleated cells. Individual myofibrils are surrounded by endomysium, a connective tissue. Groups of myofibrils are grouped into fascicles and surrounded by perimysium. Bundles of fascicles are encompassed by epimysium.

Skeletal Muscle Fiber Type Classification and Composition

Muscles have been loosely characterized as either "slow-" or "fast-" twitch, based largely on the isoforms of myosin that they express, which correlate roughly with their speed and strength of contraction[1,46-54]. This is an oversimplification, however, as muscle composition is quite heterogeneous: each muscle is not simply a collection of purely slow or fast fibers. Within the two categories of fibers, there are four general fiber types: 1) slow oxidative fibers (type 1), 2) fast oxidative fibers (type 2A), 3) fast intermediate glycolytic (type 2X), 4) fast glycolytic (type 2B)[46,55]. Although fiber types contain different subunits of myosin heavy chain (MHC), encoded by the MYH gene and related to ATPase activity[56], many fibers express a mixture of different MYH subunits[46,52,53,57,58], indicating that even characterization of fiber types by MHC subunits is an oversimplification. The following is a discussion of the general characteristics of the four

generally recognized fiber types, but further information on the biochemical processes mentioned can be found in the later section titled Metabolism on pages 17-20.

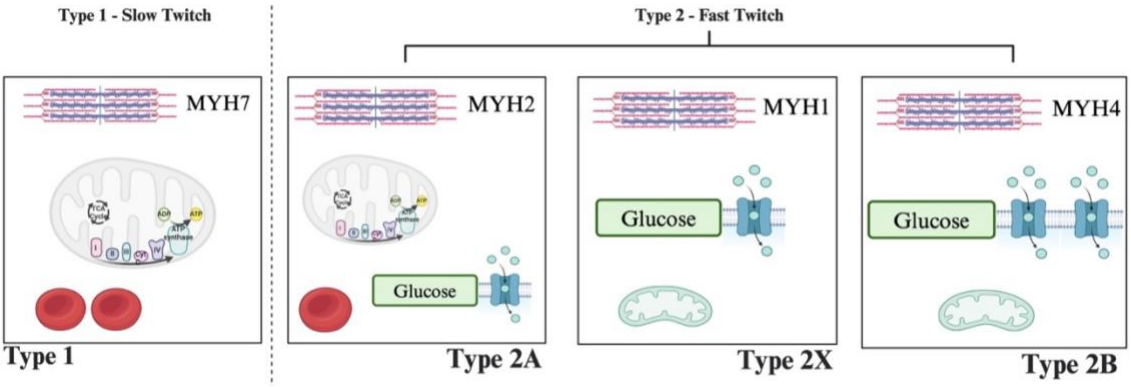

Figure 1.2. *Fiber Type Characteristics.*
Type 1 fibers are slow twitch and are oxidative, with high myoglobin content conferring bright red phenotype. Type 1 fibers have MYH7 expression. Type 2 fibers are fast twitch fibers. Type 2A fibers express MYH2 have some myoglobin content and are mostly oxidative with some glycolytic capacity. Type 2X are intermediate fast fibers that express MYH1 and are glycolytic. Type 2B fibers are the fastest fibers, expressing MYH4, are glycolytic and have low myoglobin content, making them appear paler compared to other fiber types.

Type 1 fibers are highly vascularized and contain high levels of mitochondria and myoglobin, responsible for their characteristic red appearance. As evidenced by their high mitochondrial content, type 1 fibers greatly rely on oxidative metabolism and have low glycolytic activity[59]. Their predominant utilization of aerobic respiration allows for sustained contractions with lower power requirements, e.g. in maintaining posture, and as such type 1 fibers are highly resistant to fatigue[60].

Type 2A fibers are the slowest of the fast-twitch fibers. Type 2A fibers are generally aerobic, relying on oxidative phosphorylation, and have moderate resistance to fatigue[55]. Type 2A fibers contain a relative balance of mitochondria and glycolytic

components and enzymes and contain more myoglobin that the other type 2 fibers[59]. The increased mitochondrial content in type 1 and type 2A fibers is indicative of their high oxidative activity[1].

Type 2B fibers are glycolytic and therefore rely on anaerobic glycolysis for ATP production. Type 2B fibers are the fastest fibers and they fatigue rapidly. Type 2B fibers have lower mitochondrial content compared to the other fiber types, the highest myosin ATPase activity, and the greatest force production[55].

Type 2X fibers were originally distinguished from the other type 2 fibers between 1988-1994[61-64] and have since been described as an intermediate type, between Type 2A and 2B fibers. Contraction and other twitch properties are like the other type 2 fibers but 2X fibers have intermediate fatiguability[51]. Immunohistochemical and functional assays further support an intermediate phenotype of these fibers[65-67].

Historically it was accepted that skeletal muscle fiber type was relatively delineated and simple to classify[68]. Initial distinction of fiber type was via color difference, either red (slow) or white (fast), indicative of myoglobin status[69,70]. Over time, advanced methodology allowed for more precise fiber type categorization, leading to classification of several subtypes of type 2 fibers. This methodology has grown to include histochemical staining[71], functional assays[56], microscopic evaluation[72], single fiber studies[40], and biochemical assays[73].

Skeletal muscle is highly responsive to changes in activity, disease, aging and injury and can undergo a shift in fiber types in response to these and to other stimuli[7,74,75]. Moreover, classifying muscle fiber types as simply one of four fiber types is outdated, as evidenced by growing work characterizing the existence of hybrid fiber types[7,52,57]. Evaluation at the single fiber level has been invaluable for further detailed classification and experimentation[7,58]. The factors regulating the plastic mechanisms governing muscle fiber type under different conditions are under intensive study.

Skeletal Muscle and its Role in Metabolism

Skeletal muscle is not only essential for voluntary movement, but it is also a major contributor to basal metabolism. Varying fiber type composition and localization allows for very specific functionality and metabolic capacity. Skeletal muscle has numerous roles in metabolism including but not limited to glucose uptake and storage[6,76-82], storage of amino acids[9,83-87], and perturbations in these often lead to metabolic dysfunction or disease. It is also important to note that the intersectionality of exercise, disease state, age, diet, and sex can lead to quite distinct phenotypes[15,28,88-96].

Glucose Uptake and Storage

Skeletal muscle is the primary site for glucose uptake from the bloodstream and storage as glycogen, although glycogen is also stored in the liver. Glycogen can be rapidly broken down to glucose and released into the bloodstream to reach other target tissues requiring increased energy needs.

Uptake of glucose into skeletal muscle can be insulin-dependent or independent. Insulin-dependent uptake accounts for roughly 80% of all glucose uptake[77]. In insulin-dependent uptake, post-prandial insulin release from the pancreas leads to its binding to its receptors on skeletal muscle cells. This triggers an increase in translocation of glucose transporters, primarily glucose transporter 4 (GLUT4), from intracellular stores to the cellular membrane which in turn mediates the uptake of glucose from the bloodstream into the cell facilitated by diffusion along its concentration gradient[97]. Mediation through the insulin-dependent uptake of glucose occurs via phosphatidylinositol 3-kinase (PI3K) and protein kinase B (AKT) pathways. The G protein TC10, located within lipid rafts, is also an important player in insulin-dependent glucose uptake, as it mediates changes in the actin cytoskeleton, among other processes, that lead to the effective translocation of GLUT4 to the cell membrane[98].

Insulin-independent glucose uptake is also mediated through glucose transporters, primarily GLUT1 and GLUT4, especially during contraction and exercise[77,99]. Contraction-induced uptake of glucose is mediated via downstream effects of Rac1/actin and Ca2+/calmodulin-dependent protein kinase (CAMK) signaling[82].

Once within the cytosol, glucose is phosphorylated by hexokinase, thereby making it unable to exit the cell via the GLUT transporters. Glucose-6-phosphate can be shuttled into one of four processes, from most common to least commonly used[100]: 1) glycolysis, 2) conversion to glycogen, 3) the pentose phosphate pathway[101], or 4) protein synthesis in the hexosamine pathway[102].

Perturbations in skeletal muscle glucose uptake and associated processes can lead to a host of negative impacts. Common adverse resulting physiological phenotypes include insulin-resistance[5,79,97,103], type 2 diabetes mellitus[6,77,104] and metabolic syndrome[44,88,103].

Amino Acid Reservoir

Skeletal muscle also functions as the largest reservoir in the body for amino acids, both as free amino acids and in the form of protein[39]. Interestingly, amino acids are found in the cytoplasm surrounding the contractile apparatus, as there is not a specific dedicated location within the myofibers for their storage[46]. Therefore, when tissues other than muscle exhibit a need for amino acids, myofibers must activate one of the proteolytic systems: ubiquitin-proteasome, autophagy-lysosomal, or caspase-mediated protein cleavage[105]. Activation of proteolysis includes inhibition of the mTOR pathway, as low levels of amino acids inhibit mTOR[106]. In response, mTOR inhibition activates the autophagy pathway to provide amino acids to other tissues in need. It has also been documented that in low amino acid conditions the forkhead box O (FOXO) transcription factors are activated to induce proteasomal and lysosomal degradation[107]. Low levels of amino acids also induce myogenesis by activating satellite cells to differentiate.

Metabolic Shifts and Disease

Aging, as well as acute and chronic illnesses can contribute to changes in metabolic needs and lead to muscle wasting, or atrophy. Atrophy is characterized by a

combination of a net loss of proteins, organelles and cytoplasm[108], and is accompanied by decreased fiber diameter and force production, as well as increased fatiguability[109].

Atrophy can be categorized into three categories: 1) physiologic[109], 2) pathologic[110], or 3) neurogenic[110,111]. Physiologic atrophy results from disuse of muscle leading to increases in protein degradation and decreased protein synthesis[109]. Pathologic atrophy is generally related to conditions such as aging or starvation[110]. Lastly, neurogenic atrophy results from dysfunction or damage of innervating nerves. Many pathways that can mediate atrophy including proteasomal, calpain, and autophagic-lysosomal mechanisms of protein degradation[13,32,108,109,111-117]. Many factors also impact protein regulation of protein synthesis and degradation, including TNF-α, glucocorticoids, myostatin and other activin receptor type-2B (ACVRIIB) ligands, ROS, FoxO3, PI3/Akt, and NF-κB[109-112,114]. Muscular atrophy and the associated degradation of protein and release of amino acids can be a response to a need for amino acids in other tissues for local protein synthesis, as well as muscle disuse, cachexia, or myopathy.

Branched Chain Amino Acid Catabolism

Regulation of branched chain amino acid (BCAA) catabolism is vital to maintaining myofibrillar balance of protein synthesis and degradation[81,84-87,118-121]. BCAA catabolism involves two primary enzymatic steps, 1) branched-chain amino transferases (BCAT) and 2) branched-chain ketoacid dehydrogenase complex (BCKDH). There are three subunits to the BCKDH complex, E1 through 3, in which dihydrolipoamide branched chain transacylase E2 (DBT) has the transacylase activity. DBT accepts and

then transfers acyl groups from the E1 subunit of BCKDH to coenzyme A. Any perturbations in DBT's expression could cause major metabolic fluctuations within the cell.

The most studied post-translational modifications of BCKDH involves the branched chain ketoacid dehydrogenase kinase (BDK). It is known that BCKDH activity is lower in skeletal muscles due to the higher expression of BDK, compared to DBT, than when compared to other tissues[122].

Demonstrated in rats, high expression levels of BCKDH are indicative of a tissue's need to reduce intracellular protein concentrations to reduce protein load, and conversely tissues that need to conserve synthesis of critically important proteins have lower expression of BCKDH[123,124]. It has been established that dietary protein levels in male rats were reversibly, inversely related to both plasma T3 and T4 levels[125]. It has further been shown that BDK activity increases with a concomitant decrease in BCKDH activity during a hyperthyroid induced state[126].

Activation of BCAA degradation is mediated through leucine-derived alpha-ketoisocaproate (KIC)[127]. KIC is the result of the transamination of lysine resulting from BCAT activity[128]. Once converted to KIC roughly 95% of ingested KIC promotes release of BCKDH kinase from the BCKDH complex, this action then activates the complex's activity[129].

Obesity

The first recognition of obesity as a disease was by the American Association of Clinical Endocrinologists in 2012[130]. Obesity is now a well-known, worldwide health condition that is highly prevalent in the United States[131]. An obese classification is typically defined in terms of body mass index (BMI)[130,132]. The World Health Organization defines obesity at a BMI greater than or equal to 30, in which BMI = weight (kg)/height^2 (m^2)[132]. Since the first recognition of obesity as a serious health condition there has been extensive research into its etiology and debate about its classification within the medical field[133-152].

Monogenic Obesity

Monogenic obesity results from mutations in a single gene. The first gene identified in monogenic obesity is the satiety gene LEP, encoding the leptin protein, which regulates food intake and energy expenditure[153-155]. Mutations in genes within the leptin-melanocortin system resulting in obesity include leptin and leptin receptors (LEPR)[135,140,153,154,156-158], melanocortin 4 receptor (MC4R)[135,141,143], proopiomelanocortin (POMC)[135,136,143], single-minded homolog 1 (SIM1)[143], brain-derived neurotrophic factor (BDNF)[143], neurotrophic tyrosine kinase receptor type 2 (NTRK2)[143], proprotein convertase subtilisin/kexin type 1 (PCSK1)[135,140,143,159] and PPARγ2[146,160-164]. LEPR deficiencies disrupt signaling cascades including the JAK-STAT, PI3K and ERK pathways[140,141,154,156].

These genes can also confer behavioral phenotypes that can promote a shift towards an obese phenotype. For example, in addition to altering metabolism, dysregulation of the MC4R pathway impacts eating behavior[136,147,165,166]. Hormones and neural peptides also play a significant role in modulating behavior associated with eating, satiety, and appetite. These include neuropeptide Y (NPY), agouti-related peptide (AgRP), ghrelin, cholecystokinin, leptin, and insulin[167-169].

Polygenic Obesity

Genome-wide association studies (GWAS) have identified hundreds of genes involved in polygenic obesity, each contributing varying small degrees of predisposition to an individual's presentation of obesity[134,138,142,148,152,170,171]. Etiology and categorization surrounding polygenic obesity is difficult to determine as the penetrance of different genotypes and the severity of the resulting obesity can vary greatly, even among individuals who share the same genetic alterations.

Syndromic Obesity

Syndromic obesity is broadly categorized as resulting from a collection of clinical measures related to genetics, neurodevelopment, and obesity[143,172-174]. Specifically, syndromic obesity includes the association of obesity with developmental delay, dysmorphic features, and congenital malformations[172]. Examples of these syndromes include Prader-Willi[175,176], Bardet-Biedel[177,178], Pseudohypoparathyroidism[179,180] and SIM1 related[181,182].

Sexual Dimorphism of Obesity

It has only been within the last several decades that research has really expanded to elucidate the role and impact of sexual dimorphism in many basal and disease states. The relationship of obesity to sex itself was only first described in 1996[183]. It has been the subject of many studies since then, generally showing that females are more protected against obesity due to the influence of sex hormones[21,184-189]. This protection is conferred by estrogen, estradiol, and their associated receptor's roles in modulating energy expenditure and in regulation of appetite[190-194].

Females are generally considered to be protected against obesity compared to males primarily attributed to the presence of estrogen, its role in influencing adipose tissue function and overall adipose distribution[195]. Females generally have a gynoid adipose distribution whereas males display an android distribution[196,197]. The android distribution is associated with significant differences in protein[198] and mitochondrial content[199,200], enzymatic activity[196,197,201], and mortality and risk profiles[202-208]. This distinction in phenotype becomes less defined following menopause in females as there is a shift in the deposition of visceral adipose tissue[190], which does not necessarily mean there is a shift to the android phenotype. Following ovariectomy, female mice lose resistance to high-fat diet induced obesity, increase visceral adipose tissue, and show a reduction in leptin sensitivity[184]. However, these changes can be reversed by treatment with estradiol[185].

Thyroid Hormones

Function

Thyroid hormones (THs) are essential for normal development and regulate several physiological processes including metabolism[20,25,26,163,209-216], body temperature and energy expenditure[25,215,217], heart rate[218,219], and neuronal development and signaling[220-223]. THs, triiodothyronine (T3, the active form) and thyroxine (T4, the prohormone form), are potent regulators of metabolism that are produced and controlled by the negative feedback loop of the hypothalamic-pituitary-thyroid axis (HPT)[224-227].

Mechanism of Action and Deiodinases

The HPT axis starts in the hypothalamus with the release of thyrotropin-releasing hormone (TRH) which acts upon the pituitary gland to stimulate the release of thyroid-stimulating hormone (TSH) into the portal system[224]. TSH then acts on the thyroid gland to induce the release of THs, primarily T4, into the bloodstream. Once in the bloodstream, THs can enter target tissues via carrier-mediated monocarboxylate transporters 8 and 10 (MCT8 and MCT10 respectively)[228-230] (Process shown in Figure 1.3).

Figure 1.3. *Thyroid Hormone Receptor Mediated Transcription.*
(1) THs enter the cell from the bloodstream via carrier mediated transporters. (2) Once in the cytosol, T4 must be converted to T3, the active form, (3) which can then translocate to the nucleus. Once within the nucleus, (4) T3 binds THR which triggers the (5) release of a co-repressor (shown as a red circle). (6) Dimerization with Retinoid X receptor takes place, and the complex recruits the co-activator complex (complex shown as a green circle). The entire complex can then bind to the TRE within the gene of interest's regulatory region and thereby influence transcription.

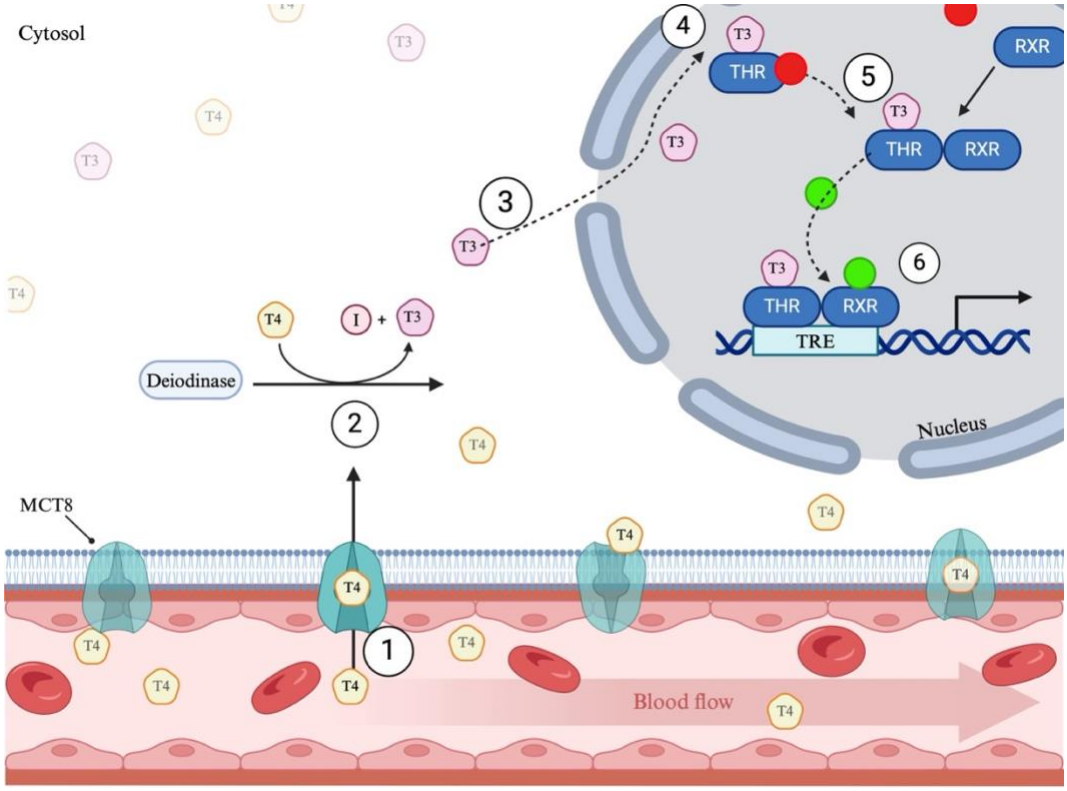

T3 binds to TRs with a K_D = to 0.06 nM whereas T4 binds to TRs at a lower affinity of K_D = 2 nM[231]. As such, it is essential that T4, the inactive form of the thyroid hormones, is converted to the active form, T3. T3 is essential for the regulation of metabolism in most tissues including the liver, brain, kidneys, and skeletal muscles[232]. The conversion of T4 to T3 is catalyzed by one of the three iodothyronine deiodinases (DIO1-3)[232-235].

DIO1 is responsible for catalyzing both the activation and inactivation of thyroid hormones by removing one iodine, to activate, or additional iodines, to inactivate[236]. DIO1 acts in its role as a scavenger enzyme to deiodinate inactive thyroid hormone

molecules, which typically have iodines in the incorrect positions[237]. DIO1 is highly expressed within the kidney, liver, and thyroid[238].

DIO2 activates the conversion of T4 to T3[239-241] and DIO2 activity is significantly increased in slow-twitch muscle[241]. This increased activity is likely linked to the fact that slow-twitch muscles are more responsive to thyroid hormones[26,27,242]. In congruence with DIO2's increased activity, it is upregulated in hypothyroidism and downregulated in hyperthyroidism[215].

DIO3 is expressed at only low levels across tissue types in healthy individuals[232,234] and is responsible for inactivating both T3 and T4, to T2 and rT3 respectively. DIO3 can modulate localized levels of THs regardless of serum concentration of THs in a 'cell-autonomous manner'[243]. DIO3 is critically important in the development of the fetal brain for appropriate timing of thyroid action in developmental stages[244,245]. DIO3 is also seen in high levels in highly proliferative cancers, which can lead to local hyperthyroidism and thus inactivation of TH transcriptional activity[246].

Thyroid Hormone Receptors (THRs) and Thyroid Response Elements (TREs)

Following its conversion from T4 in the cytoplasm, T3 can translocate to the nucleus where it binds to nuclear thyroid hormone receptors (THRs). THRs bind to T3-response elements (TREs) in promoter regions and function as transcription factors to regulate T3 target gene expression[247,248]. TREs are specific DNA sequences with the

canonical sequence half-site sequence AGGTCA[249], although other, closely related sequences can also be functional.

TREs can either consist of the half-site sequence as either a palindrome or separated by four nucleotides as either direct repeats or as an inverted palindrome[250] (Table 1.1). THRs bind to the TRE as a protein dimer, either as a homodimer or as a heterodimer with another member of the retinoid X receptor (RXR) nuclear receptor family[249,251-254], liver X receptor[255] or PPARs[256]. TREs are typically found in regulatory regions of genes and can either act as enhancers (positive TRE) or silencers (negative TRE)[250] and possess corepressor or coactivator activity to further regulate transcription[257-259]. Confirmation of transcriptional THR targets is traditionally evaluated using electrophoretic mobility shift assays (EMSAs), serum-based immunoassays and LC/MS.MS techniques[260] and reporter assays such as luciferase assays[260-263].

TRE Sequence Type	Sequence
Consensus	AGGTCA
Direct Repeat	AGGTCAnnnnAGGTCA
Everted Repeat	TGACCCnnnnAGGTCA
Inverted Repeat	AGGTCA TGACCT

Table 1.A. Consensus and Common TRE Sequences.

Humans have four THRs produced at two loci, the THRA locus on chromosome 17 and the THRB locus on human chromosome 3. The THRA locus produces TRα1 and TRα2 while the THRB loci produces TRβ1 and TRβ2. Differences within the four THR

include TRα2 alone is unable to bind T3[264], TRα1 and TRα2 differ at their C-terminal region due to the expression of an alternative exon; and TRβ1 and TRβ2 differ at their amino termini for the same reason[265].

TRα1 and TRα2 can bind DNA in their monomeric form and are both expressed in various tissues. They both can interact with hormone response elements (HREs), however as previously noted TRα2 is not able to bind T3[264]. TRβ1 and TRβ2 typically will form heterodimers with retinoid X receptors (RXR) and is the most transcriptionally activate of the THRs.

Although there are other isoforms of THR, they exist as truncated forms and their function *in vivo* is unknown[266,267]. Active THR subunits are all comprised of an N-terminal domain, a DNA binding domain, and a T3 ligand binding domain which allow THRs to act as ligand-activated transcription factors. Each isoform has separate ligand-independent and dependent actions[268,269].

Thyroid Hormones and Sex Hormones

THs impact the bioavailability of other hormones throughout the body, especially in terms of female reproductive system[270,271]. Alterations in serum sex hormone levels leads to changes in circulating levels of key metabolic factors including leptin, growth hormone and insulin-like growth factor-1[185,272,273], as well as influencing adipose distribution[197,198,203,274,275]. As testosterone inhibits, and estradiol stimulates, leptin expression males are more prone to metabolic pathologies[276]. Ultimately, sex hormones

impact a variety of processes including the HPT axis, body weight, fat distribution, and appetite[277,278].

Metabolism

The dynamism and versatility of skeletal muscle are closely linked to their metabolic properties, including their ability to use multiple substrates via different biochemical pathways, as well as their ability to adapt to everchanging energy demands.

Substrate Source

Substrate selection in skeletal muscle is influenced by ongoing demands of the body, including activity and exercise intensity and duration of activity, as well as nutritional status. Potential substrates include glucose, fatty acids, and amino acids. Glucose is primarily derived from the diet as carbohydrates or stored as glycogen. Skeletal muscle is the primary storage site of glycogen, with approximately a four-fold more than the amount stored in the liver. Fatty acids can be mobilized from adipose tissue in times of need, and amino acid utilization predominantly occurs during intense exercise or fasting in healthy individuals, or muscle atrophy or cachexia in individuals with disease.

Pathways for Energy Utilization

Glycolysis

As mentioned previously, of the potential target tissues during insulin mediated glucose uptake, skeletal muscle accounts for the maximal glucose uptake of roughly 80%

of the total glucose[279]. Glycolysis is a cytosolic process in which glucose is broken down into pyruvate. In aerobic conditions, pyruvate is then dependent on oxygen availability for entry into the Krebs Cycle (citric acid cycle). For anaerobic glycolysis, pyruvate is converted to lactate.

Krebs Cycle

The Krebs Cycle, also known as the tricarboxylic acid (TCA) cycle, takes place in the mitochondrial matrix. In this pathway, with fatty acids or pyruvate produced from glycolysis, there is a production of NADH, $FADH_2$, and ATP. The Krebs Cycle within skeletal muscle is detailed in great depth in Schiafinno, et. al 2015[280].

Electron Transport Chain (ETC)/Oxidative Phosphorylation

The inner mitochondrial membrane harbors the electron transport chain (ETC). The ETC consists of five protein complexes that create an electrochemical gradient via redox reactions[281]. As electrons move to each successive complex, protons are pumped from the matrix to the inner membrane space. Once in the inner membrane space, protons can be used for oxidative phosphorylation. The protons power the ATP synthase to produce ATP[75]. Oxidative phosphorylation is a process that requires oxygen as the source of electrons and results in the production of reactive oxygen species (ROS)[282] as well as ATP.

Lactate Production

While lactate is often not thought of as an energy source but rather a waste product, it is in fact useful as a circulating carbohydrate source. Lactate is produced in times of cellular stress in which the levels of oxygen present are insufficient for the ATP demands of the cell[283]. Lactate is then available as an energy source in other tissues with greater access to oxygen, or it can be transported to the liver for gluconeogenesis[75].

Modulation of Energy Production

In response to muscle contraction and movement, skeletal muscle can rapidly alter its metabolic properties. At maximal activity, ATP turnover rate can reach levels exceeding 100-fold than those seen at rest[284]. This increase in ATP consumption can lead to about a 20-fold increase in overall whole-body metabolism[284]. The high mitochondrial content within most fibers in human skeletal muscle allows for maximal rates of oxygen consumption, associated with up to a 100-fold increase in TCA cycle activity[285,286]. Furthermore, exercise training can result in increased mitochondrial density, shift in substrate choice, and show significant differences in enzyme activity for specific metabolic pathways in skeletal muscle[2,4,7,96].

THs can influence metabolic pathways and energy production in a variety of manners. THs influence lipolysis and lipogenesis, glycogenolysis and gluconeogenesis, phosphofructokinase and fructose 1,6-diphosphatase, hexokinase and glucose-6-phosphate, and protein synthesis and catabolism[287]. Binding of THs to the receptors on mitochondria lead to increased ATP production and activation of transcription.

Hypothyroidism results in impaired oxidative phosphorylation within the mitochondria, and hyperthyroidism impairs work capacity of muscles.

Mu-Crystallin

Expression of Mu-Crystallin

Mu-crystallin is a 34 kDa cytosolic protein encoded by the *CRYM* gene that has a role both as a ketimine reductase and a NADPH-dependent thyroid hormone binding protein[288-290]. The only disease in which CRYM has so far been identified as the causal agent is a specific form of non-syndromic deafness in which one of two amino acid changes at the C-terminus of the protein, (K314T, X315Y), alter thyroid signaling in the fibrocytes of the cochlea[291].

CRYM expression has been documented in multiple tissues including brain, heart, kidney, prostate, inner ear, and skeletal muscle[292]. Within the human population, expression of mu-crystallin in muscle is highly variable, with approximately 70% of the population expressing little to no detectable mu-crystallin whereas the remaining population expresses high levels of mu-crystallin. There is also considerable variation in CRYM expression among family members[292].

Function of Mu-Crystallin and Current Studies

As previously mentioned, since CRYM's discovery two main functional roles have been identified, 1) role as a ketimine reductase and 2) as a thyroid hormone binding protein. Most of the literature surrounding Crym has focused on characterization of the

role of Crym as a ketimine reductase in the brain[128,293]. As ketimine reductases reduce imine bonds, research has examined its role in neuronal lysine metabolism[128,294].

Lysine Metabolism

Lysine metabolism occurs via one of two pathways, 1) saccharopine pathway or 2) pipecolic acid pathway. The saccharopine pathway is better characterized than the pipecolic pathway. The saccharopine pathway takes place within the mitochondria, where lysine is converted through a series of reactions into α-aminoadipic acid and glutamate[128,294,295]. An extensive detailed history of the elucidation of the saccharopine pathway can be found in Matthews 2020[295].

Lysine degradation via the pipecolic acid pathway results in the production of pipecolic acid, but the exact mechanism is not yet fully understood. Adding to this complexity is the lack of distinct localization to a cellular compartment, as this pathway has enzymes within the mitochondria, cytosol, and the peroxisome. Interestingly, it has been suggested that Crym may mediate the conversion of Δ1-piperideine-2-carboxylate to pipecolic acid in the cytosol[293].

Of importance, intermediates such as alpha-aminoadipate semialdehyde in the lysine metabolism pathway are quite toxic[296,297] leading to impaired mitochondrial function. Lysine functions also as a precursor for carnitine synthesis, which facilitates the transfer of fatty acids into the mitochondria for β-oxidation[298]. Decreased carnitine synthesis can lead to muscle atrophy due to inefficient transport of fatty acids into the

mitochondria. This results in decreased energy production, an increase in muscle fatiguability and impaired muscle recovery[299,300].

Thyroid Hormone Binding Protein

It is presumed that mu-crystallin plays a role in regulation of free intracellular T3 levels, perhaps by sequestering T3 in the cytosol to impede T3's access to its receptors in the nucleus[288,289]. As mentioned previously, T3 binds to TRs with a K_D = to 0.06 nM. The mu-crystallin binds T3 with a K_A = 2nM[301], which represents a relatively strong binding, but not as strong as T3 to TRs.

Research on mu-crystallin's role as a thyroid hormone binding protein outside of the brain, specifically on mu-crystallin's influence on metabolism via its thyroid hormone binding capacity, is limited [162,302]. To probe the prospective role of mu-crystallin in modulating metabolism, our lab has generated a line of transgenic mice, in the C57BL/6 background, with skeletal-muscle specific high-expression (SM-HE) of *Crym*.

Previously Published Research

We published data obtained with these *Crym*-tg mice maintained on standard chow that demonstrated that SM-HE of mu-crystallin increased the levels of T3 in *tibialis anterior* muscles (~200-fold increase), though with minimal changes in circulating T4 (1.2-fold decrease)[302]. We also detailed a concurrent, small but statistically significant, 13.7% shift in respiratory exchange ratio towards an increase in utilization of fat as an energy source with paralleled expected changes in mRNA and proteomic data[302].

We also documented that male *Crym*-tg mice did not display significant differences in several other physiologic, morphologic, and cellular parameters. Some of these measures that did not show significant differences include but are not limited to: body composition, mass of individual fat pads, fiber types, overall fiber number, grip strength, maximum treadmill running speed, maximal rate of twitch force contraction/relaxation, specific isometric force of contraction, and voltage-induced Ca^{2+} transients[302]. Of note, however, these studies only evaluated male mice.

Work has also been done with male SV/129 mice in which the *Crym* gene has been inactivated by homologous recombination within the first and second coding exons[303]. Initial publications detailed the phenotype of *Crym*-KO mice and showed no significant differences in growth, heart rate, or hearing. There was a significant decrease in circulating serum THs, with decreased levels of both T4 and T3[303]. Interestingly, following radio-labeled T3 injection, *Crym*-KO mice showed a faster time to reach peak concentration in the brain, heart, liver and kidney and faster clearance of radiolabeled T3 from the assessed target tissues[303]. The authors proposed that this was likely indirect evidence that *Crym* plays an important role in mediating translocation of T3 to the nucleus.

Additional studies conducted by the same group challenged male *Crym*-KO mice with low- and high-fat diet (LFD and HFD, respectively) interventions. Following 10-weeks on diet, no significant differences were seen in mice on LFD. However, *Crym*-KO

mice showed a significant increase in body mass on the HFD when compared to non-littermate controls[162]. Further evaluation of these mice on HFD showed no changes in glucose or insulin tolerance. When they evaluated gene expression in the liver, there was a significant increase in peroxisome proliferator-activated receptor γ (PPARγ) activation, tumor necrosis factor α (TNFα), and Acetyl-CoA carboxylase (Acc1)[162] in mice on the HFD. They found no significant differences seen in expression of POMC[162] or other behavior-associated genes in either group.

Conclusion

Obesity is continuing to increase in the United States and worldwide, with serious long-term health consequences and healthcare-related costs. Research has focused on understanding the complex etiology of obesity and on potential treatments. Traditional interventions, such as increased physical activity, change in diet, and behavioral therapy, are often insufficient or difficult to comply with. As such, complete understanding of the regulation of whole-body metabolism is essential to identify new pharmacotherapeutic interventions that can be utilized in conjunction with conventional treatment modalities.

As skeletal muscle is responsible for a large portion of basal metabolic rate it is an ideal target tissue to study. THs are potent regulators of metabolism, while mu-crystallin is a thyroid hormone binding protein that can be found expressed in high levels in ~20% of the human population.

For these reasons, we evaluated the role of high, muscle-specific expression of mu-crystallin as a modulator of metabolism in mice placed on diets of low- or high-fat chow. The work presented here evaluates physiological implications of SM-HE of mu-crystallin and the resulting whole-body phenotype, and the cellular and molecular consequences. In Chapter 2 we reveal sexually dimorphic differences in basal endogenous mu-crystallin expression across several mouse strains and across various muscle depots. Utilizing our *Crym*-tg mouse line in Chapter 3 we demonstrate sex-dependent and diet-specific changes in body composition, relative and cumulative fiber cross sectional area, and transcriptomic changes in metabolic genes, and specifically those involved in branched chain amino acid catabolism. The data presented in Chapter 3 provides evidence that mu-crystallin may primarily mediate its metabolic effects through its role as a ketimine reductase and not through its role as a thyroid hormone binding protein as we previously hypothesized. Finally in Chapter 4 we show that SNP rs3843259 is not a good predictor of high mu-crystallin expression in human skeletal muscle.

Chapter 2 Determining Endogenous Skeletal Muscle *Crym* Expression in Males and Females in Commercially Available Mouse Strains

Introduction

Various mouse, and rat, strains have been manipulated via genetic and/or diet interventions to elucidate the direct and downstream effects of obesity. Monogenic and polygenic mutations as well as environmental factors are common targets of interest to interrogate a wide range of intracellular, intercellular, and systemic processes that impact whole-body metabolism. These factors are frequently related, but not limited, to satiety[141,147] and neuronal signaling[136,304-306], glucose homeostasis and blood glucose transport[6,307], energy intake and expenditure[37,308], hormone (dys)regulation[25,213], obesogens[137] and epigenetic modifications[309-311].

The most notable monogenic models of obesity in mice are the *ob/ob*, *db/db*, *s/s*, Tubtub/J mice[312]. Perhaps the most studied and exemplary model of such a strain is the *ob/o*b (ob = obese) strain of C57BL/6J mice. While *ob/ob* mice were first characterized in 1949 at Jackson Laboratories, the gene responsible for the obese phenotype was not characterized until 1994, when it was identified as a monogenic mutation in the leptin gene[313]. *Ob/ob* mice present with rapid weight gain due to hyperphagia and decreased energy expenditure, along with other attributes associated with obesity, including dysregulated glucose tolerance and insulin sensitivity, defective thermogenesis, dyslipidemia, and even infertility[157].

Knowing that mu-crystallin is a thyroid hormone binding protein, we were interested in the potential metabolic phenotype resulting from variations in *Crym* expression. Our prior work indicates that mice expressing high levels of mu-crystallin in their skeletal muscles show a significant increase in intracellular thyroid hormone concentrations[302]. As T3 has a major influence on lipid metabolism, we were interested to determine whether obesity-prone strains of mice exhibit levels of endogenous mu-crystallin expression that differ from those of obesity-resistant strains. We hypothesized that increased levels of mu-crystallin would be found in obesity-resistant strains, consistent with the idea that this would lead to increases in intracellular T3 and, as T3 is a potent regulator of metabolism, this increase would result in subsequent alterations in whole body metabolism. The results of these studies could reveal if different endogenous levels of mu-crystallin in skeletal muscle impact the tendency of different strains of mice to become obese or to resist obesity.

Therefore, we evaluated selected mouse strains for endogenous levels of mu-crystallin and compared them with metabolic phenotypes for each strain found in current literature. We selected a subset of commercially available strains of interest from Jackson Laboratories. Since we have previously published that mu-crystallin inherently varies by skeletal muscle group in our transgenic line[302], we did not want to presume that expression across strains did not follow suit. We evaluated multiple tissues in case endogenous levels vary by muscle in the other strains as well.

The current classification methods for fiber typing are a crude system that does not typically account for hybridization of fiber types. Furthermore, it is well known that fiber type distribution varies significantly by muscle group, and so to test our hypothesis that mu-crystallin affects metabolic homeostasis, it was important to evaluate canonically slow- and fast-twitch based muscle groups. For our studies we selected the following muscles: *tibialis anterior, gastrocnemius, quadriceps, soleus* and *diaphragm.* The *tibialis anterior* muscle in C57BL/6 mice primarily consists of fast-twitch fibers[314,315], as noted in Figure 2.1. *Gastrocnemius* muscle contains both fast- and slow-twitch fiber types, the proportion of which varies based on factors such as age and physical utilization. *Soleus* muscle is primarily slow-twitch (Type I) fibers. *Quadriceps* also have a mix of fast- and slow-twitch muscle fibers. The *diaphragm* is primarily comprised of fast-twitch fibers. Of note, we did not select the *ob/ob* strain but rather selected the background strain C57BL/6J.

Figure 2.1. *Fiber type distribution in select muscle groups of C57BL/6 mice.*
Data was collected from readily available literature. Data includes *tibialis anterior, soleus,* and *gastrocnemius* fiber type distribution of C57BL/6 mice[315,316].

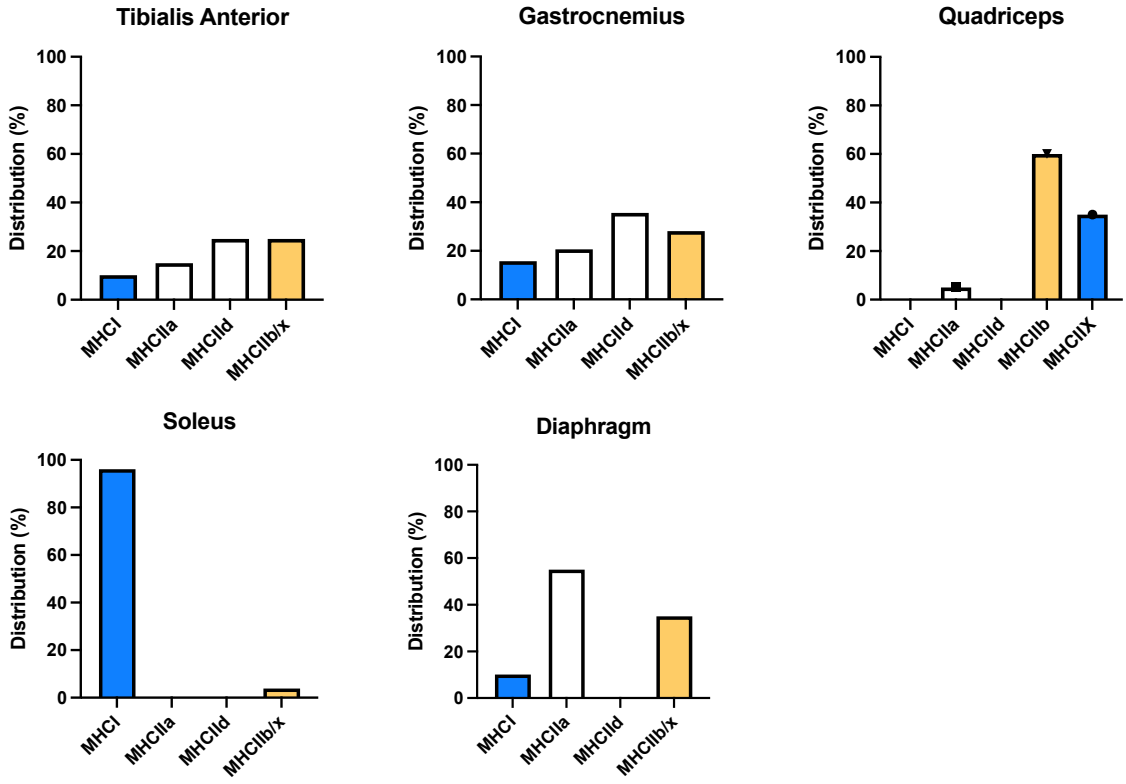

Strain Selection

Obesity Prone Strains

C57BL/6J

C57BL/6J is the most widely used obesity-prone inbred strain of mice and is often used as the background for obesity-related studies[317]. The benefits of using the C57BL/6J mouse is its longevity, ease of breeding and ease of introducing genetic mutations. Common interventions used in studying obesity include manipulation of caloric load or diet composition, exercise, and other environmental perturbations. Jackson Laboratory notes the ease of C57BL/6J's high-fat diet-induced obesity phenotype with concomitant hyperglycemia and hyperinsulinemia[318,319]. Of five strains considered, AKR/J, C3H/HeJ, DBA/2J, SWR/J and C57BL/6J, readily available data from Jackson Laboratory states that the latter is the least glucose tolerant [320,321]. Furthermore, with

high-fat diet intervention, skeletal muscles of C57BL/6J mice show a shift toward more oxidative fiber types and a significant decrease in respiratory exchange ratio as measured in CLAMS cages[18].

C57L/J and AKR/J

Utilizing quantitative trait loci mapping (QTL), the Jackson Laboratories evaluated C57L/J and AKR/J mice via selective DNA pooling to identify regions related to their obesity phenotypes. The *Obq3* locus of AKR/J mice, located within chromosome 2, confers increased adiposity, more prominently in males than in females[322]. The AKR/J strain is also more responsive to dietary fat-induced weight gain. *Obq4* in C57L/J mice, on chromosome 17, also showed a more pronounced phenotype in males compared to females, and differentially affects inguinal fat deposits[322].

129X1/SvJ

129X1/SvJ mice are another inbred strain of obesity-prone mice. When compared to three other strains, C57BL/6, FVB/N, DBA/2, 129X1/SvJ mice had the lowest fasting blood glucose and insulin levels as well as significantly increased *in vivo* insulin secretion[323]. However, high-fat diet fed 129X1/SvJ mice are more glucose intolerant and insulin resistant than C57BL/6, DBA/2 and FVB/N mice[324].

Obesity Resistant Strains

BALB/cJ

BALB/cJ mice are considered an obesity-resistant strain of mice. When challenged with a high-fat diet for 6 weeks, they do not present with changes in body mass or blood glucose levels[325]. BALB/cJ are also reasonably protected from high-fat diet-induced glucose intolerance[326].

SWR/J

Swiss SWR/J mice develop polydipsia and nephrogenic diabetes insipidus (polyuria) as they age[327]. Of note, polydipsia is more pronounced in female mice than in males. To achieve maximal weight gain, these mice need a chow with high dietary fat and with as little protein content as possible[151]. Following high-fat diet, when compared to the AKR/J strain of mice, SWR/J mice showed slightly lower plasma glucose and insulin levels[328,329]. The AKR/J and SWR/J strains are also distinguishable by the differences in their adipocyte insulin sensitivity[328]. AKR/J mouse adipocytes demonstrate an increased sensitivity to insulin, which is increased following high-fat diet intervention[328]. On the contrary when SWR/J mice are fed a high-fat diet their adipocytes show a decreased sensitivity to insulin[328].

C3H/HeJ

The C3H/HeJ strain was selected for its insulin resistance and resistance to diet-induced obesity. C3H/HeJ mice have a loss-of-function mutation in the Toll-like Receptor 4 (TLR4) gene that may be linked to the strains documented low body fat, but how this mutation effects changes in adiposity remains unknown[330].

Other Notable Strains

DBA/2J

The DBA strain of mice is the oldest of all inbred murine strains. DBA/2J mice, as well as AKR/J mice, show elevated levels of leptin and insulin with increased adiposity[331]. Crossing DBA/2J mice with New Zealand obese (NZO) mice, with the QTL locus *Nidd/DBA* located on chromosome 4, implicates four potential candidate genes for type 2 diabetes[332]. The *Nidd/DBA* mice present with hyperglycemia, reduced plasma insulin and loss of beta-cells[332]. However, there are conflicting reports on whether or not this strain is obesity-prone or -resistant[158,331,333,334].

SJL/J

SJL/J mice were of interest to us as our laboratory also conducts studies on dysferlinopathies and facioscapulohumeral muscular dystrophy (FSHD). The dysferlin gene in the SJL/J strain has a splice-site mutation that results in decreased expression of dysferlin[335]. This leads to decreased muscle mass due to progressive loss of muscle while concomitantly increasing several markers of muscular pathology[336]. One hundred percent of SJL/J mice, by six to eight months of age, show clear myopathy[336]. Interestingly, SJL/L mice regenerate muscle faster following injury than BALB/c mice[337,338].

Methods

Mice

All experiments were performed in compliance with the policies and procedures of the University of Maryland, Baltimore's Institutional Animal Care and Use Committee

(IACUC). All strains were procured from Jackson Laboratories (Bar Harbor, ME) at three to four months of age. Strains included C57BL6/J (000664), C57L/J (000668), AKR/J (000648), BALB/cJ (000651), SWR/J (000689), 129X1/SvJ (000691), C3H/HeJ (000659), DBA/2J (000671), and SJL/J (000686).

Protein Extraction

Following euthanasia of the mice, tissues of interest (*diaphragm*, *gastrocnemius, soleus, tibialis anterior* and *quadriceps)* were collected, snap-frozen in liquid nitrogen and stored at -80^{o} C. Protein was extracted in RIPA Buffer (R0278-50 ML, Sigma-Aldrich), prepared with cOmplete Mini, EDTA-free protease inhibitor tablets (11836170001, Sigma-Aldrich; 10 mL of RIPA buffer to every protease inhibitor tablet). Tissue was weighed and 100 µL per 10 mg of tissue of RIPA/protease inhibitor solution was added, along with two 5 mm steel beads (69989; Qiagen, Hilden, Germany). Samples were placed in a TissueLyser LT (Qiagen) at 50 oscillations/sec for 3 min, briefly vortexed, placed on ice for 2 min, followed by a second round of 50 oscillations/sec for 3 min. Samples were sonicated for 10 sec and subjected to centrifugation at 14,000 x g for 30 min at 4^{o}C. The supernatant was transferred to a new microfuge tube and protein concentration was determined with Protein Assay Dye Reagent Concentrate (Bradford Assay; 5000006, Bio-Rad).

Automated Capillary Immunoassay (Abby)

Analysis was performed with Protein Simple's Simple Western system, Abby, according to the manufacturer's instructions for the 12-230 kDa protein separation

module (#SM-W004; Protein Simple a Bio-Techne Brand, Minneapolis, MN). Protein extracted from whole tissue lysates was prepared with 10x Sample Buffer (#042-195; ProteinSimple) to generate an overall protein concentration of 1.0 mg/ml for each sample generated. The primary antibody for mu-crystallin (SC-376687; Santa Cruz Bio) was diluted to 1:25 in Protein Simple's Antibody Diluent 2. A primary antibody to a control protein, aconitase-2 (ab129069; Abcam, United Kingdom), was used at 1:200, and multiplexed with mu-crystallin. Samples were run as technical triplicates. Compass software (Compass for SW 4.0 Mac Beta; Protein Simple) was used to visualize the electropherograms and to analyze each peak of interest to calculate the area under the curve (AUC). The peak signal-to-noise ratio was set at $\geq$ 10 automatically by the software. Due to slight capillary-to-capillary variations in the readout of molecular mass, peaks identified close to the calculated mobility were allowed a 10% range in variance (as automatically set by the Abby system). AUC was analyzed with two-way ANOVA, fitted with a main effects only model, comparing each group to C57BL/6J, using a Fisher's LSD test, with significance set at $p<0.05$.

Considerations

We used the capillary-based immunoassay system by Biotechne's Protein Simple devices, specifically Abby. As these experiments progressed an improved and more precise methodology was established for normalizing protein expression that was not available initially for this system. The development of the total protein normalization module allowed us to move away from using a single housekeeping protein for normalization, as we were already aware that traditional housekeeping proteins were not

available for us to use in our studies (previously published Aconitase2 as a control protein for these assays).

Results

Expression of endogenous mu-crystallin in males of eight murine strains were compared to endogenous mu-crystallin levels in C57BL/6/J mice. 129X1/SvJ and DBA/2J mice showed a significantly higher levels of endogenous mu-crystallin in the tibialis anterior compared to C57BL/6J males. The remaining murine strains did not differ significantly from C57BL/6J (Figure 5.2).

For budgetary reasons, we chose to analyze fewer strains of female mice. We found no significant differences in the expression of endogenous mu-crystallin in the tibialis anterior muscles in any of the female strains when compared to C57BL/6J. However, DBA/2J mice had a statistically significant increase in endogenous mu-crystallin expression when compared to C57BL/6J female mice in soleus, gastrocnemius, and quadriceps muscles. Lastly, female BALB/cJ mice showed a statistically significant increase, approximately 3-4-fold, in endogenous mu-crystallin expression in the quadriceps and gastrocnemius compared to C57BL/6J females (Figure 2.2).

Figure 2.2. *Endogenous mu-crystallin expression in select skeletal muscles of commercially available mouse strains.*
Mu-crystallin protein expression, normalized to the control protein Aconitase 2, in various muscles of different strains of male and female mice, assayed quantitatively by ProteinSimple technology. Strains are respectively grouped by obesity prone, obesity resistant and other selected strains, as indicated by the dotted line separating the three groups above.
* $p<0.05$, ** $p<0.01$, *** $p<0.001$

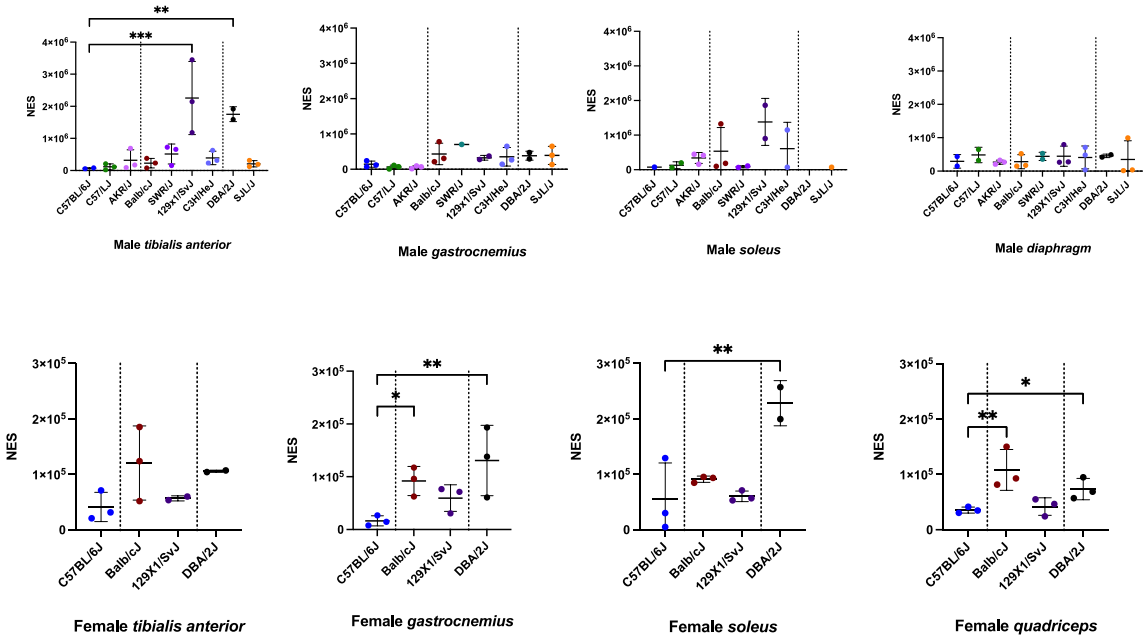

Discussion

Our prior work revealed that mice with skeletal muscle specific high levels of mu-crystallin showed a significant increase in intracellular thyroid hormone concentrations[302]. We hypothesized that higher levels of mu-crystallin would be found in obesity-resistant strains and would align with metabolic phenotypes documented for these mice within the literature. The results of these studies could potentially reveal whether endogenous levels of mu-crystallin in skeletal muscle are indicative of the tendency of different strains of mice to become obese or to resist obesity. However, our results argue against this hypothesis.

The only significant change seen in mu-crystallin expression for the male mice evaluated was found in the *tibialis anterior* muscle of 129X1/SvJ and DBA/2J. 129X1/SvJ and DBA/2J males had a statistically significant increase in mu-crystallin

expression compared to C57BL/6J mice (Figure 2.2). As for the female mice evaluated, we found statistically significantly increased mu-crystallin expression in several muscles of female DBA2/J and Balb/cJ mice when compared to C57BL/6J controls (Figure 2.2).

The metabolic properties of skeletal muscles track closely with their composition of slow, fast fatiguable and fast fatigue resistant muscle fibers. Specification of fiber types depends on a variety of factors, including thyroid hormone activity[29,47,339], which can dramatically impact skeletal muscle homeostasis, function and repair[20]. Thyroid hormones directly influence myosin heavy chain (MHC) gene expression, a key determinant of fiber type [90], and exposure to increased levels of T3 shifts fiber type by decreasing expression of MHC typical of type-1(slow) fibers and enhancing expression of MHC typical of type-IIA (fast fatigue resistant) fibers[22,23,29,340-342].

Furthermore, sex plays an important role in fiber type variation[28,95,343,344]. Sex-specific differences in humans have been documented via measurement of the cross-sectional area (CSA) of several fiber types. CSA for fiber types I, IIA and IIB were evaluated in men and women, and men had significantly increased CSA for each fiber type when compared to females[344]. In addition, CSA of fibers within the males showed that IIA fibers were the largest of the different fiber types (IIA>I>IIB) but in females the largest fiber type as measured via CSA was type I (I>IIA>IIB)[344]. Many factors have been well studied in the regulation and expression of MHC in various skeletal muscles, including age, sex, and hormone status[27,28,345-347]. In addition to the role of sex in fiber type presentation, the interplay of thyroid and sex hormones have also been

evaluated[14,43,89,90]. A study in rats showed that T3 treatment did not alter MHC composition in males, but in females the T3 treatment influenced a fiber type shift from IIA to IIB[345].

The selected muscle groups presented here inherently exhibit a range of fiber type compositions, from about half type I fibers in the soleus to primarily fast twitch fibers in the gastrocnemius and tibialis anterior muscles. Contrary to our hypothesis, our data does not indicate that obesity-resistant strains have an overall increase in mu-crystallin expression in any of the muscles evaluated. However, we did find that there are both sex-specific and muscle-specific differences in the expression of endogenous mu-crystallin across murine strains.

We previously reported that increased mu-crystallin expression in skeletal muscle leads to increased levels of T3[302]. Circulating thyroid hormone levels are primarily T4, the pro-hormone form, which must be converted to T3 in the cell. The enzymes that are responsible for conversion of thyroid hormone to active and inactive forms, and vice versa, are encoded by the deiodinase (DIO) genes[234]. DIO1 is responsible for catalyzing both the activation and inactivation of thyroid hormone[236], DIO2 activates the conversion of T4 to T3[239-241], and DIO3 is responsible for inactivating both T3 and T4.

There are fiber type specific differences in the expression of the deiodinases. DIO1, while able to fulfill both the activation and the inactivation of thyroid hormones, has been considered relatively inefficient compared to DIO2 activation (activating the

conversion from T4 to T3) which has a 700-fold increase in efficiency[348]. Limited evidence also shows significant variations in the expression of the deiodinases with fiber composition and murine strain[349]. DIO2 expression has been documented in all hindlimb muscles of C57BL/6 mice[241]. DIO2 activity is significantly increased in slow-twitch compared to fast-twitch muscle[241] likely due to the fact that slow-twitch muscles are more responsive to thyroid hormones[26,27,242]. It also follows that DIO2 is upregulated in hypothyroidism and downregulated in hyperthyroidism[215]. It has also been shown that loss of DIO2 leads to an increase in body mass and a greater reliance on carbohydrates as an energy source[350]. DIO3 is not likely a major contributor as it has been noted to be lowly expressed across tissue types[232,234].

It is possible that the muscle-specific differences that we have noted could be due to differences not only in fiber type composition and distribution by muscle group, but also to the inherent variability in fiber type composition and distribution across strains, which is relatively little studied[351]. Nevertheless, the results we report here strongly suggest that the different metabolic phenotypes of the mouse strains we have studied are not directly linked to their levels of expression of mu-crystallin in their skeletal muscles.

Chapter 3 Metabolic Consequences of Skeletal Muscle Specific High Expression (SM-HE) of mu-Crystallin Following Low-and High-Fat Diet Interventions are Diet and Sex-Specific

Introduction

Obesity is an epidemic in the United States and is associated with increased risk for many conditions such as insulin resistance[5,79,149,163,328,332,352], type 2 diabetes mellitus[144,319,353-355], cardiovascular disease[139,207,275], infertility[157,309,356,357], and cancer[355,358,359]. The related healthcare costs are over $147 billion annually[131]. Although traditional treatments for obesity include changes in diet as well as increased physical activity, many individuals are unable to follow these treatments[360]. Pharmacotherapeutic targets to treat obesity, which has many genetic contributors, could significantly reduce health-related costs.

The current molecular targets for the treatment of obesity include hormone signaling[159,166,361-365], lipases[366,367], the melanocortin-4 receptor (MC4R) pathway[141,182,368]. These targets include leptin, ghrelin, glucagon-like pepetide-1 (GLP-1), glucose-dependent insulinotropic peptide (GIP), among others. This has led to the targeted therapeutics with the active ingredient semaglutide (found in Wegovy or Ozempic), tirzepatide (Zepbound), retatrutide (Mounjaroa, not currently FDA approved). As potent regulators of metabolism, thyroid hormones are an attractive candidate for reducing obesity. Increasing the levels of thyroid hormones can be dangerous for non-hypothyroid individuals, however, so an indirect target is needed.

The thyroid hormone binding protein, mu-crystallin, may play a role in controlling thyroid hormone levels and therefore affect metabolism. mu-Crystallin (CRYM) is a 34 kDa protein with ketimine reductase activity that readily forms homodimers and binds both T3 and T4 in an NADPH-dependent manner[303]. Mu-crystallin is expressed in the cerebral cortex, kidney, heart, and skeletal muscle, among other tissues[292]. Approximately 20 percent of the population expresses high levels of the protein mu-crystallin in skeletal muscle, while the rest of the population expresses little to none[292]. Skeletal muscle is a major target of thyroid hormone signaling. Skeletal muscle-specific high expression (SM-HE) of mu-crystallin in *Crym*-tg male mice increases T3 levels in muscle 192-fold and promotes a shift in metabolism from glycolytic to oxidative pathways[302]. Consistent with the metabolic changes, SM-HE muscle shows increased expression of genes and proteins involved in fatty acid oxidation and decreased expression of gene products involved in glycolytic metabolism, as well as some members of the insulin signaling pathway[302]. These changes occur in the absence of any overt alteration in skeletal muscle structure and function.

Here we focus on the consequences of SM-HE of mu-crystallin in mice exposed to low- and high-fat diets (LFD, HFD). We hypothesized that SM-HE of mu-crystallin would promote oxidative metabolism in mice on HFD preferentially. We found otherwise: our results show that SM-HE of Crym in mice on HFD or LFD does not alter glycolytic or oxidative metabolism, but instead reduces lean muscle mass in *Crym*-tg males on LFD and in females on HFD. This suggests that high levels of *Crym* promote

protein catabolism in mice in a diet- and sex-dependent manner. Mu-crystallin's ability to reduce lean mass is consistent with its activity as a ketimine reductase in the lysine[128,293] degradation pathway.

Materials and Methods

Mice

C57BL/6 male and female mice transgenic for the SM-HE of *Crym* in skeletal muscle, described in Kinney[302], were bred at the University of Maryland, Baltimore. Mice were periodically rederived from back crosses with C57BL/6 from the colony at the University of Maryland, Baltimore. Genotyping used the following primers:

forward: TGGCCACGCGTCGACTAGTACG;
reverse: AATTCGTACTAGTCGACGCGTGGCC

All procedures were approved by the Institutional Animal Care and Use Committee, University of Maryland School of Medicine.

Diet Interventions

Four to 6-week-old homozygotic male and female *Crym*-tg and C57BL/6 littermate controls were placed on either high-fat diet (HFD; 60% kcal derived from fat; Cat. No. D12492) or sucrose-matched low-fat diet (LFD; 10% kcal derived from fat; Cat. No. D12450J) from Research Diets Inc. (New Brunswick, NJ) for 16 weeks. Weights were recorded weekly, and water was provided *ad libitum*. Glucose and insulin tolerance

tests (GTT and ITT) were performed prior to and following testing in indirect calorimetry cages. After 16 weeks, mice were anesthetized with isoflurane then euthanized via cervical dislocation, tissues were collected, snap-frozen in liquid nitrogen and kept at -80° until analysis.

Body Composition Analysis

Body composition for total fat mass, lean mass, and water content was determined in a quantitative magnetic resonance instrument (Echo-MRI-100; Echo Medical Systems, Waco, TX) at the Mouse Phenotyping Core, Johns Hopkins University School of Medicine.

Indirect Calorimetry

Indirect calorimetry and tolerance tests were conducted at the Center for Metabolism and Obesity Research, Johns Hopkins University School of Medicine. LFD-fed or HFD-fed WT and *Crym*-tg male and female mice were assessed daily for body weight, food intake, physical activity, and whole-body metabolic profile in an open-flow indirect calorimeter (Comprehensive Laboratory Animal Monitoring System, CLAMS; Columbus Instruments, Columbus, OH). Initially, mice had *ad libitum* access to food and water for 3 days to allow them to acclimate to the calorimetry chambers, as monitored by stable body weights, food intakes, and diurnal metabolic patterns. Data were collected on day 4 under *ad libitum* feeding conditions for analysis. Mice were then monitored during a subsequent 24-hour period of food deprivation, followed by a similar period of refeeding. Next, running wheels were inserted into the chambers and mice were

monitored for an additional 7 days, with data again collected on day 4. Rates of oxygen consumption (V_{O_2}; $mL \cdot kg^{-1} \cdot h^{-1}$) and carbon dioxide production ($\dot{V}_{CO_2}$; $mL \cdot kg^{-1} \cdot h^{-1}$) in each chamber were measured every 24 min. Respiratory exchange ratio ($RER = \dot{V}_{CO_2}/\dot{V}_{O_2}$) was calculated by CLAMS software (version 5.16) to determine the use of carbohydrates (RER = 1.0) versus fats (RER = 0.7) as energy sources (without accounting for protein oxidation as a possible alternative). Energy expenditure (EE) was calculated as $EE = \dot{V}_{O_2} \times [3.815 + (1.232 \times RER)]$. General and ambulatory physical activities were measured from breaks in infrared beams in the metabolic chamber, and wheel rotations during voluntary exercise were counted. Average metabolic values, summed food intakes, and physical activities were calculated per mouse and averaged across all mice for statistical analysis by Student's *t*-test.

Glucose and Insulin Tolerance Testing

For glucose tolerance tests (GTT) prior to and after the indirect calorimetry experiments, mice were fasted overnight (16 hours) before glucose injection. Glucose (Sigma, St. Louis, MO) was reconstituted in sterile saline (0.9 g NaCl/L) and injected intraperitoneally (IP) at 1 mg/g body weight. Blood glucose was measured with a glucomoter (NovaMax Plus, Billerica, MA) at 0, 15, 30, 60, and 120 min after injection.

For insulin tolerance tests (ITT) prior to and after the CLAMS experiments, food was removed 2 hours before insulin injection. Insulin was diluted in sterile saline and injected at 1.0 U/kg body weight IP. Blood glucose was measured at 0, 15, 30, 60, and 90 min after insulin injection using the glucometer.

Protein Extraction

Tissues of interest were collected following the CLAMS studies and terminal GTT and ITT assays, snap-frozen in liquid nitrogen and stored at -80º C. Protein was extracted in RIPA Buffer (R0278-50 ML, Sigma-Aldrich), prepared with cOmplete Mini, EDTA-free protease inhibitor tablets (11836170001, Sigma-Aldrich; 10 mL of RIPA buffer to every protease inhibitor tablet). Tissue was weighed and 100 µL per 10 mg of tissue of RIPA/protease inhibitor solution was added along with two 5 mm steel beads (69989; Qiagen, Hilden, Germany). Samples were placed in a TissueLyser LT (Qiagen) at 50 oscillations/sec for 3 min, briefly vortexed, placed on ice for 2 min, followed by a second round of 50 oscillations/sec for 3 min. Samples were sonicated for 10 sec and subjected to centrifugation at 14,000 x g for 30 min at 4ºC. The supernatant was transferred to a new microfuge tube and protein concentration was determined with Protein Assay Dye Reagent Concentrate (Bradford Assay; 5000006, Bio-Rad).

RNA Extraction and cDNA Synthesis

RNA was extracted as follows. Tissue was placed in a 2 ml tube with 1 mL of TRIzol Reagent (Thermo Fisher Scientific) and processed once with the TissueLyser as above. Samples were checked for complete homogenization and, if incompletely homogenized, processed again in 30 sec cycles with checks for complete homogenization after each cycle. Samples were vortexed briefly, inverted to mix at room temperature for 5 min, and subjected to centrifugation at 12,000 x g for 10 min at 4ºC. Supernatant was removed into a new 1.5 mL RNase-free tube and 200 µL of chloroform was added. The

sample was vortexed for 15 sec, then left at room temperature for 3 min. After a second centrifugation at 12,000 x g for 15 min at 4°C, the top (clear) layer was removed into a new 1.5 mL RNase-free tube and 500 µL of ice-cold isopropanol was added. Tubes were vortexed and inverted several times and then left at room temperature for 10 min. Centrifugation at 12,000 g for 10 min at 4°C generated a white pellet of RNA, which was washed with 1 mL of ice-cold 75% ethanol and collected again by centrifugation (10,000 x g for 5 min at 4°C). After drying at room temperature, the pellet was dissolved in 35 µL of RNase-, DNase-free water at 60°C for 10 min RNA samples were stored at -80°C until use.

qRT-PCR

Total RNA isolated with TRIzol was incubated with QuantiTect Reverse Transcription Kit (205313; Qiagen) to generate cDNA. qRT-PCR was performed on a CFX Connect thermal cycler (Bio-Rad) using the cDNA and PrimeTime Gene Expression Master Mix (1055772; IDT, Coralville, IA) in 20 uL reaction volumes following the manufacturer's protocol for the PrimeTime qPCR Probe Assay. Data were normalized to our previously identified housekeeping gene *Nom1*[302] and expressed as relative mRNA levels using the delta delta Ct method. Primers used are as follows;

Crym:

Forward: 5'-GAGATGTTCGGGTCTGTTCAT-3'.

Reverse: 5'-GGCTTTACCCATTCACCAAATAA-3'.

Probe: 5'-/FAM/TCATCACAG/ZEN/TCACCATGGCAACAGA/3IABkF Q/-3'.

Nom1:

Forward: 5’--TAAACCCAGAGTTCACTTCCTAC-3'.

Reverse: 5’-CCTTCTCGCAACATTCCCA-3'.

Probe: 5'-5HEX/TCGTCTTCA/ZEN/GTTTCCATCAACAGTGCA/3IABkFQ/3'.

Custom PrimePCR Assay

Using BioRad’s customization tool, PrimePCR, we designed a 96-well plate array to assay 14 genes of interest with validated SYBR green primers. Genes included *Ube2d1, Mib1, Psme4, Deptor, Esr1, Ckmt2, Irs2, Stat5b, Calm3, Pi3kr1, Ppara, Nfkbia, Ppargc1a, Eif4ebp1,* with *Nom1* as the control and *Crym* as an interplate control. Genes of interest were selected after matching previously identified genes of interest (GOIs) within RNA-seq data for *Crym*-tg mice on normal chow[302] to GOIs used on other commercially available metabolic arrays (See Appendix A Figure A.11 for full list and assay IDs).

Automated Capillary Immunoassay (Abby)

Analysis was performed with Protein Simple’s Simple Western system, Abby, according to the manufacturer’s instructions for the 12-230 kDa protein separation module (#SM-W004; Protein Simple a Bio-Techne Brand, Minneapolis, MN). Protein extracted from whole tissue lysates were prepared with 10x Sample Buffer (#042-195; ProteinSimple) to generate an overall sample protein concentration of 1.0 mg/ml for each sample generated. The primary antibody for µ-crystallin (SC-376687; Santa Cruz Bio) was diluted 1:25 in Protein Simple’s Antibody Diluent 2. Compass software (Compass

for SW 4.0 Mac Beta; Protein Simple) was used to visualize electropherograms, followed by analysis of each peak of interest to calculate the area under the curve (AUC). The peak signal-to-noise ratio was set at ≥ 10 automatically by the software. Due to slight capillary-to-capillary variations in the readout of molecular mass, peaks identified close to the calculated mobility were allowed a 10% range in variance (as automatically set by the Abby system). AUC was analyzed with two-way ANOVA, fitted with a main effects only model, comparing each group to C57BL/6J, using a Fisher's LSD test, with significance set at $p<0.05$. (*As noted in the introduction, this method of normalizing protein with total protein normalization is the current best practice quantitation method.*)

Considerations

Most of this work is conducted in our laboratory's Crym transgenic model of skeletal-muscle specific high-expression of mu-crystallin. It is important to note that while we utilize littermate controls ideally larger sample sizes than what we have used would help reduce variance, however due to cost and time constraints we had to limit our cohort numbers.

Results

Crym-tg mice that highly express mu-crystallin specifically in skeletal muscle (SM-HE) have been previously described[302]. Data published on male *Crym*-tg mice fed regular chow demonstrate a small but significant shift (13.7%) from glycolytic towards oxidative metabolism as determined by respiratory exchange ratio[302]. Further evidence of

this shift is a change in profile of transcriptomic and proteomic data consistent with a shift from fast to slow contractile and glycolytic to oxidative genes[302].

Here we examine the impact of low- or high-fat diets (LFD and HFD, respectively) on the metabolism, body composition and gene expression in both male and female *Crym*-tg mice, as well as sex-specific differences related to these diets, before and after voluntary running. Experimental design and timeline can be seen in Figure 3.1.

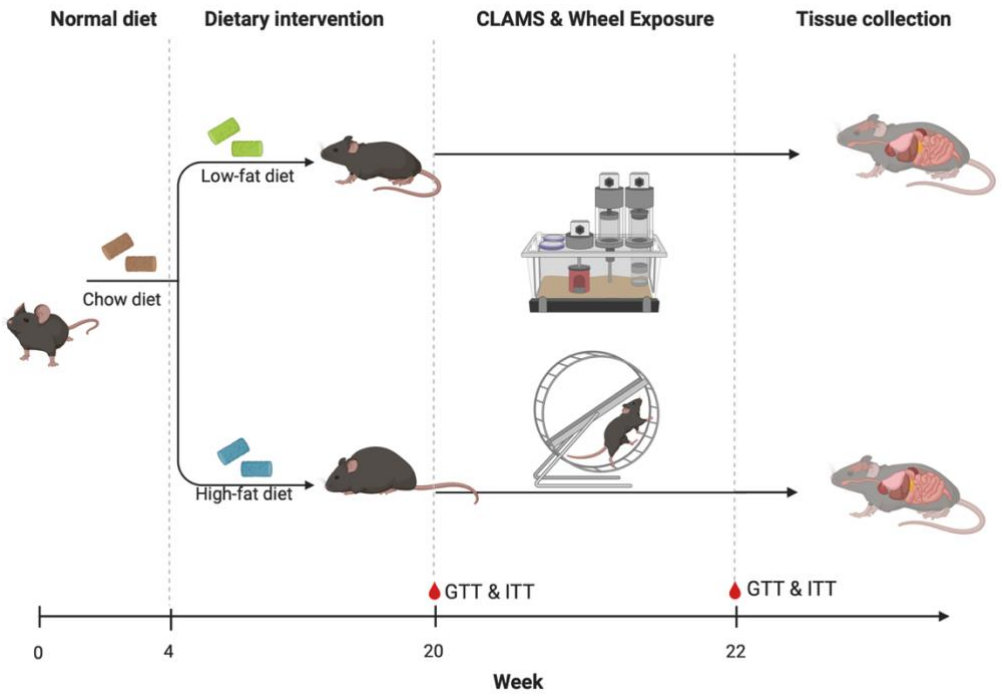

Figure 3.1. *Experimental Design for Diet Intervention Studies of Male and Female Crym-tg and Littermate Control Mice.*
Experimental design includes two separate cohorts undergo dietary intervention, of either low- or high-fat diet for a sixteen-week period. Indirect calorimetry in CLAMS cages, and glucose and insulin tolerance tests were then administered for baseline metabolic measures, followed by voluntary wheel exposure and repeated CLAMS data collection. Post-metabolic data collection, mice were euthanized, and tissue collected for further evaluation.

Low-Fat Diet

We evaluated the effect of LFD intervention on SM-HE *Crym*-tg mice for changes in body mass and overall body composition, from 4 to 16 weeks of age. Male *Crym*-tg mice on the LFD weighed approximately 3 grams less than WT controls at the 16-week time point ($p < 0.05$) (See Figure 3.2A). Quantitative nuclear magnetic resonance (Q-NMR) analysis of this group indicated that this was due to a significant decrease in lean muscle mass, with no changes in fat (Figure 3.2B-C) mass. Female *Crym*-tg mice on the LFD showed no significant differences in body mass or body composition (Figure 3.2D-F).

We subjected *Crym*-tg and WT mice on the LFD to glucose and insulin tolerance tests (GTT and ITT). We found no significant differences in female *Crym*-tg mice compared to WT (Figure 3.2I-J). However, while *Crym*-tg males demonstrated no significant changes in glucose tolerance, they showed a small decrease in insulin sensitivity compared to WT littermates (Figure 3.2G-H). This suggests that uptake of glucose into skeletal muscle in the male *Crym*-tg mice is slightly impaired.

Figure 3.2. *Body Composition, GTT, and ITT Data of Male and Female Mice Following Low-Fat Diet Intervention.*
Following LFD, *Crym*-tg mice show sex specific differences in body mass and body composition, as well as insulin tolerance. Body weights and composition of *Crym*-tg and wildtype (WT) male and female mice fed a low-fat diet (LFD). A. Body weights of male *Crym*-tg and WT fed LFD starting at 4 weeks of age $p < 0.05$. B-C. Body composition of male *Crym*-tg and WT male mice fed LFD for 16 weeks. $p < 0.05$. D. Body weights of female *Crym*-tg and WT mice fed LFD starting at 4 weeks of age. E-F. Body composition analysis of female *Crym*-tg and WT male mice fed LFD for 16 weeks. G-K. Blood glucose levels in response to glucose or insulin tolerance testing in male and female

Crym-tg and WT mice. N = 6 for all groups. Data for *Crym*-tg are in red and WT in blue. Students t-test with a $p < 0.05$.

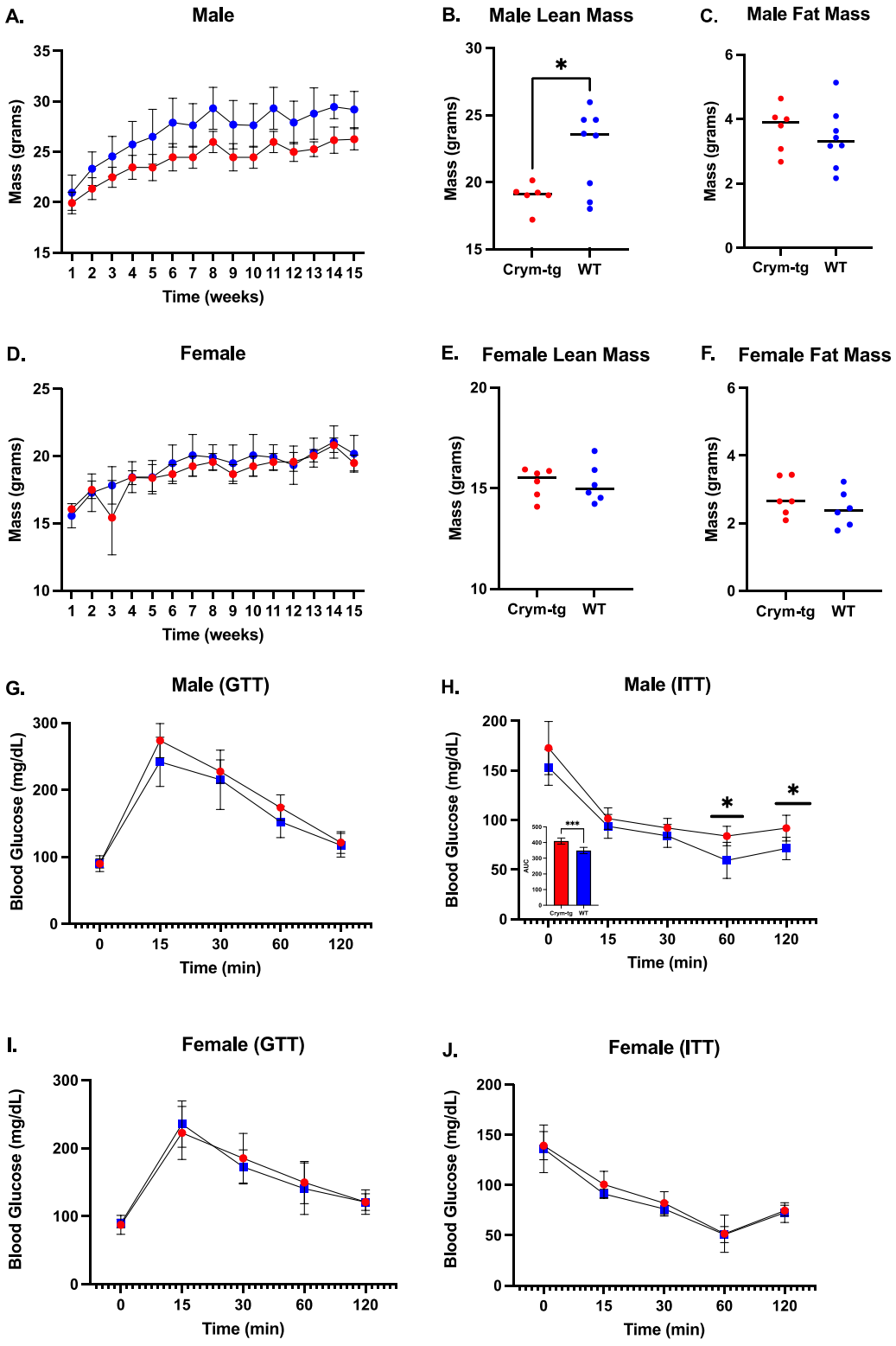

We then studied the *Crym*-tg mice and their WT littermates in Comprehensive Laboratory Animal Metabolic System (CLAMS) indirect calorimetry cages. We acclimated mice to cages for a period of three days with *ad libitum* feeding and then on day four measured the following metabolic parameters: food intake, physical activity (total and ambulatory), respiratory exchange ratio (RER), and energy expenditure (EE). On day four, we subjected the mice to a 24-hour food deprivation and, following refeeding, repeated our CLAMS studies. Lastly, the mice were acclimated to a running wheel for seven days, when the final CLAMS studies and GTT and ITT were conducted. A summary of our results for the low-fat CLAMS data is in Appendix A Table A.1.

Our first measurements only showed significant differences via decreased respiratory exchange ratio (RER) of male *Crym*-tg male during the light cycle (Figure 3.3A). This suggests that male *Crym*-tg mice on LFD during the light cycle show more basal fat oxidation than WT mice. This shift in RER does not appear to account for the significant difference in overall lean body mass in these mice. Both male and female *Crym*-tg mice showed no significant differences in food intake, energy expenditure (EE) or activity throughout the initial 24-hour period in which measurements were done (See Figure 2B-J).

Figure 3.3. *CLAMS Indirect Calorimetry Data Following Low-Fat Diet Intervention.* CLAMS data shows minimal changes in male *Crym*-tg mice and not females following LFD. CLAMS indirect calorimetry data for male and female *Crym*-tg and WT mice on LFD for 16 weeks. Changes in male *Crym*-tg and WT (A) respiratory exchange ratio, (B) energy expenditure, (C) total activity, (D) ambulatory activity, (E) caloric intake over 24-hour *ad libitum* cycle. $p < 0.05$ There are no distinct changes in female *Crym*-tg and WT (F) respiratory exchange ratio, (G) energy expenditure, (H) total activity, (I) ambulatory

activity, (J) caloric intake over 24-hour *ad libitum* cycle. N = 6 for all groups. Data for *Crym*-tg are in red and for WT in blue.

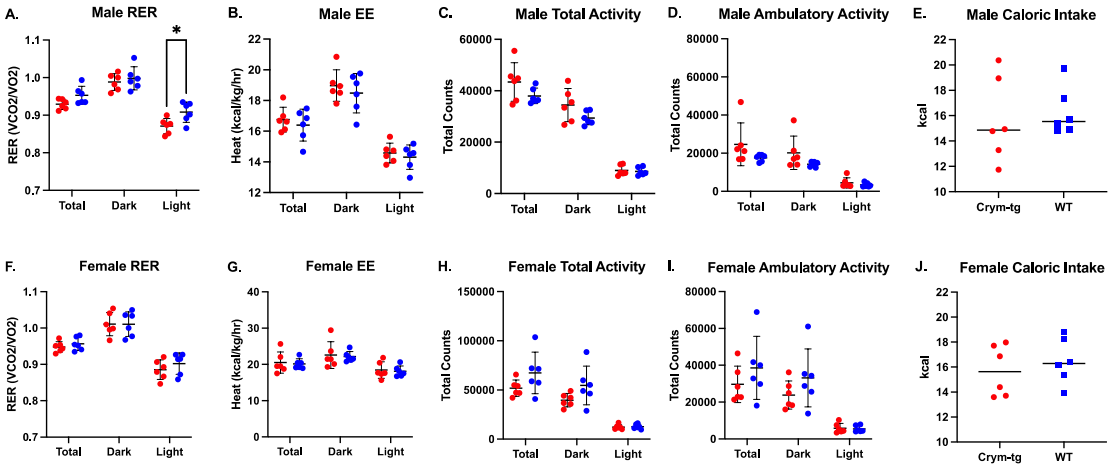

We repeated our CLAMS measurements during the fasting and refeeding period. We found minimal changes in metabolic parameters of the male mice with no significant changes in any parameters measured of the female cohort (Appendix A Figures A.1 and A.2). These data suggest that LFD diet leads to change in overall body mass and body composition in male *Crym*-tg mice compared to their littermate controls, but that these changes do not correlate with specific metabolic parameters as measured via CLAMS cages. Of note, these changes were not seen in females, suggesting that high levels of mu-crystallin in skeletal muscle has differing effects in males versus females.

In the final experimental period, we determined if voluntary wheel running would affect the changes we reported above. In this case, mice were acclimated to voluntary running wheels within the CLAMS cages for 7 days after the fasting/refeeding period and then tested over a 24-hour period. Male *Crym*-tg mice on the LFD showed a significant decrease in RER during the light cycle that did not translate to an overall shift in RER

over the 24-hour period (Figure 3.4A). Males showed no significant changes in total, ambulatory or wheel activity (Figure 3.4G-I). Of the six *Crym*-tg and six WT mice in the experiment, however, three transgenics and two WT mice did not utilize the running wheel at all. It is not clear what was driving this behavior. Figure 3.4J shows traces of wheel activity for those mice that utilized the wheel throughout the experiment.

Figure 3.4. CLAMS Data for Mice on Low-Fat Diet Following Voluntary Wheel Running. Following voluntary wheel exposure *Crym*-tg mice show minimal changes in metabolic parameters with a distinct pattern of decreased running wheel activity. Following voluntary wheel acclimation male *Crym*-tg and WT mice showed little differences in (A) respiratory exchange ratio, (B) energy expenditure, (C) caloric intake, (G) total activity, (H) ambulatory activity and (I) wheel activity. Of note male *Crym*-tg and WT mice voluntary wheel activity was minimal (see text). Female *Crym*-tg and WT mice show no alterations in (D) RER, (E) EE, (F) caloric intake, (K) total activity, or (L) ambulatory activity. (M) Female *Crym*-tg compared to WT trended to show decreased running wheel activity. (N) Wheel activity traces for *Crym*-tg and WT female mice suggest that *Crym*-tg mice tend to run less than WT ($p < 0.09$). (O-P) Male *Crym*-tg and WT mice show no differences in GTT or ITT following wheel exposure. (Q-S). Post-wheel exposure GTT showed minimal changes in which *Crym*-tg mice had lower blood glucose levels at one time point. The significant difference seen in R-S could likely be due to differences in basal blood glucose levels during the ITT. * $p< 0.05$ and ** $p < 0.01$

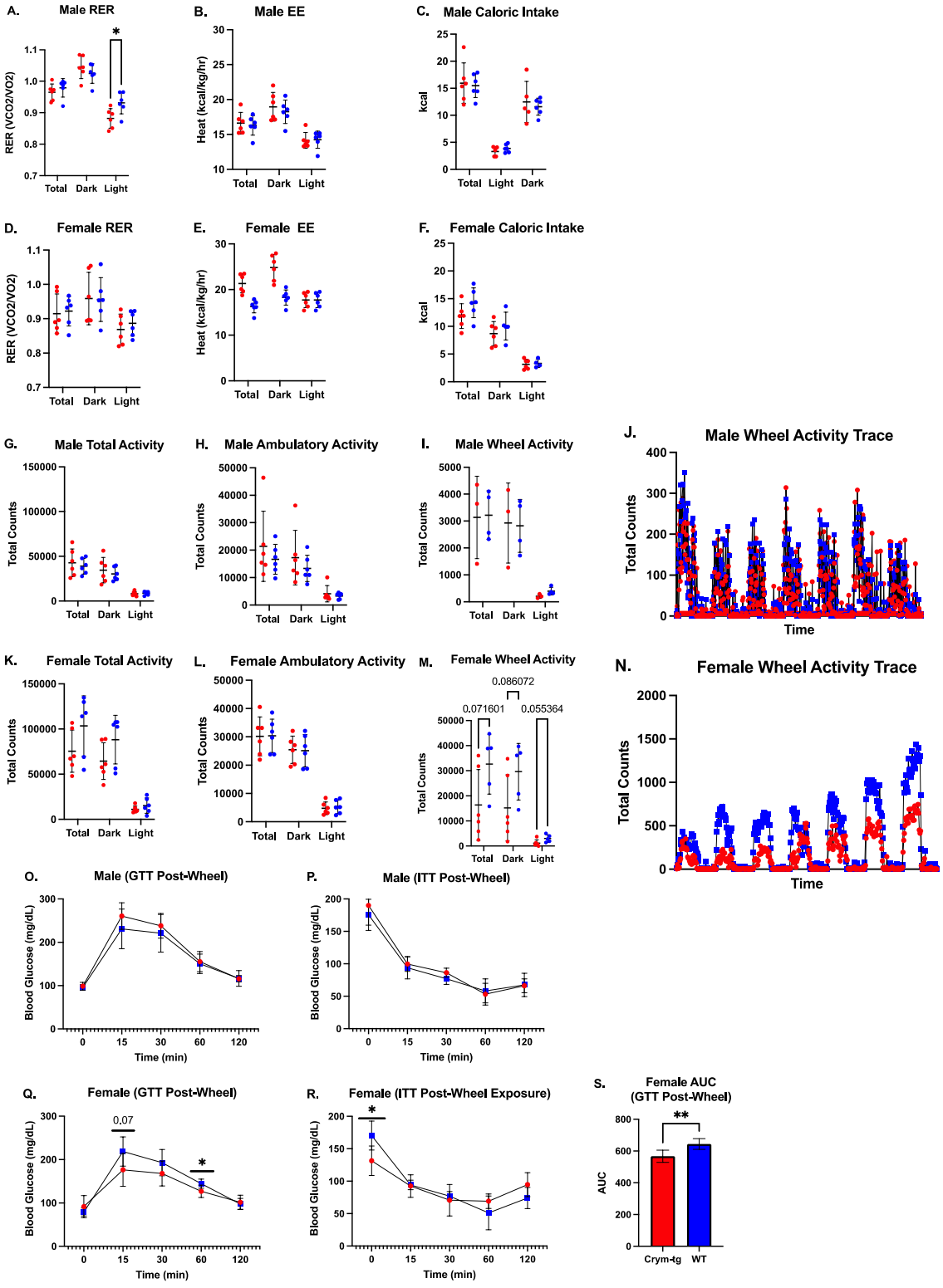
A.
Male RER
RER (VCO2/VO2)
Total Dark Light
B.
Male EE
Heat (kcal/kg/hr)
C.
Male Caloric Intake
kcal
Total Light Dark
D.
Female RER
E.
Female EE
F.
Female Caloric Intake
G.
Male Total Activity
Total Counts
H.
Male Ambulatory Activity
I.
Male Wheel Activity
J.
Male Wheel Activity Trace
Time
K.
Female Total Activity
L.
Female Ambulatory Activity
M.
Female Wheel Activity
0.086072
0.071601
0.055364
N.
Female Wheel Activity Trace
O.
Male (GTT Post-Wheel)
Blood Glucose (mg/dL)
Time (min)
P.
Male (ITT Post-Wheel)
Q.
Female (GTT Post-Wheel)
0.07
R.
Female (ITT Post-Wheel Exposure)
S.
Female AUC
(GTT Post-Wheel)
AUC
Crym-tg WT

LFD female *Crym*-tg mice exposed to the wheels showed no significant changes in RER, EE, or caloric intake (Figure 3.4D-F), although their running activity significantly decreased in the light cycle. While total and ambulatory activity showed no significant differences, female *Crym*-tg mice showed a significant decrease in running activity in the light cycle (Figure 3.4K-N, $p<0.05$). Consistent with this, these mice trended to running less in the dark and over the full 24-hour period, although the differences did not reach significance ($p = 0.086$ and $p = 0.072$ respectively, Figure 3.4M). Overall wheel running by the female mice during this period tended to show a distinct pattern (Figure 3.4N), but this too did not reach statistical significance, perhaps due to our small sample size.

Crym-tg male mice showed no significant differences compared to WT during the fasting period (Appendix A, Figure 1A-E). During the refeeding period, *Crym*-tg male mice showed a decrease in RER throughout the light cycle and the full 24-hour period (Appendix A, Figure 1F), as well as a decrease in caloric intake through the light cycle (Appendix A, Figure 1E). They showed no significant differences in EE, or total or ambulatory activity (Appendix A, Figure 1B-D).

Upon the fasting/refeeding period for female *Crym*-tg mice on LFD only showed a significant difference in EE, which decreased during the dark cycle compared to WT (Appendix A, Figure A.2B). This change in EE was independent of changes in RER or activity (Appendix A, Figure 2A-J).

After wheel running, we again subjected the mice to glucose or insulin tolerance tests (Figure 3.2G-J). The male mice showed no significant differences in either GTT or ITT, unlike pre-wheel exposure, when male *Crym*-tg mice had significantly decreased insulin sensitivity compared to WT. This suggests that exercise may have improved the insulin intolerance of the male *Crym*-tg mice. Interestingly, female mice that previously did not display a difference in GTT or ITT showed increased sensitivity to glucose, especially at later timepoints, with no change in insulin sensitivity (Figure 3.4Q-S). This suggests that glucose regulation might be compromised after exercise in females with high intramuscular levels of *Crym* fed LFD.

To complete the experiment, we euthanized the mice and collected tissue for further analysis. We first evaluated fiber cross-sectional area (CSA) both by genotype and by sex. Comparing *Crym*-tg and WT males we found a left shift in fiber CSA both in relative distribution and cumulative frequency distribution, and a right shift in female *Crym*-tg mice when compared to WT controls (Figure 3.5). A left shift is indicative of an increase in the number of fibers with a decreased CSA, which can result from a variety of factors, such as atrophy or changes in muscle composition. Comparison of male and female *Crym*-tg mice shows a minimal difference in the cumulative frequency distribution, in which females are slightly right shifted, indicating larger CSA. However, when comparing WT males and females, female WT have a pronounced left shift, or smaller CSA of fibers, when compared to males. Often a left shift, or smaller CSA can be a result of disuse, again or disease state that indicate muscle weakness or impaired

function. WT females on HFD have a pronounced left shift in fiber CSA when compared to males (Figure 3.6).

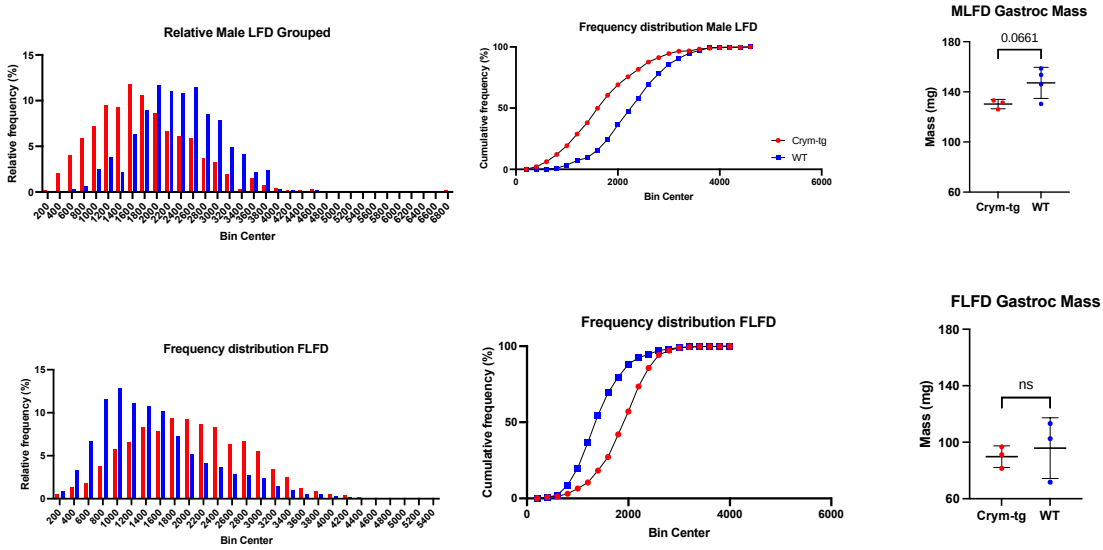

Figure 3.5. *Relative and Cumulative Fiber CSA Distribution Following Low-Fat Diet Interventions of Crym-tg mice compared to wildtype littermate controls.*
Both male and females show a distinct shift in relative frequency and cumulative distribution of cross-sectional area of fibers found within the *gastrocnemius*. The change in CSA is independent of change of mass in both males and females, although male *gastrocnemius* mass trends towards significance (p=0.0561).

Figure 3.6. *Relative and Cumulative Fiber CSA Distribution Following Low-Fat Diet Interventions by Sex.*
Both *Crym*-tg and WT mice show sex-specific shifts in relative and cumulative fiber CSA following low-fat diet intervention. The distinct shift in relative frequency and cumulative distribution of cross-sectional area of fibers are found within the *gastrocnemius*.

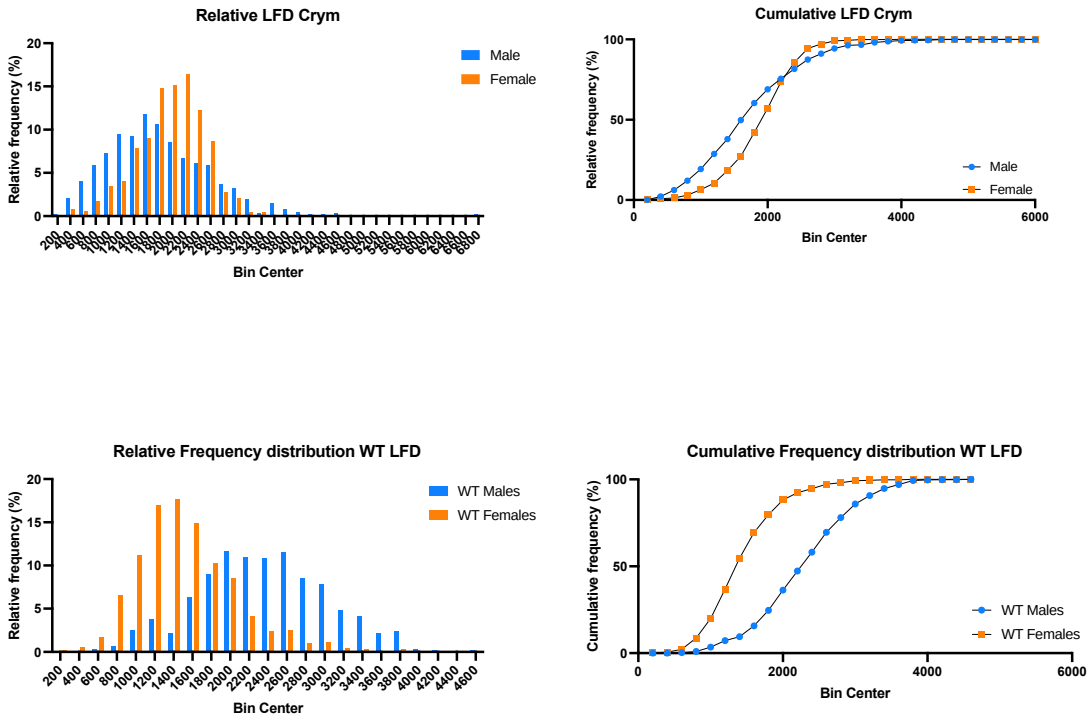

We studied a subset of mRNAs that were differentially expressed in our original RNA-seq performed in *Crym*-tg male mice on standard chow[302]. As we were uncertain of the likely mechanism that caused male *Crym*-tg mice to have lower lean mass, we selected following DEGs from various pathways. These include translational repressor *Eif4ebp1,* the negative regulator of TOR *Deptor*, ubiquitin associated *Mib1* and *Ube2d1,* proteasomal activator *Psme4*, peroxisomal *Ppara* and *Ppargc1a*, calcium binding *Calm3*, estrogen receptor *Esr1,* insulin receptor substrate *Irs2,* transcription factor *Stat5b*, PI3K regulator *Pi3kr1*, NFKB inhibitor *Nfkbia,* and mitochondrial creatine kinase *Ckmt2.* None of these showed a significant change in LFD male *Crym*-tg mice, and only *Ckmt2* showed a statistically significant decrease in female *Crym*-tg mice (Figure 3.7).

As we did not see a significant shift towards either glycolytic or oxidative metabolism in *Crym*-tg mice when compared to littermate controls via indirect calorimetry, we shifted our evaluation to mu-crystallin's other known function as a ketimine reductase. STRING analysis of the RNAseq data show several genes related to lysine metabolism that are differentially expressed[302]. Decreased levels of lysine impacts branched-chain amino acid (BCAA) catabolism[294,295]. We found that mRNAs encoding *Pcca, Dbt* and *Bcat2* mRNA significantly decreased in LFD male *Crym*-tg mice compared to littermate controls ($p<0.05$). All three genes are linked to BCAA catabolism. We did not see a change in expression of three other genes analyzed from this pathway, *Bckdhb*, *Mgea5,* or *Mut* (Figure 3.8).

Figure 3.7. Relative Expression of GOIs Following LFD in *tibialis anterior* lysates. qRT-PCR array of selected metabolic genes identified previously in RNA-seq datasets for *Crym*-tg mice on regular chow using *tibialis anterior* lysates. N = 6 for all groups. Data for *Crym*-tg are in red and for WT in blue. ($p < 0.05$).

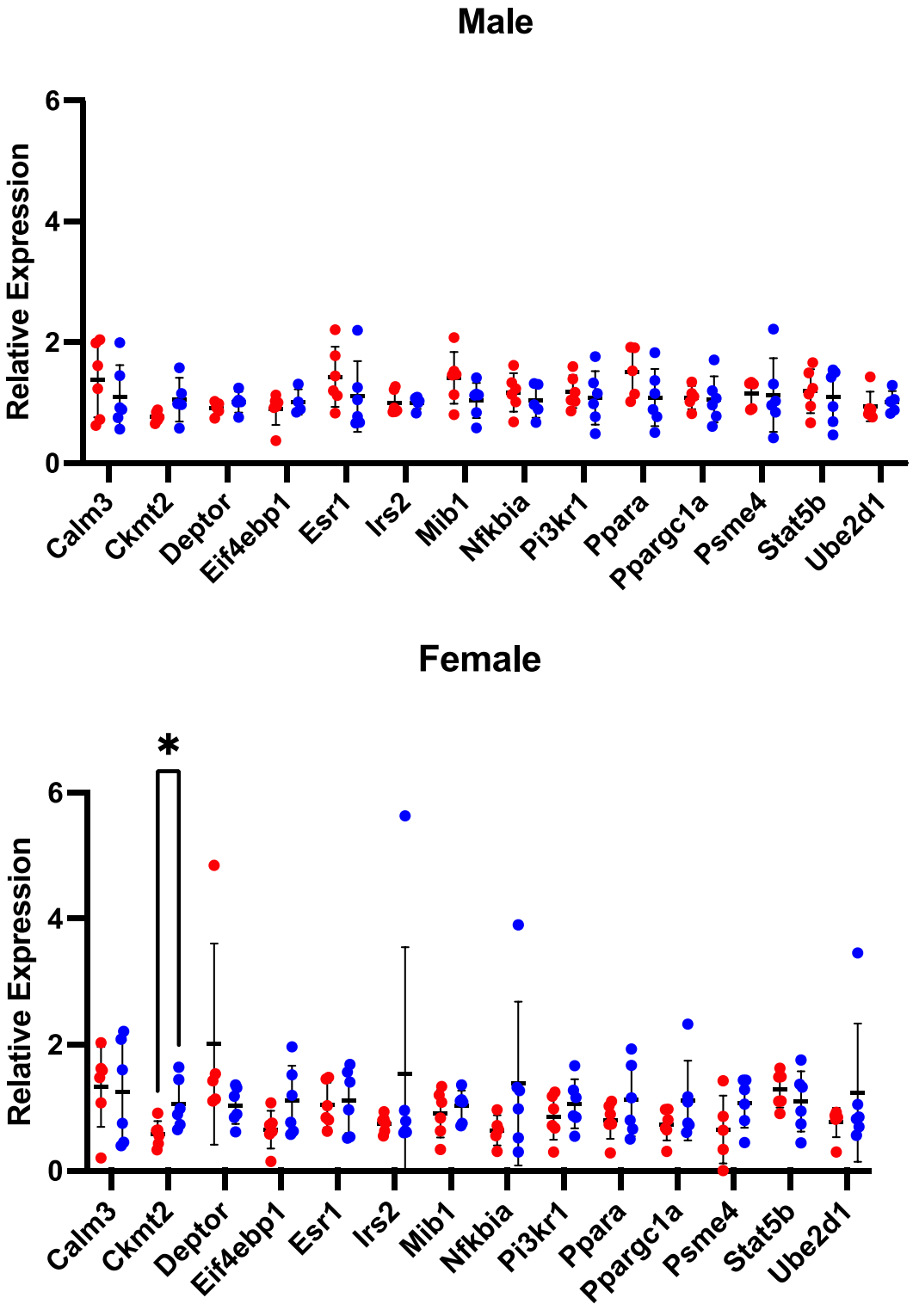
Male
Relative Expression
0
2
4
6
Calm3
Ckmt2
Deptor
Eif4ebp1
Esr1
Irs2
Mib1
Nfkbia
Pi3kr1
Ppara
Ppargc1a
Psme4
Stat5b
Ube2d1
Female
*
Relative Expression
0
2
4
6
Calm3
Ckmt2
Deptor
Eif4ebp1
Esr1
Irs2
Mib1
Nfkbia
Pi3kr1
Ppara
Ppargc1a
Psme4
Stat5b
Ube2d1

qRT-PCR analysis and capillary-based immunoassay in LFD males showed no significant differences in *Ckmt2* protein expression (Appendix A Figure A.4.). Further capillary-based immunoassays showed no significant changes in *Dbt* protein levels of LFD males (Appendix A Figure A.3).

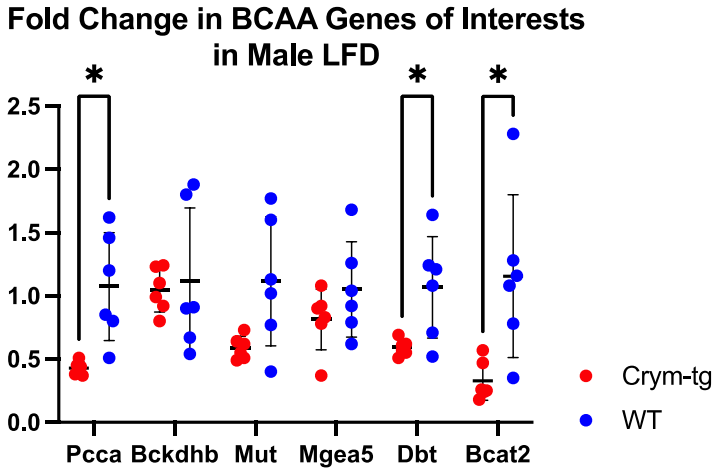

Figure 3.8. *Relative Expression of BCAA GOIs in Male Mice Following LFD in gastrocnemius lysates.*
qRT-PCR array of selected branched-chain amino acid (BCAA) catabolism genes using *tibialis anterior* lysates. N = 6 for all groups. Data for *Crym*-tg are in red and for WT in blue. ($p < 0.05$).

High-Fat Diet

We also studied the effects of a HFD on *Crym*-tg and WT mice. Between 4 and 16 weeks of age, male *Crym*-tg mice did not show a measurable change in overall mass or body composition compared to their WT littermates (Figure 3.9A-C). In contrast, the mass of *Crym*-tg females on HFD were approximately 5 g lighter than WT controls (p value = 0.0179, Figure 3.9D). QNMR analysis of the female mice showed a significant decrease in the females' lean mass but not fat mass (Figure 3.9D-F), mirroring the

differences in body composition seen in males on LFD (Figure 3.2A). Unlike our results with the LFD, however, GTT and ITT showed no differences between male and female *Crym-tg* mice and their WT littermates in either assay.

Figure 3.9. *Body Composition, GTT and ITT Data of Male and Female Mice Following High-Fat Diet Intervention.*
Body weights and composition of Crym-tg and WT male and female mice fed a high-fat diet (HFD) A. Body weights of male Crym-tg and WT fed HFD starting at 4-6 weeks of age. B-C. Body composition analysis of male Crym-tg and WT male mice fed HFD for 16 weeks. D. Body weights of female Crym-tg and WT fed HFD starting at 4-6 weeks of age. E-F. Body composition analysis of female Crym-tg and WT male mice fed HFD for 16 weeks. G-K. Blood glucose levels in response to glucose or insulin tolerance testing in male and female Crym-tg and WT mice. (Male Crym-tg, n = 8 and WT n = 5), (Female Crym-tg n = 6, WT n = 5). ($p < 0.05$) Crym-tg are labeled in red and WT in blue.

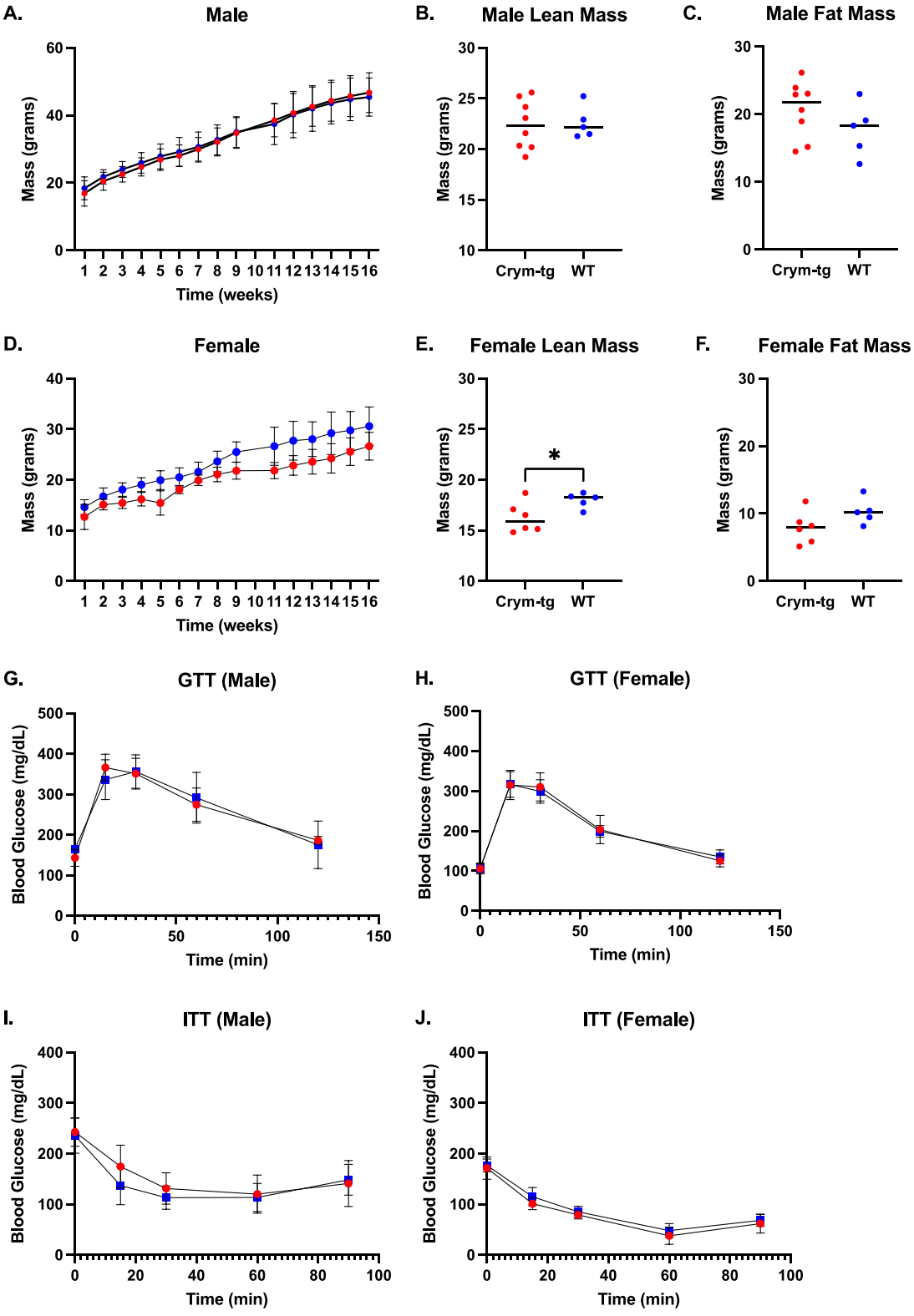
A.
Male
Mass (grams)
Time (weeks)
B.
Male Lean Mass
Mass (grams)
Crym-tg
WT
C.
Male Fat Mass
Mass (grams)
Crym-tg
WT
D.
Female
Mass (grams)
Time (weeks)
E.
Female Lean Mass
*
Mass (grams)
Crym-tg
WT
F.
Female Fat Mass
Mass (grams)
Crym-tg
WT
G.
GTT (Male)
Blood Glucose (mg/dL)
Time (min)
H.
GTT (Female)
Blood Glucose (mg/dL)
Time (min)
I.
ITT (Male)
Blood Glucose (mg/dL)
Time (min)
J.
ITT (Female)
Blood Glucose (mg/dL)
Time (min)

Subsequent studies of these mice in CLAMS cages showed a significant decrease in RER and EE in male *Crym*-tg mice, consistent with a shift towards oxidative metabolism similar to our previous results with male *Crym*-tg mice on normal chow[302]. Caloric intake was also significantly decreased (Figure 3.10E). These changes did not correlate with changes in total or ambulatory activity (Figure 3.10A-D) or the lack of change in body composition. A summary of the complete results for the HFD CLAMS data is in Appendix A Table A.2.

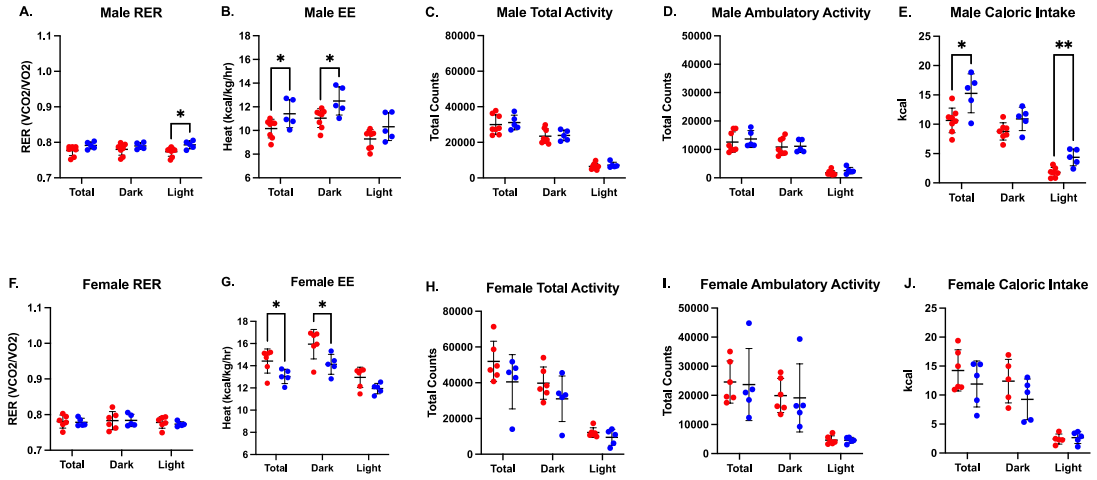

Figure 3.10. *CLAMS Indirect Calorimetry Data Following High-Fat Diet Intervention.* Following *ad libitum* feeding on HFD, male *Crym*-tg and WT mice show changes in (A) RER, (B) EE, and (E) caloric intake but not (C) total activity, or (D) ambulatory activity. Female *Crym*-tg mice on an *ad libitum* HFD show (G) a significantly increased EE compared to WT mice. There are no differences seen in (F) RER, (H) total activity, (I) ambulatory activity, and (J) caloric intake. ($p < 0.05$) *Crym*-tg are labeled in red and WT in blue.

Unlike the males, female *Crym*-tg mice demonstrated a significant increase in EE without changes in RER, total or ambulatory activity, or caloric intake (Figure 3.10F-J). The increase in EE does not appear to be sufficient to account for the change in mass of the female *Crym*-tg compared to WT.

The only significant change we found in metabolism upon fasting and refeeding of mice on a HFD was a decrease in caloric intake in male *Crym*-tg mice with refeeding during the light cycle (Appendix A Figure A.5). Congruent with results during *ad libitum* feeding, female *Crym*-tg mice increased in EE, in this case solely during the fasting dark cycle (Appendix A Figure A.6). We found no other significant differences (Appendix A Figure A.6). These data suggest that a HFD leads to changes in body mass and composition in female *Crym*-tg mice that do not correlate with any of the metabolic parameters measured in CLAMS cages.

Following voluntary wheel exposure both male and female *Crym*-tg mice on the HFD did not differ significantly from WT in RER, EE, total activity, ambulatory activity, or wheel activity (Figure 3.11). There were no measurable changes in any of the outcomes measured compared to those obtained in the absence of wheels. The male WT mice appeared to segregate into subgroups, one that utilized the wheels and one that did not (5 did and 4 did not). Consistent with these results, we did not find any differences in GTT or ITT in male and female *Crym*-tg or WT mice after voluntary running compared to the baseline levels measured earlier (Figure 3.9G-J).

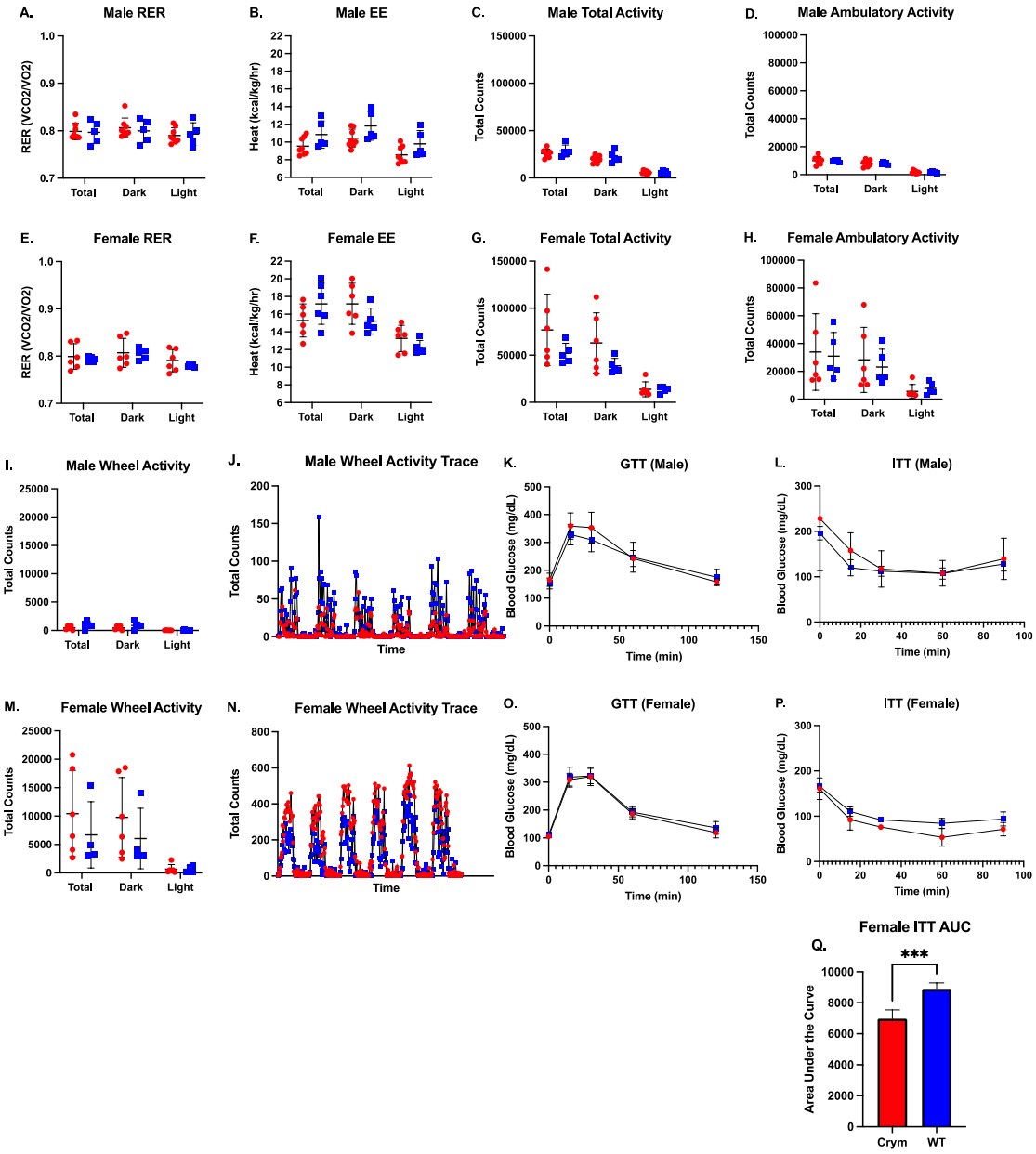

Figure 3.11. CLAMS Data for Mice on High-Fat Diet Following Voluntary Wheel Running.

Male *Crym*-tg and WT mice show no differences in (A) RER, (B) EE, (C) total activity or (D) ambulatory activity. Likewise, there were no differences in female *Crym*-tg and WT mice in (E) RER, (F) EE, (G) total activity or (H) ambulatory activity. (I-J) There were no significant changes in wheel activity of male mice, though in J it appears to show a trend for decreased running activity in *Crym*-tg mice. (K-L) Post-wheel exposure there are no changes seen in either GTT or ITT in male mice. (M-N) Female mice do not show a significant difference in wheel activity. (O-Q) Post-wheel exposure GTT for female mice show no difference however, female *Crym*-tg mice are statistically more sensitive to insulin stimulation. ($p < 0.05$) *Crym*-tg are labeled in red and WT in blue.

Following the final GTT and ITT testing of the *Crym*-tg and WT mice, we collected tissue, it was then snap-frozen, followed by extraction of RNA and protein from the *tibialis anterior* and *gastrocnemius* muscles for qRT-PCR and capillary-based immunoassay analysis of mRNA and protein expression levels. As above, we examined fiber cross-sectional area and distribution, and the same subset of metabolic genes.

Male *Crym*-tg mice following HFD show a distinct right shift in relative and cumulative fiber cross-sectional area (CSA) in *gastrocnemius* when compared to WT, with no statistically significant changes in *gastrocnemius* mass (Figure 3.12). Conversely, female *Crym*-tg mice on HFD show a slight left shift in CSA distribution and frequency in *gastrocnemius* when compared to WT, also with no significant change in *gastrocnemius* mass. When evaluating whether this could be a sexually dimorphic variation based on genotype, we evaluated CSA of males and females of *Crym*-tg mice separately from males and females of WT mice (Figure 3.13). Interestingly, we saw that in WT mice males and females did not show a notable difference in frequency distribution, unlike the results noted for LFD WT mice (Figure 3.13). Further evaluation would be necessary to determine if these shifts in CSA confer differences in other functional parameters including grip strength, maximal force production, endurance, and muscle fatiguability for both the LFD and HFD cohorts.

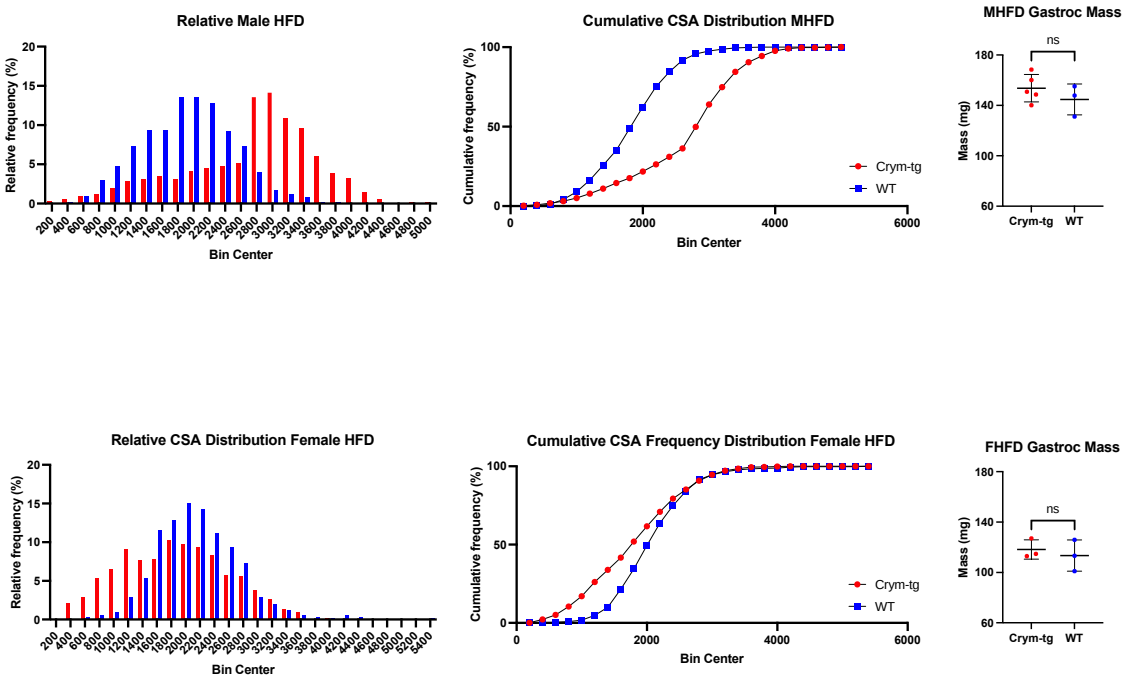

Figure 3.12. Relative and Cumulative CSA Distribution Following High-Fat Diet Interventions of Crym-tg Mice Compared to Wildtype Littermate Controls.

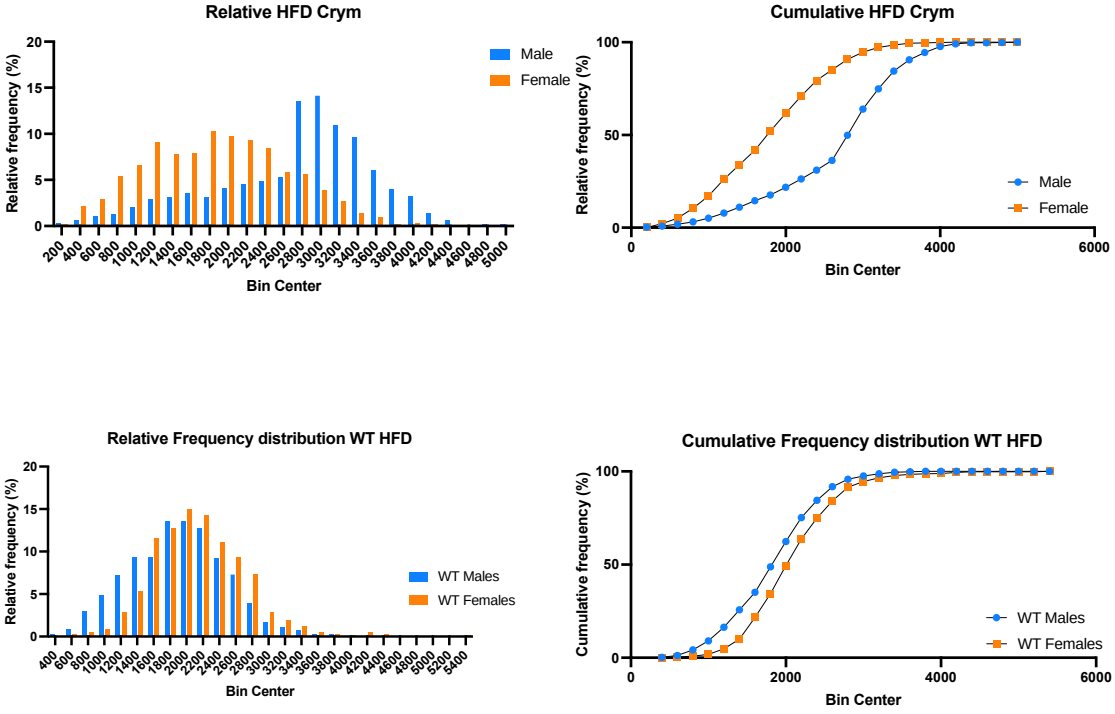

Figure 3.13. *Relative and Cumulative Fiber CSA Distribution Following High-Fat Diet Interventions Exhibit Sex-Specific Differences by Genotype.*

While we noticed that male *Crym*-tg mice tend not to run, with three of the six mice not utilizing the running wheel, however there was no statistical significance. Whereas, female *Crym*-tg mice tend to run more than their WT counterparts (again with no statistical significance).

We again evaluated the same set of genes of interest as the LFD cohort (Figure 3.7) to determine if these pathways could be differentially expressed due to diet intervention. HFD *Crym*-tg male mice show a statistically significantly increase in expression of *Irs2* and decrease in expression of *Calm3* (Figure 3.14). HFD *Crym*-tg females showed significant increases in expression of *Calm3, Ckmt2, Deptor, Irs2, Mib1, Nfkbia, Ppargc1a, Stat5b, and Ube2d1* (Figure 3.14). The only significant decrease in HFD female *Crym*-tg mice gene expression was for *Ppara.*

Capillary-based immunoassay in HFD females show a statistically significant decrease in *Ckmt2* protein expression in HFD females (Appendix A Figure A.8). Further capillary-based immunoassays showed no significant changes in the mitochondrial marker, *VDAC,* protein levels of HFD female muscle (Appendix A Figure A9).

Figure 3.14. *Relative Expression of GOIs Following HFD in tibialis anterior lysates.* qRT-PCR array of selected metabolic genes identified previously in RNA-seq datasets for *Crym*-tg mice on regular chow using *tibialis anterior* lysates. N = 6 for *Crym*-tg mice and N=5 for WT. Data for *Crym*-tg are in red and for WT in blue. ($p < 0.05$). *Crym*-tg are labeled in red and WT in blue.

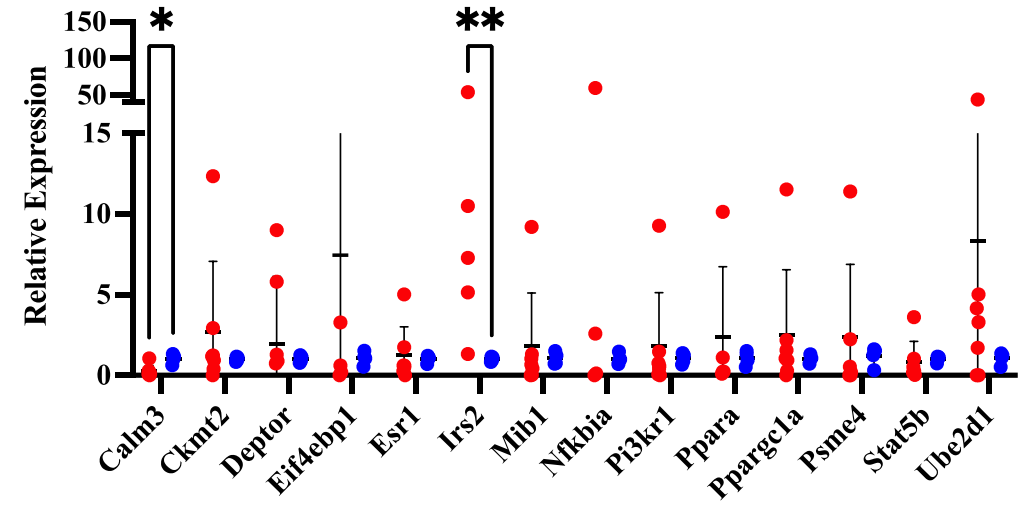

A. Male

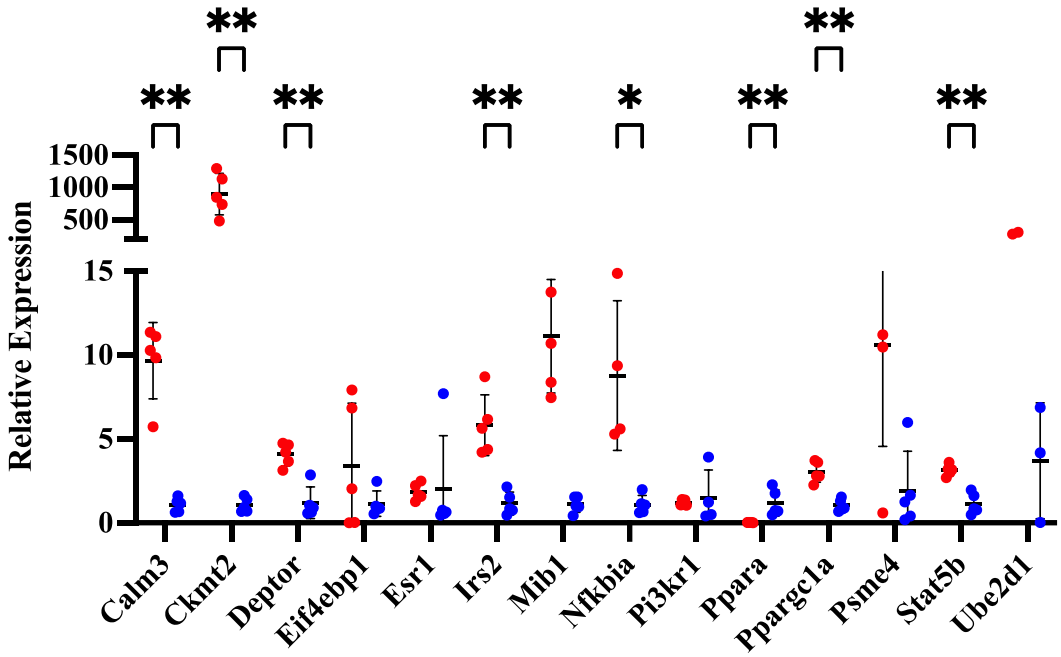

B. Female

Further assays of mRNA levels of genes involved in BCAA catabolism showed that *Mgea5, Dbt* and *Bcat2,* but not *Pcca*, *Bckdhb*, or *Mut* levels significantly increased in HFD *Crym*-tg females compared to littermate controls (Fig. 3.15; $p<0.05$). Capillary-

based immunoassay of *Dbt* protein expression levels did not show differences in HFD females (Appendix A Figure A.7).

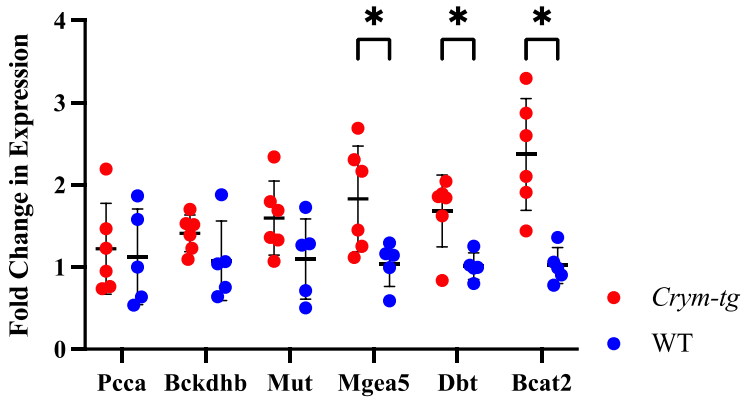

Figure 3.15. *Relative Expression of BCAA GOIs Following HFD in gastrocnemius of female mice.*
qRT-PCR array of selected BCAA genes using *tibialis anterior* lysates. N = 6 for all groups. Data for *Crym*-tg are in red and for WT in blue. ($p < 0.05$).

Discussion

Skeletal muscle is the largest organ by mass, comprising approximately 40 percent of the human body. Perturbations in skeletal muscle physiology and metabolism can have dramatic impacts on health. An important participant in modulating metabolism are the thyroid hormones, T3 and T4, which increase resting metabolic rate via increasing maximal oxygen consumption[214,218,369,370]. Our work focuses on the intersection of whole-body metabolism and the effects of high levels of expression of the thyroid hormone binding protein, mu-crystallin, in skeletal muscle of transgenic mice. Our results have revealed that *Crym*-tg mice show sex- and diet-dependent shifts in metabolism, body mass and composition. Most prominently, high levels of skeletal muscle specific high expression (SM-HE) of mu-crystallin, which is seen in 15-20% of the human population[292], causes a significant decrease in lean mass in male mice on low-fat diet and in female mice on HFD.

mu-Crystallin is little studied in the context of whole-body metabolism. We have previously shown that our *Crym*-tg mice have 192-fold more T3 in skeletal muscle tissue than WT mice. Although we did not examine the translocation of T3 and its associated receptors to the nucleus, we previously showed that the effects of SM-HE of *Crym* on metabolism in male mice maintained on a standard chow included a shift from glycolytic pathways and towards genes associated with oxidative metabolism, consistent with a shift in RER towards increased fatty acid as an energy source[302]. This shift was accompanied by an expected shift in gene expression towards genes used in slow twitch muscle and away from those used in fast twitch muscle. Here we extend our studies to include both male and female mice maintained on low- and high-fat diets (LFD and HFD, respectively). We anticipated that, by promoting oxidative metabolism, SM-HE of *Crym* would reduce HFD-induced weight gain in both sexes. Contrary to our expectations, our results suggest that *Crym* promotes the loss of lean muscle tissue in a sex-and diet-dependent manner.

At the outset of our studies, we hypothesized that increased levels of mu-crystallin would enhance fatty acid metabolism in skeletal muscle and translate to corresponding changes in body mass and composition. We assumed that the increase in intramuscular T3 in the *Crym*-tg mice does not impede the ability of T3 to translocate to the nucleus to activate thyroid response elements (TRE), which drive expression of genes controlling oxidative metabolism. Alternatively, intracellular T3 may increase but the increased levels of mu-crystallin would reduce the free concentration of the hormone,

thereby inhibiting binding of T3 to its receptors and impeding its translocation to the nucleus. Our results indicate that the effects of Crym overexpression are more complex, as we see a loss in lean rather than fat mass that manifests in diet- and sex-specific ways. The fact that a high Crym level in muscle can reduce lean mass without corresponding changes in metabolic parameters in mice on HFD or LFD suggests that it either is mediated through disuse atrophy or, more likely, that it promotes protein catabolism. Notably, CLAMS technology cannot measure the metabolic contribution of protein as an energy source. Nevertheless, the effects of *Crym* SM-HE that we document are consistent with *Crym*'s ketimine reductase activity, which plays a key role in the catabolism of lysine, which in turn influences protein catabolism.

STRING analysis of our original RNAseq dataset[302], from male mice on standard chow, identified several differentially expressed genes related to lysine metabolism. Lysine is an essential amino acid that must come from the diet. Ishida et. al evaluated changes in protein metabolism in a study that altered dietary lysine in rats, first at deficient levels then increased to sufficient[12]. The mice on low dietary lysine had a lower body mass than control counterparts, but when dietary lysine was increased to sufficient levels, they showed significant compensatory growth, as measured via decreased protein catabolism and concomitant increased rated in protein synthesis[12]. The high levels of mu-crystallin, expressed in the muscles of *Crym*-tg mice may therefore reduce the levels of lysine in muscle to limit protein synthesis and promotes protein catabolism, leading to the decrease in lean mass we report.

Congruent with some of our results, we found that the expression of several genes encoding enzymes involved in branched chain amino acids (BCAA) catabolism were also increased in *Crym*-tg muscle. It seems likely to us that a decrease in lysine could account for this effect. Intermediates in the lysine metabolism pathway such as alpha-aminoadipate semialdehyde are quite toxic[296,297] and can impair mitochondrial function, and mutations in the dehydrogenase that leads to its production is responsible for pyridoxine-dependent seizures[297]. Alterations in lysine content also impacts collagen and carnitine synthesis. Collagen is crucial for collagen cross-linking which maintains mitochondrial integrity.

Lysine is also a precursor for carnitine synthesis, which facilitates the transfer of fatty acids into the mitochondria for β-oxidation[298]. Carnitine also enhances nonoxidative glucose disposal under euglycemic hyperinsulinemic conditions, indicating that glucose being taken up into skeletal muscle or adipose tissue might be for glycogen synthesis, lipogenesis, or other metabolic pathways and not immediate energy production. Perturbations, specifically decreases in carnitine synthesis, can lead to muscle atrophy as fatty acids cannot efficiently enter the mitochondria to produce energy, leading to increased muscle fatiguability and impaired muscle recovery[299,300].

In conjunction with decreased lysine, BCAA catabolism could also lead to the effects that we see in our studies. BCAA catabolism involves two primary enzymatic steps, the first of which involves branched-chain amino transferases (BCAT), and the second uses the branched-chain ketoacid dehydrogenase complex (BCKDH). There are

three subunits to the BCKDH complex, E1 through 3, in which dihydrolipoamide branched chain transacylase E2 (DBT) is the E2 subunit that encodes the transacylase subunit. Our data demonstrated changes in DBT expression in which *Crym*-tg male mice on LFD shows significant decreases in expression while female *Crym*-tg mice show an increase in DBT expression compared to wildtype controls. As DBT's enzymatic activity is to accept and then transfer acyl groups from the E1 subunit of BCKDH to coenzyme A, any perturbations in its expression could constitute major metabolic fluxuations within the cell, potentially impacting organ, or whole-body metabolism. While we see that DBT expression is significantly decreased in LFD *Crym*-tg males versus WT and that HFD *Crym*-tg females statistically significantly increase in DBT expression compared to WT females, these changes do not completely account for the loss of lean mass reported. Further work is necessary to determine what role estrogen may play in these opposing changes in expression.

Branched-chain aminotransferase 2 (BCAT2) is a mitochondrial specific aminotransferase found primarily in skeletal muscle. Our studies show significant changes in BCAT2 in both *Crym*-tg males on low-fat diet and females on high-fat diet. Interestingly, reports of whole-body knock-out of BCAT2 in male mice leads to decreased exercise capacity as well as a leaner body composition compared to controls[87,119]. The She et. al study supports the data that we have demonstrated here in that our male *Crym*-tg mice with decreased BCAT2 levels have relatively reduced exercise activity as well as lower lean muscle mass.

The most studied post-translational modifications of BCKDH have focused on branched chain ketoacid dehydrogenase kinase (BDK). It is known that BCKDH activity is lower in skeletal muscles due to the higher expression of BDK, compared to the E2 subunit of BCKDH, than when compared to other tissues[122]. BDK-KO mice show low skeletal muscle concentrations of BCAAs. Further work by Ishikawa on these KO mice shows decreased myofibrillar protein content and decreased post-translational modifications of key proteins in the mTORC1 signaling pathway that promote protein synthesis, S6K1 and eIF4eBP[84].

Increases in the activity of BCKDH are indicative of a tissue's need to reduce intracellular protein concentrations, whereas tissues that need to conserve synthesis of critically important proteins have lower BCKDH activity. As BDK activity increases with a concomitant decrease in BCKDH activity during a hyperthyroid induced state[126], THs are likely to regulate protein catabolism. This would be consistent with our observation that important enzymatic regulators of BCAA are altered in our studies.

As thyroid hormones are potent regulators of metabolism, and our transgenic mice show highly elevated levels of intracellular T3, it is curious that our results suggest that such high levels do not have more overt effects. Notably, in our prior work we did evaluate the number of TRE containing genes that were differentially expressed and identified very few, less than ten[302]. Although our studies here show that *Crym*'s effects seem to be primarily mediated by its enzymatic activity, rather than by its ability to bind T3. However, it is possible that an interplay of mu-crystallin's two functional roles that

allows for further complexity in metabolic phenotype than we have been able to evaluate. Mu-crystallin's impact on the thyroid hormone signaling pathway and regulation of thyroid hormone responsive gene expression remains to be explored.

Chapter 4 Defining the Association of SNP rs3848259 Allele Incidence and Endogenous CRYM Expression in *vastus lateralis* Skeletal Muscle

Introduction

Obesity is a complex and dynamic disease characterized by a positive energy balance, increased adiposity, and altered metabolism. The prevalence of obesity within the United States and its territories has continued to dramatically increase over the last decade. Many areas around the country have reached or exceeded a staggering 40% of their population as self-reportedly obese[131]. Of the states and its territories, only six had a prevalence at or below 30%, notably with none below 20 percent[131]. However, factors such as education, gender, race and ethnicity, and age contribute to disparities in obesity prevalence. For example, the rate of adult individuals with self-reported obesity dramatically decreases as level of education increases[131,195].

Obesity prevalence is associated with a substantial increase in health-care related costs per obese individual, culminating in an approximate $147 billion USD spent annually on obesity-related healthcare costs[131]. Obesity is associated with a wide array of other health issues including, but not limited to, cardiovascular diseases[139,275], insulin resistance[149,163,332], diabetes mellitus[144,353,354], infertility[356,357], obstructive sleep apnea[371,372], and cancer[355,358,359]. With the current increase in incidence of obesity and associated comorbidities, there is a considerable need for treatments and related interventions. First line interventions include lifestyle modifications consisting of dietary changes, increased exercise activity and behavioral therapy[360]. However, for many

individuals these interventions alone are insufficient and therefore targeted pharmacotherapeutics are often suitable in conjunction with lifestyle modifications.

The etiology of obesity is often multi-faceted, as many genetic and environmental influences, such as obesogens[137], may impact any given individual. Over the years an increasing number of genes have been linked to obesity prevalence and severity[37,134,135,138,140-143,146,148,152-156,159,163,164,170,305]. These genes can act alone, as well as in conjunction with other genes and environmental and lifestyle factors. These factors can generally be grouped as follows: monogenic, polygenic, and syndromic obesity. Pharmacotherapeutics have been developed to help treat obesity in individuals in conjunction with lifestyle modifications based on these categories.

There are several current pharmacotherapies for obesity that target lipases[366,367], hormonal signaling[361-363], and the melanocortin-4 receptor (MC4R) pathway[368]. Included are lipase inhibitors[366,367], glucose-dependent insulinotropic polypeptide (GIP) mimetics[373], glucagon-like peptide-1 (GLP-1) receptor agonists[365,374-378] and dual GIP and GLP-1 agonists[166,363,373,379]. Thyroid hormones are also major metabolic contributors and thus another potential therapeutic targets for developing treatments for obesity. Targeting T3 levels directly can be dangerous and as such an indirect target would be preferable. As we study the thyroid hormone binding protein, mu-crystallin, we posited that mu-crystallin was an attractive pharmacotherapeutic target[209].

According to GTex, approximately 15-20% of the human population expresses high levels of mu-crystallin and the remainder of the population expresses little to none[292]. This expression incidence is consistent with the frequency of the single nucleotide polymorphism (SNP) rs3848259, which is found upstream of the CRYM gene, in the promoter region[380]. We postulated that the presence of this SNP could predict the protein expression levels of CRYM and therefore make for a simple diagnostic marker. This would allow for a less invasive approach, to predict an individual's CRYM expression levels, as to assays requiring traditional muscle biopsies.

Materials and Methods

Human *vastus lateralis* muscle biopsies

Two *vastus lateralis* muscle biopsies were performed with local anesthesia, one before the start of a three-hour hyperinsulinemic-euglycemic clamp and the second at 120 min during the clamp procedure. Wet muscle was immediately frozen in clamps cooled in liquid nitrogen and stored at -80°C. Muscle biopsies were provided by Dr. Alice Ryan and funded by VA Merit Award Clinical Service R&D 1153486.

gDNA Extraction

Approximately 25mg of each skeletal muscle sample was placed into 1.5ml microfuge tubes. gDNA extractions were completed using Invitrogen's PureLink Genomic DNA Isolation Kit (K1820-01) and associated standard mammalian tissue protocol. Modifications in the standard protocol included replacing the recommended

elution buffer with 100ul of UltraPure DNase/RNase-Free Water (Invitrogen, 10977015), preheated to 90°C and the second elution step was eliminated.

Protein Extraction

Approximately 25mg of each sample was used for protein extraction. Protein was extracted in RIPA Buffer (R0278-50 ML, Sigma-Aldrich), prepared with cOmplete Mini, EDTA-free protease inhibitor tablets (11836170001, Sigma-Aldrich; 10 mL of RIPA buffer to every protease inhibitor tablet). Each sample was placed into a 2ml microfuge tube with 250µL of RIPA/protease inhibitor solution along with two 5 mm steel beads (69989; Qiagen, Hilden, Germany). Samples were placed in a TissueLyser LT (Qiagen) at 50 oscillations/sec for 3 min, briefly vortexed, placed on ice for 2 min, followed by a second round of 50 oscillations/sec for 3 min. Samples were sonicated for 10 sec and subjected to centrifugation at 14,000 x g for 30 min at 4ºC. The supernatant was transferred to a new microfuge tube and protein concentration was determined with Protein Assay Dye Reagent Concentrate (Bradford Assay; 5000006, Bio-Rad).

Automated Western Blotting (Abby)

Analysis was performed with Protein Simple's Simple Western system, Abby, according to the manufacturer's instructions for the 12-230 kDa protein separation module (#SM-W004; Protein Simple a Bio-Techne Brand, Minneapolis, MN). Protein extracted from whole tissue lysates were prepared with 10x Sample Buffer (#042-195; ProteinSimple a Bio-Techne Brand, Minneapolis, MN) to generate an overall sample protein concentration of 1.0 mg/ml for each sample generated. The primary antibody for

μ-crystallin (SC-376687; Santa Cruz Bio) was prepared to a dilution of 1:25 in Protein Simple's Antibody Diluent 2. A primary antibody to a control protein, aconitase-2 (ab129069; Abcam, United Kingdom), was used at 1:200. The primary and control antibodies were multiplexed. Samples were run as technical triplicates. Compass software (Compass for SW 4.0 Mac Beta; Protein Simple) was used to visualize the electropherograms, followed by analysis of each peak of interest to calculate the area under the curve (AUC). The peak signal-to-noise ratio was set at ≥ 10 automatically by the software. Due to slight capillary-to-capillary variations in molecular weight readout, identified peaks at a molecular weight of interest were allowed a 10% range in variance in molecular weight (as automatically set by the Abby system). AUC was analyzed with Two-way ANOVA, fitted with a main effects only model, $p<0.05$. (*As noted in the introduction, this method of normalizing protein with control protein and not total protein normalization, is not the current best practice quantitation method.*)

rhAmp SNP Genotyping Assay

rhAmp SNP Genotyping assay from IDT was used for SNP allele detection at rs3848259. Genomic DNA extraction from participants *vastus lateralis* muscle biopsies were completed following the protocol on page page 85. The SNP Assay utilized was a predesigned assay from IDT for human CRYM for rs3848259, with design ID Hs.GT.rs3848259.G.1. gDNA for participant samples were prepared according to IDT's rhAmp SNP genotyping protocol, to a final concentration of 5ng/μl in IDTE at pH 7.5. DNA control templates (gBlocks) for reference, alternate and heterozygous alleles were procured from IDT and diluted to 500 copies/μl in IDTE at pH 7.5. Heterozygous

gBlocks are comprised of pooled equal parts of reference and alternate gBlock preparations. Final reaction volume per well was 10 μl as per determined by IDT. The remainder of the protocol, thermocycling details and analysis were completed following IDT's user guidelines.

Results

To determine whether the presence of SNP rs3848259 predicts endogenous mu-crystallin expression in humans, we first needed to ascertain the SNP allele frequency of our samples. Figure 4.1A shows the results of the allele frequency call for each sample, run in triplicate. As expected, most of our samples were identified as possessing the reference allele, two were heterozygotic and the remaining two were identified to have the alternate allele present (Figure 4.1A).

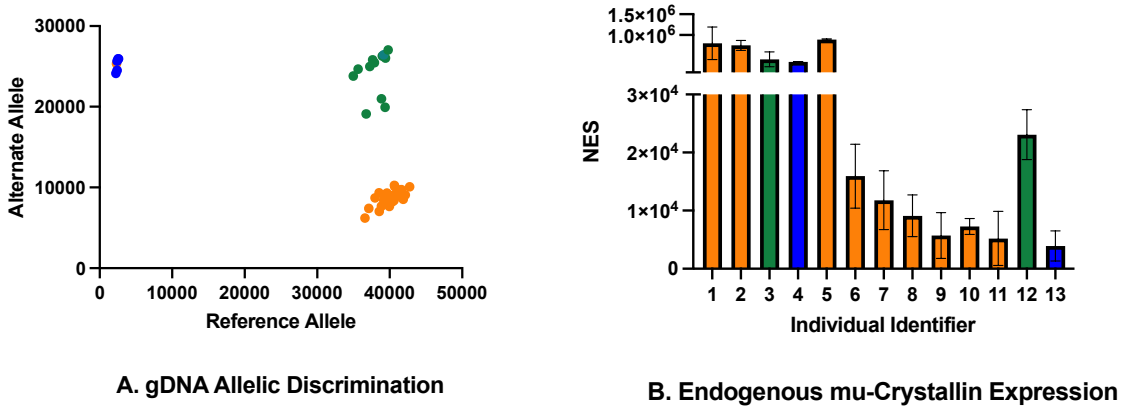

Figure 4.1. *Allelic Discrimination and Endogenous mu-Crystallin Expression in vastus lateralis biopsies.*
A) Allelic discrimination for SNP rs3848259 in individual samples clearly separated in resulting reference, heterozygote, and alternate allele genotypes (orange, green, and blue, respectively). B) Endogenous mu-crystallin expression of individual *vastus lateralis* samples were also determined and bar colors correspond to identified genotype (orange is reference, green is heterozygote and blue is alternate allele). Samples were run in technical triplicate.

Each sample was assayed for endogenous protein levels of mu-crystallin, shown in Figure 4.1B. Of the samples assayed for mu-crystallin expression, 5 of the 13 were determined to be high-expressers and the remaining 7 low-expressers (individual identifiers 1-5 and 7-13 respectively). When comparing SNP allele determination and protein expression levels of mu-crystallin, no discernible association between the two was evident.

The samples analyzed in Figure 4.1 were provided from time 0 min of a glucose clamp experiment. Utilizing individual samples for 120 min of the glucose clamp procedure allowed us to further investigation of the potential role for mu-crystallin in modulating skeletal muscle metabolic phenotype.

We assayed for changes in mu-crystallin expression during hyperinsulinemic-euglycemic clamp by comparing expression levels at time 0 to the 120 min timepoint (Figure 4.2). There were no statistically significant changes in mu-crystallin protein levels in either the mu-crystallin low- or high- expressors over this period (Figure 4.2). Analyzing all samples together, timepoint 0 and 120 min, regardless of basal expression level did not significantly alter *in vivo* mu-crystallin expression (Figure 4.3).

Figure 4.2. *Mu-Crystallin Expression During Hyperinsulinemic and Euglycemic Clamp.* Mu-crystallin expression is not significantly altered from the start (0 min) to 120 min during glucose clamp in *vastus lateralis* muscle biopsies. Even when accounting for normal versus impaired glucose tolerance, there is no evidence of significant differences in mu-crystallin levels. NES is the normalized experimental signal, the normalization of mu-crystallin expression to the aconitase-2 expression levels in each sample.

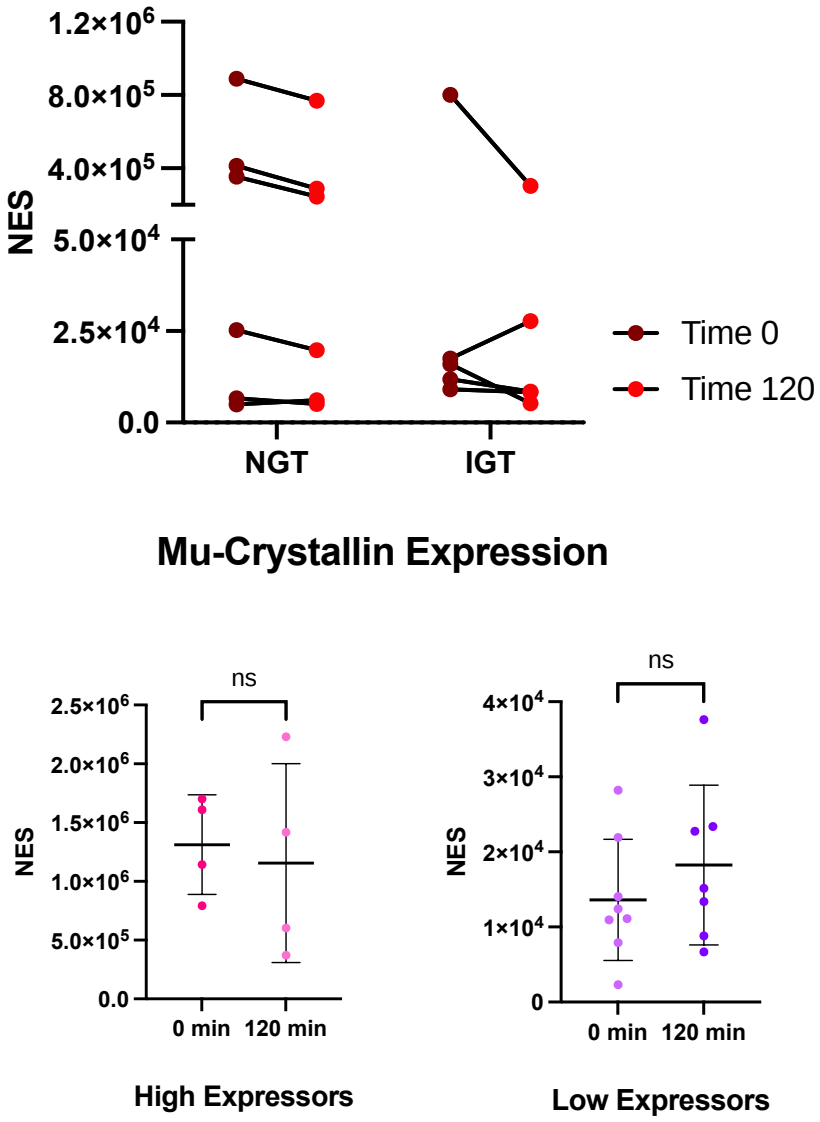

Figure 4.3. *NES of mu-Crystallin Expression at Time 0 and 120min of Hyperinsulinemic-Euglycemic Clamp in Normal Glucose Tolerant (NGT) and Impaired Glucose Tolerant (IGT) Participants.*
Mu-crystallin expression is not significantly different in NGT or IGT participants from time 0 to time 120 of hyperinsulinemic-euglycemic clamp.

Lastly, linear regression analysis of the low- and high-CRYM expressors was conducted with several identifiers including body weight, lean body mass, body mass index (BMI), fasting blood glucose, fasting insulin levels, and maximal volume of

oxygen consumed (VO_2 max) determined during a graded exercise treadmill test (Figure 4.4). If significant, these analyses would show associations between mu-crystallin expression level and the parameter identified, but importantly would not denote causation. There were no significant differences in the parameters analyzed when comparing low- versus high-mu-crystallin expressors (Figure 4.4) as determined via the regression coefficient of the slope (Table 4.1).

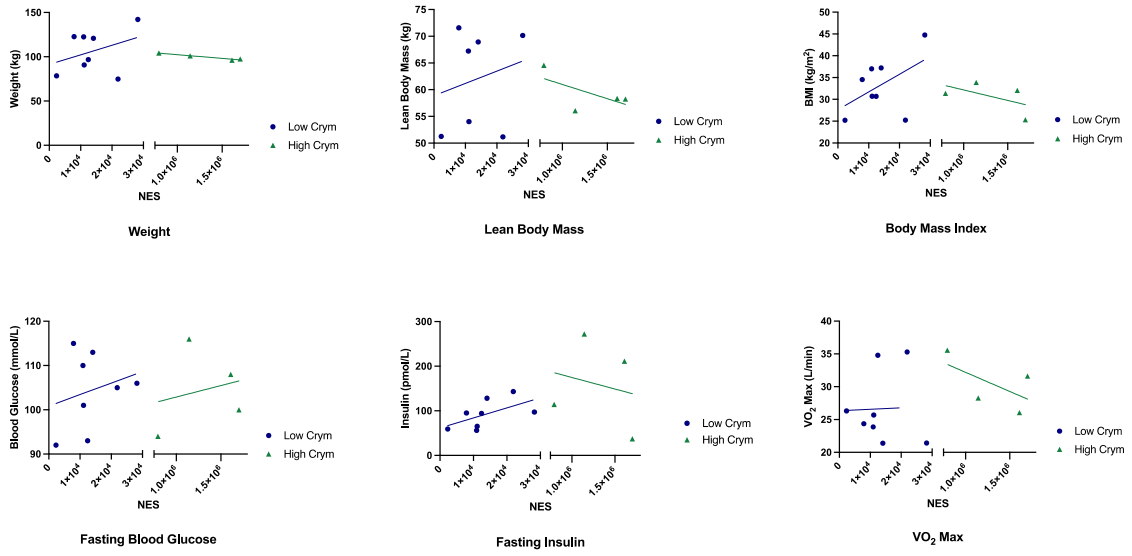

Figure 4.4. *Linear Regression Analysis of Low- and High-CRYM Expressors with Various Measured Parameters.*
Linear regression analysis does not reveal significant differences between basal low- or high expressors of mu-crystallin in any category analyzed (weight, lean body mass, body mass, fasting blood glucose, fasting insulin and VO_2 max of participants). See Table 4.1 for statistical analysis summary.

Table 4.A. *Linear Regression Analysis Results for Low- and High-Expressors of mu-Crystallin Associated with Figure 4.4.*
Statistical data for the linear regression analysis used in Figure 4.4 does not show significantly non-zero slopes individually nor significant differences between low- and high-expressors.

Linear Regression Analysis Details			
Parameter x NES of mu-crystallin		Low Expressors	High Expressors
Lean Mass	**Slope**	**Y = 0.0002304*X + 58.87**	**Y = -5.326e-006*X + 66.31**
	F	0.239	1.23
	DFn, DFd	1, 5	1, 2
	P value	0.6456	0.3829
	Is slope significantly non-zero?	Not Significant	Not Significant
BMI	**Slope**	**Y = 0.0004074*X + 27.63**	**Y = -4.806e-006*X + 36.97**
	F	1.979	0.8586
	DFn, DFd	1, 6	1, 2
	P value	0.2091	0.4519
	Is slope significantly non-zero?	Not Significant	Not Significant
VO2 Max	**Slope**	**Y = 2.239e-005*X + 26.34**	**Y = -5.826e-006*X + 38.02**
	F	0.006545	1.096
	DFn, DFd	1, 6	1, 2
	P value	0.9382	0.4051
	Is slope significantly non-zero?	Not Significant	Not Significant
Glucose	**Slope**	**Y = 0.0002602*X + 100.8**	**Y = 5.188e-006*X + 97.69**
	F	0.3827	0.1112
	DFn, DFd	1, 6	1, 2
	P value	0.5589	0.7705
	Is slope significantly non-zero?	Not Significant	Not Significant
Weight (kg)	**Slope**	**Y = 0.001087*X + 91.35**	**Y = -8.361e-006*X + 110.8**
	F	0.904	30.03
	DFn, DFd	1, 6	1, 2
	P value	0.3784	0.0317
	Is slope significantly non-zero?	Not Significant	Significant
Insulin	**Slope**	**Y = 0.002250*X + 61.49**	**Y = -5.169e-005*X + 226.3**
	F	2.931	0.0929
	DFn, DFd	1, 6	1, 2
	P value	0.1377	0.7893
	Is slope significantly non-zero?	Not Significant	Not Significant

Discussion

With the increasing prevalence and severity of obesity worldwide it is imperative to develop effective interventions to combat this growing concern. Traditional treatment modalities include lifestyle modifications; change in diet, increased physical activity and participation in behavioral therapy. Although these strategies are highly supported in the literature these lifestyle modifications are difficult to adhere to long-term for many

individuals. As a result, many pharmacotherapeutic agents are being developed although few have been approved to aid in weight management. Of the agents on the market, the mechanism of action typically entails targeting melanocortin-4 receptor signaling, lipases or glucagon related pathways.

Thyroid hormones are potent regulators of metabolism and therefore theoretically an ideal candidate for pharmacotherapeutic intervention. As direct treatment of individuals without hypothyroidism with T3 can lead to adverse effects, modulating intracellular T3 levels indirectly would offer an alternative way of exploring thyroid hormone as a weight management pharmacotherapy.

Our work has sought to evaluate mu-crystallin's potential role in the modulation of metabolism because of its known function as a thyroid hormone binding protein. We hypothesized that allele presence at rs3848259 upstream of the CRYM gene could be indicative of skeletal muscle protein expression levels of mu-crystallin and that alternate allele frequency would correlate with the approximate 70 percent of the population that express little to no mu-crystallin. Concomitantly, we posited that the alternate allele frequency would parallel the approximate 15 percent of individuals that are high mu-crystallin expressors. Our data did not support this hypothesis in this limited sample set as we did not observe a discernible association between mu-crystallin expression with SNP rs3848259 incidence or other sample identifiers that we assessed.

In summary, within the limitations of this study, SNP rs3848259 does not serve as a genetic marker for mu-crystallin expression or other metabolic related phenotypes. If mu-crystallin can indeed be utilized as an indirect protein target to modulate thyroid hormone metabolic impact, our effort to potentially reduce the invasiveness necessary in determining intramuscular levels of mu-crystallin was not successful. Thus, the factors that control the levels of expression of mu-crystallin in human skeletal muscle remain to be identified.

Chapter 5 Conclusions and Future Directions

Background

The prevalence and severity of obesity continues to rise[131,132] leading to an increasing need to develop weight management interventions. Traditionally, interventions include changes in diet, increase in physical exercise activity, and participation in behavioral therapy[360]. For many individuals though, these interventions are insufficient, thus highlighting the need for pharmacotherapeutics. Current pharmacotherapeutics involve targeting lipases[366,367], hormonal signaling[361-363], and the melanocortin-4 receptor (MC4R) pathway[368]. Utilizing a pharmacotherapy for obesity that targets thyroid hormones (TH) is also a potential avenue, but as direct targeting of THs can be quite dangerous for individuals that have normal levels, an indirect target is needed. Mu-crystallin is a TH binding protein, it is of great interest to determine its impact in TH signaling and TH mediated gene expression as it may be an indirect target for THs.

The goal of this work was to further characterize the role of the thyroid hormone binding protein mu-crystallin in modulating metabolism. Roughly 70% of the population expresses little to no mu-crystallin whereas the remainder of the population express high levels[292]. Even if mu-crystallin cannot be a target for obesity interventions, this work could provide valuable insight to the complex and dynamic metabolic processes. Indeed, our findings suggest that the predominant effect of mu-crystallin in muscle is to modulate muscle mass in a sex- and diet-specific dependent manner.

Prior Findings

Our previously published work demonstrated that male *Crym*-tg mice on standard chow had a small but significant shift in RER, with a 13.7% increase in fatty acid oxidation as an energy source when compared to wildtype C57BL/6 controls[302]. We also previously demonstrated a shift in gene expression via RNAseq transcriptomic and LC.MS/MS proteomic data that supported these findings[302]. Within these studies, male *Crym*-tg mice did not display significant differences in various other physiologic, morphologic, and cellular parameters including but not limited to: body composition, mass of individual fat pads, fiber types, overall fiber number, grip strength, maximum treadmill running speed, maximal rate of twitch force contraction/relaxation, specific isometric force of contraction, and voltage-induced Ca^{2+} transients[302]. Of note, however, is that these earlier studies did not include female *Crym*-tg mice.

Hypothesis

Following initial characterization and analysis of the *Crym*-tg line of mice generated by our lab, it was of great interest to determine diet and/or sex-specific differences resulting from the skeletal-muscle specific high-expression (SM-HE) of mu-crystallin. As it is well documented that the activities and impact of THs are is altered in pre-menopausal females when compared to males[21,90,184-189], we sought to determine the metabolic effects of high expression of mu-crystallin in skeletal muscle when mice of both sexes were stressed with low- or high-fat diets.

We hypothesized that SM-HE of mu-crystallin would confer protection against obesity in mice on HFD, based on our earlier findings that it promotes a shift towards an increase in fatty acid metabolism. In conjunction with this hypothesis, we postulated that SM-HE of mu-crystallin would reveal a prominent phenotype in mice on HFD regardless of sex, as HFD leads to obesity in both male and female mice.

Main Findings

In Chapter 2 we tested whether obesity-prone strains of mice would express lower endogenous levels of mu-crystallin while obesity-resistant strains would express higher levels of mu-crystallin. Our data from various strains and different muscles within those mice did not show any correlation between mu-crystallin expression in skeletal muscle and the susceptibility of obesity. Nonetheless, we did see sex-specific differences in Crym expression in different muscles. For example, we only documented significant differences in mu-crystallin expression in the *tibialis anterior* of male mice. Meanwhile, females of the strains we evaluated did not show significant differences in endogenous mu-crystallin within the *tibialis anterior* but did show significant differences in the *gastrocnemius, soleus,* and *quadriceps.* These sex-specific differences are likely attributable to the documented sex-specific differences that are published concerning fiber type variation[28,48,95,343,344]. Specifically, fiber type composition within each muscle varies to some degree and females generally have a smaller cross-sectional area for all fiber types compared to men. Men tend to have a greater cross-sectional area as well as greater distributions percentages of all type 2 fibers (2, 2A, 2X). Whereas females had greater distribution of type 1 fibers[93]. Nevertheless, the data in Chapter 2 indicate quite

varied expression level of mu-crystallin across strains. While our results do not show a relationship between mu-crystallin expression and obesity presentation, our data does suggest that further skeletal muscle evaluation would likely benefit from multiple strain analysis. Evaluation across strains of fiber CSA and fiber typing would provide valuable insight on not only characterization but of the physiological and functional importance in utilizing specific muscles for experiments.

Furthermore, in Chapter 3, we postulated that SM-HE of mu-crystallin would confer protection against DIO in both male and female mice when compared to wildtype littermate controls when subjected with a high-fat diet (HFD), with little variation in outcomes of mice subjected to a low-fat diet (LFD). Our hypothesis was disproved as SM-HE of Crym had no effect on fat accumulation. Rather, lean muscle mass was affected in sex- and diet-specific ways. Male *Crym*-tg mice on LFD had a statistically significant decrease in body mass resulting from decreased lean mass with no changes in females on LFD. Conversely, female *Crym*-tg mice on HFD had a statistically significant decrease in body mass resulting from decreased lean mass with no changes in male mice on HFD. These changes were not detected by measuring metabolic parameters via CLAMS cages. Of note, the data obtained with CLAMS cages are limited to indirect measurement of carbohydrate and fat metabolism and not protein metabolism.

We then shifted our focus to evaluating the potential role of protein catabolism for facilitating these differences in lean body mass, as mu-crystallin also has a functional role as a ketimine reductase. This activity is well defined in the brain but not within skeletal

muscle. Therefore, we started by evaluating changes in genes related to protein catabolism at the transcriptomic and proteomic levels. To keep costs at a minimum, we did not utilize RNAseq or LC/MS.MS analysis, but rather selected a subset of genes from various pathways and proteins implicated in modulating metabolic phenotypes for analysis via qRT-PCR and capillary-based immunoassays.

Results on the mRNA level again showed sex- and diet specific differences. Without a clear target identified in males on LFD and having determined many genes were differentially expressed in females on HFD, we then pivoted to evaluating changes in mRNA levels and protein levels of genes relating to branched-chain amino acid metabolism. Within the genes selected, males on LFD showed statistically significant decreased expression of *Pcca, Dbt,* and *Bcat2.* Females on HFD showed statistically significant increases in *Mgea5, Dbt,* and *Bcat2.* Further work, documented in Appendix I, details the initial results and analysis of proteomic data of the tissue from the LFD male mice and HFD female mice. Further evaluations are necessary to determine which BCAA related genes may be functionally different at the protein level. This would provide further insight as to how these lean mass changes are started.

Evaluation of whether these differences in lean mass are due to atrophy or inherent impairment of myogenesis further studies would have to be conducted. The decrease in lean muscle in male *Crym*-tg mice and in individual fiber cross-sectional area may result from disuse atrophy, as we saw that only three of our six *Crym*-tg males utilized the running wheel. As for the increase in CSA of female *Crym*-tg mice with the

concomitant decrease in lean muscle mass may be a result of a compensatory mechanism to maintain force production. Further testing of these mice for grip strength, maximum treadmill running speed, maximal rate of twitch force contraction/relaxation, specific isometric force of contraction, and voltage-induced Ca^{2+} transients would provide better insight to how these differences we document are being mediated.

Finally in Chapter 4, we evaluated the potential role of SNP rs3843259 as a marker for predicting basal endogenous levels mu-crystallin expression in humans. The alternate SNP allele presence in rs3843259 varies with approximately the same frequency as the frequency of individuals who express high levels of mu-crystallin[292]. To test the possible link between this SNP and Crym expression, we extracted RNA and protein from participant human *vastus lateralis* muscle biopsies and analyzed them via SNP genotyping assay (rhAmp SNP genotyping assay by IDT) and capillary-based immunoassays. We observed reference, alternate and heterozygous individuals within our sample group, but failed to find a relationship between SNP allele presence and endogenous protein expression levels of mu-crystallin. Using linear regression, we also did not see any statistically significant parameters associated with low versus high mu-crystallin expression. These parameters include participant features such as BMI, VO_2 max, lean body mass, etc. We concluded that the SNP rs3843259 allele presence does not correlate with the expression levels of mu-crystallin.

Of note, limitations in this chapter include our limited sample size as well as limitations of the capillary-based immunoassays utilized within Chapter 4. Specifically, the

capillary-based immunoassays now have an improved method for normalizing signal, utilizing total protein normalization rather than to an individual house-keeping gene that was not available at the time of these experiments. With the use of the newer method of total protein normalization, I would expect a much lower degree of variance within our groups. In our initial characterization of male *Crym*-tg mice on standard chow, aconitase-2 was a sufficient control, however we noted greater variability in its expression throughout initial diet study evaluations. This variability in expression is particularly important to note as aconitase-2 is a mitochondrial enzyme that converts citrate to isocitrate in the TCA cycle[381]. As such, since the newer method was available, we moved away from normalization with aconitase-2 to the total protein method and saw better refinement in terms of decreased variability. This gave us greater confidence in the results we reported for Chapter 3, however it would be best to re-evaluate strain specific expression and human *vastus lateralis* expression of mu-crystallin to confirm our findings more definitively.

Future Directions

As the data provided in this body of work has several factors identified in both potential mechanism of action and in factors influencing phenotypic presentation, it is imperative to explore both avenues. Factors for the mechanism of action include the two functional roles of mu-crystallin as a 1) ketimine reductase and 2) TH binding protein. It is possible that one of these functions is primarily responsible for the data but there is also the possibility of some level of interaction of these roles modulates the degree of variation described here. In females, estrogen can also bind to half-sites of TREs and

therefore impair thyroid hormone receptor binding. As such, it is possible that mu-crystallin's theorized ability to increase T3 translocation to the nucleus may not be sufficient to influence TRE gene transcription. Therefore, it is possible that mu-crystallin's role as a ketimine reductase may then be as a compensatory mechanism to ensure changes in metabolism. To properly interrogate this process, in addition to diet intervention, it is necessary to evaluate the role of sex hormones in affecting the phenotypic outcomes. This would imply that mu-crystallin expression itself would not necessarily be influenced by the presence of sex hormones, but that changes in mu-crystallin expression levels impacts the ability of sex hormones to influence metabolism in specific dietary conditions.

Mechanism of Action

To further resolve if these results are the functions of mu-crystallin's role as a TH binding protein or as a ketimine reductase, repeating these studies with mice that undergo a thyroidectomy or radioactive iodine intervention would be a valuable source of data.

In parallel with the thyroidectomy experiments, evaluation of branched-chain amino acid catabolism's role in these diet- and sex-specific differences needs to also be considered. One such experiment could introduce BCAA supplementation to male and female mice on either LFD or HFD and repeating the experiments previously described and utilized in Chapter 3. Specialized formulations of the LFD and HFD chow could include BCAA-rich or BCAA-deficient LFD and HFD. If BCAA catabolism is a key determinant in the results described here in Chapter 3, we would expect to see at least a

partial amelioration in the differences noted in body composition, gene expression differences, and relative and cumulative fiber CSA distributions of the BCAA enriched diet mice. This experimental design would have to closely monitor caloric intake and recognize differences in caloric intake could dramatically alter results if not controlled properly.

Factors Affecting Phenotypic Presentation

Moving this research forward will require elucidation of the role of sex hormones in modulating the phenotypes described in our diet studies. These studies utilize mice with normal hormone levels. Cohorts of mice on both LFD and HFD with suppressed hormone levels would be ideal next steps. These cohorts could include 1) gonadectomy of male mice, 2) estradiol treatment of male mice, 3) oophorectomy of female mice and 4) testosterone treatment of female mice. The mice should then be evaluated for metabolic parameters (including glucose and insulin tolerance tests), CLAMS measurements, body composition analysis and tissue analysis as previously described and completed in Chapter 3. If the differences we see in female mice on HFD are mediated in part by the levels of estrogen, then one would expect that oophorectomy of female mice could reduce or ameliorate the phenotype of decreased lean mass, and results would more likely resemble those seen in male mice. The opposite would be true for male mice treated with estradiol, and that these results would further be compounded with gonadectomy in the context of low-fat diet intervention. To learn if some our results were due to disuse atrophy, we have to use hindlimb immobilization combined with the diet studies and the associated tests we described.

Conclusions

My research has elucidated the whole-body phenotype, cellular and molecular variations in response to SM-HE of mu-crystallin in the *Crym*-tg mouse line. Our data give clear evidence of a more complex mechanism than previously predicted for the role of mu-crystallin in modulating glycolytic versus aerobic metabolism and instead points to a dominant role of Crym in determining muscle lean mass in sex- and diet-specific ways. This is not completely surprising as TH action is greatly influenced by sex hormones. While we propose that the differences documented in Chapter 3 are likely due to mu-crystallin's function as a ketimine reductase, that does not preclude the potential for altering metabolism as well, via binding and release of intracellular T3. The idea that mu-crystallin regulates the phenotypes described here via both its ability as a ketimine reductase and as a TH binding remains highly attractive. Nevertheless, it is clear is that mu-crystallin neither predisposes to nor protects against obesity. Further studies of how mu-crystallin regulates muscle metabolism are likely to reveal novel interactions that open new avenues for understanding atrophy and other muscle disorders.

Appendix A. *Additional Figures and Tables for Chapter 3*

Low-Fat Diet Data

Table A.1. Complete CLAMS calorimetry data for all LFD experiments.
Indirect calorimetry analyses of male and female *Crym*-tg and WT littermates following 16 weeks of low-fat diet are shown. All data are expressed as means + SD. All significant data ($p < 0.05$) are noted in bold and underlined text and trending values ($p < 0.09$) are *italicized*. Key: WT, wildtype; VO2, rate of oxygen consumption; VCO2, rate of carbon dioxide production; RER, respiratory exchange ratio; EE, energy expenditure.

	WT		Crym-tg		p-value	WT		Crym-tg		p-value	WT		Crym-tg		p-value
	Mean	St Dev	Mean	St Dev		Mean	St Dev	Mean	St Dev		Mean	St Dev	Mean	St Dev	
Male, Low Fat diet	*Ad libitum, dark cycle*					*Ad libitum, light cycle*					*Ad libitum, 24 h*				
n	6		6			6		6			6		6		
Body weight, g											28.1167	1.5105	24.9833	0.9559	**0.0016**
Food Intake, kcal	11.2677	0.8738	10.4951	0.1878	0.2230	3.5869	1.2970	1.9327	1.1136	*0.0517*	14.8546	1.2407	12.7050	1.2919	**0.0148**
VO2, ml/kgLM/h	3724.3775	261.1997	3744.6225	189.8602	0.8810	2960.7379	94.9116	2981.5150	133.0854	0.7619	3342.5173	174.1488	3362.9353	153.5480	0.8338
VCO2, mg/kg/LM/h	3735.2621	239.8313	3821.9337	128.9691	0.4537	2598.9854	133.7762	2518.2305	122.1780	0.3005	3167.3028	156.1915	3169.6670	69.0527	0.9736
RER, VCO2/VO2	1.0025	0.0233	1.0207	0.0429	0.3826	0.8766	0.0326	0.8442	0.0489	0.2065	0.9396	0.0121	0.9324	0.0382	0.6662
EE, kcal/kgLM/h	18.4767	1.2796	18.9726	1.0282	0.4764	14.3091	0.7991	14.5768	0.6459	0.5377	16.3934	1.0410	16.7536	0.8048	0.5178
Total activity, beam breaks	29459.6667	3921.2814	32077.6667	7454.0572	0.4640	8866.3333	1673.2830	8711.6667	2964.7829	0.9136	38326.0000	4791.3428	40789.3333	9720.5953	0.5899
Ambulatory Activity, counts	14036.1667	2254.8510	18585.1667	8904.8145	0.2530	3103.8333	863.6340	4235.0000	3860.5571	0.4996	17140.0000	2560.5735	22820.1667	12595.4302	0.3044
	Fasting, dark cycle					*Fasting, light cycle*					*Fasting, 24 h*				
Food Intake, kcal	0.0000	0.0000	0.1155	0.2583	0.2967	0.0000	0.0000	0.0462	0.1033	0.2967	0.0000	0.0000	0.1617	0.3616	0.2967
VO2, ml/kgLM/h	3018.1548	133.3629	3125.8158	328.6328	0.4787	2245.9122	79.4833	2299.1820	222.4582	0.5951	2630.6995	86.8485	2712.2041	273.2095	0.5038
VCO2, mg/kg/LM/h	2294.0335	123.9590	2357.9552	227.3925	0.5667	1664.2313	97.7548	1659.2877	157.6711	0.9505	1977.9125	96.5533	2008.3201	188.7461	0.7370
RER, VCO2/VO2	0.7569	0.0165	0.7502	0.0068	0.4180	0.7390	0.0314	0.7177	0.0078	0.1780	0.7478	0.0234	0.7339	0.0041	0.2260
EE, kcal/kgLM/h	14.3404	0.6558	14.8297	1.5332	0.4938	10.6183	0.4010	10.8157	1.0416	0.6765	12.4728	0.4374	12.8212	1.2747	0.5430
Total activity, beam breaks	38019.3333	9504.9916	35774.4000	7809.7632	0.6832	10368.0000	5265.0801	8014.0000	1913.8606	0.3708	48387.3333	14312.3438	43788.4000	9666.1516	0.5573
Ambulatory Activity, counts	22703.0000	6972.1399	23728.2000	10171.9819	0.8473	5001.1667	3885.9730	4059.0000	2829.8817	0.6633	27704.1667	10416.8924	27787.2000	12988.7040	0.9909
	Refeed, dark cycle					*Refeed, light cycle*					*Refeed, 24 h*				
Food Intake, kcal	15.4385	0.5014	16.8784	4.6401	0.4649	5.8007	0.7964	4.1118	0.7639	**0.0061**	21.2392	1.1780	20.9902	5.0602	0.9087
VO2, ml/kgLM/h	3496.8112	241.6093	3661.5300	292.1984	0.3319	2801.4709	149.7111	2837.9909	200.0213	0.7367	3148.2692	185.0869	3250.4057	243.8703	0.4493
VCO2, mg/kg/LM/h	3575.9811	244.3452	3708.3520	254.3492	0.4025	2934.6572	127.6069	2796.7470	131.5372	0.1122	3254.6047	163.6757	3253.5674	175.2306	0.9921
RER, VCO2/VO2	1.0240	0.0115	1.0152	0.0149	0.2970	1.0499	0.0275	0.9861	0.0435	**0.0157**	1.0370	0.0180	1.0008	0.0278	**0.0280**
EE, kcal/kgLM/h	17.7460	1.2200	18.5376	1.4270	0.3465	14.3032	0.7157	14.2727	0.8966	0.9513	16.0204	0.9036	16.4088	1.1427	0.5438
Total activity, beam breaks	32590.6667	8060.5125	40380.8000	8549.9819	0.1547	8188.3333	2351.4918	11411.4000	2790.5341	*0.0670*	40779.0000	6799.1830	51792.2000	11153.8538	*0.0740*
Ambulatory Activity, counts	17995.0000	5796.8134	25451.2000	10243.6726	0.1619	3292.8333	1291.5684	6121.6000	2875.3843	*0.0574*	21287.8333	5166.1947	31572.8000	13074.5523	0.1084
	Wheel, dark cycle					*Wheel, light cycle*					*Wheel, 24 h*				
Food Intake, kcal	11.5885	1.5584	12.4586	3.7965	0.6183	3.8885	0.7485	3.3110	0.8762	0.2680	15.4770	2.2021	15.9454	3.7296	0.7965
VO2, ml/kgLM/h	3597.8350	350.8832	3718.7603	410.0002	0.5951	2870.9641	252.2965	2882.0602	226.7295	0.9377	3242.5830	295.4482	3311.8122	308.1670	0.6996
VCO2, mg/kg/LM/h	3674.3044	278.4538	3879.3543	413.2142	0.3372	2673.1316	232.3391	2553.4052	234.6798	0.3954	3184.8398	238.2513	3233.3805	307.1703	0.7660
RER, VCO2/VO2	1.0246	0.0311	1.0449	0.0363	0.3234	0.9315	0.0351	0.8820	0.0312	**0.0273**	0.9791	0.0293	0.9653	0.0262	0.4096
EE, kcal/kgLM/h	18.2526	1.6705	18.9663	2.0570	0.5243	14.2460	1.2269	14.1409	1.1396	0.8809	16.2942	1.4089	16.6181	1.5431	0.7122
Total activity, beam breaks	30289.3333	7490.4748	34579.5000	14211.4134	0.5278	8694.8333	1978.6838	8115.6667	2461.3465	0.6629	38984.1667	8829.7555	42695.1667	15520.7910	0.6218
Ambulatory Activity, counts	13371.5000	4799.1699	17283.3333	9946.5218	0.4059	3330.0000	1091.3986	4133.1667	2967.4181	0.5477	16701.5000	5439.8263	21416.5000	12773.9949	0.4249
Wheel Activity, counts	2823.2500	984.4800	2928.0000	1487.2078	0.9142	395.5000	144.2625	208.0000	76.0986	0.0997	3218.7500	903.4048	3136.0000	1534.4211	0.9314
Female, Low Fat diet	*Ad libitum, dark cycle*					*Ad libitum, light cycle*					*Ad libitum, 24 h*				
n	6		6			6		6			6		6		
Body weight, g											19.3167	1.4275	19.5667	0.7062	0.7086
Food Intake, kcal	9.0552	1.5377	7.5332	3.2779	0.3676	3.1339	0.6804	3.1249	0.8429	0.9851	11.7553	2.0030	10.6581	3.9531	0.5577
VO2, ml/kgLM/h	4576.7465	584.0810	4856.5486	517.7952	0.4005	3600.8231	276.8529	3721.3756	411.0373	0.5645	4086.5864	421.5613	4288.6684	457.5832	0.4447
VCO2, mg/kg/LM/h	4249.6363	457.3422	4433.7566	867.3693	0.6554	3139.9990	242.2676	3185.9840	509.8660	0.8458	3693.2882	*327.4054*	3808.5932	673.7310	0.7140
RER, VCO2/VO2	0.9298	0.0503	0.9072	0.0854	0.5897	0.8693	0.0376	0.8500	0.0408	0.4150	0.8997	0.0375	0.8785	0.0605	0.4828
EE, kcal/kgLM/h	22.1563	1.3921	22.5761	3.6811	0.7992	18.1305	1.4600	18.4383	2.2723	0.7858	20.1428	1.4068	20.5014	2.9296	0.7924
Total activity, beam breaks	66874.5000	22295.7467	58012.8333	16095.5463	0.4482	12437.3333	1742.2646	13555.0000	3387.9102	0.4888	79311.8333	23337.8591	71567.8333	19005.3345	0.6646
Ambulatory Activity, counts	42641.6667	16933.7888	37844.5000	16220.3276	0.6271	5580.1667	1536.3477	6762.5000	4843.5907	0.5813	48221.8333	17885.5769	44607.0000	20791.5051	0.7535
	Fasting, dark cycle					*Fasting, light cycle*					*Fasting, 24 h*				
Food Intake, kcal	0.2374	0.3696	0.4697	1.0503	0.6224	0.0513	0.0795	0.0308	0.0689	0.6618	0.2888	0.4488	0.5005	1.1192	0.6789
VO2, ml/kgLM/h	3929.8586	278.7931	3429.0520	374.9956	**0.0315**	2578.7859	122.7205	2460.8345	403.4253	0.5102	3256.5489	185.4465	2943.2210	374.2447	0.1031
VCO2, mg/kg/LM/h	3001.5821	249.6777	2612.8741	324.1983	0.0509	1872.0495	125.6795	1777.1586	344.9466	0.5437	2438.6960	178.7366	2193.5615	320.0077	0.1420
RER, VCO2/VO2	0.7610	0.0139	0.7534	0.0169	0.4296	0.7200	0.0157	0.7167	0.0229	0.7821	0.7406	0.0145	0.7350	0.0187	0.5900
EE, kcal/kgLM/h	18.6905	1.3683	16.3007	1.8273	**0.0348**	12.1443	0.6214	11.5777	1.9619	0.5170	15.4282	0.9261	13.9309	1.8196	0.1102
Total activity, beam breaks	78215.5000	27694.1238	43955.0000	20733.8650	**0.0488**	15808.6667	8681.9253	14350.4000	9105.6982	0.7922	94024.1667	35037.0373	58305.4000	29686.5366	0.1054
Ambulatory Activity, counts	53254.3333	21971.0601	28860.6000	14883.8739	*0.0647*	8972.1667	6340.4164	8636.6000	6449.9109	0.9328	62226.5000	27427.7320	37497.2000	21255.7136	0.1350
	Refeed, dark cycle					*Refeed, light cycle*					*Refeed, 24 h*				
Food Intake, kcal	14.3028	7.3171	16.6166	3.7766	0.5405	4.5751	2.3549	5.6441	0.7478	0.3586	22.0990	2.9220	22.2607	3.6023	0.9362
VO2, ml/kgLM/h	4037.3005	179.3284	3875.5704	442.0332	0.4305	3484.9117	246.5073	3492.3692	390.6505	0.9700	3760.4701	186.0856	3684.2097	404.3950	0.6876
VCO2, mg/kg/LM/h	4193.9175	245.3748	4015.3431	521.6428	0.4721	3679.7326	320.1143	3658.3643	456.0616	0.9292	3936.1392	247.5581	3837.3117	478.4269	0.6683
RER, VCO2/VO2	1.0409	0.0162	1.0362	0.0223	0.6959	1.0549	0.0225	1.0469	0.0358	0.6584	1.0479	0.0175	1.0416	0.0283	0.6604
EE, kcal/kgLM/h	20.5694	0.9840	19.7323	2.3267	0.4412	17.8285	1.3299	17.8306	2.0389	0.9984	19.1957	1.0110	18.7829	2.1257	0.6810
Total activity, beam breaks	33177.8333	6358.3052	29379.6000	6183.4862	0.3441	12184.1667	2626.3275	10952.2000	3324.7840	0.5088	45362.0000	7430.0113	40331.8000	6823.1171	0.2762
Ambulatory Activity, counts	18861.3333	5037.6460	17574.4000	8254.9109	0.7570	5631.6667	2004.9069	5224.8000	1850.5529	0.7368	24493.0000	6180.9777	22799.2000	9269.0778	0.7250
	Wheel, dark cycle					*Wheel, light cycle*					*Wheel, 24 h*				
Food Intake, kcal	10.0485	2.4933	8.6882	2.1834	0.3594	3.5035	0.7441	3.1634	0.8798	0.5118	14.2450	2.6750	11.8516	2.2385	0.1237
VO2, ml/kgLM/h	5221.2601	868.3440	4975.8717	656.7221	0.5930	3533.2518	372.1941	3624.3959	367.6820	0.6786	4391.9706	592.7372	4314.9432	472.0352	0.8084
VCO2, mg/kg/LM/h	4968.9050	657.5164	4732.1796	327.2990	0.4481	3153.1537	385.7656	3151.2866	249.0117	0.9922	4077.4079	481.3651	3959.7965	261.2837	0.6104
RER, VCO2/VO2	0.9561	0.0638	0.9588	0.0764	0.9477	0.8866	0.0371	0.8687	0.0447	0.4685	0.9220	0.0432	0.9149	0.0573	0.8132
EE, kcal/kgLM/h	26.0409	4.0791	24.8131	2.8693	0.5599	17.3641	1.8719	17.7095	1.6731	0.7431	21.7788	2.8220	21.3400	2.0866	0.7657
Total activity, beam breaks	88231.0000	26949.1819	64420.8333	20293.3309	0.1145	15156.6667	8483.5729	11067.3333	3716.1985	0.3049	103387.6667	33300.8677	75488.1667	23282.5582	0.1235
Ambulatory Activity, counts	25118.6667	5689.9633	25426.0000	4839.3438	0.9217	5254.1667	2405.4489	4771.5000	2220.8316	0.7255	30372.8333	5873.2643	30197.5000	6870.1440	0.9630
Wheel Activity, counts	29626.6000	11267.6371	15205.3333	13166.1844	*0.0861*	3011.4000	1487.2536	1150.8333	1320.0035	*0.0554*	32638.0000	11941.6126	16356.1667	14078.2795	*0.0716*

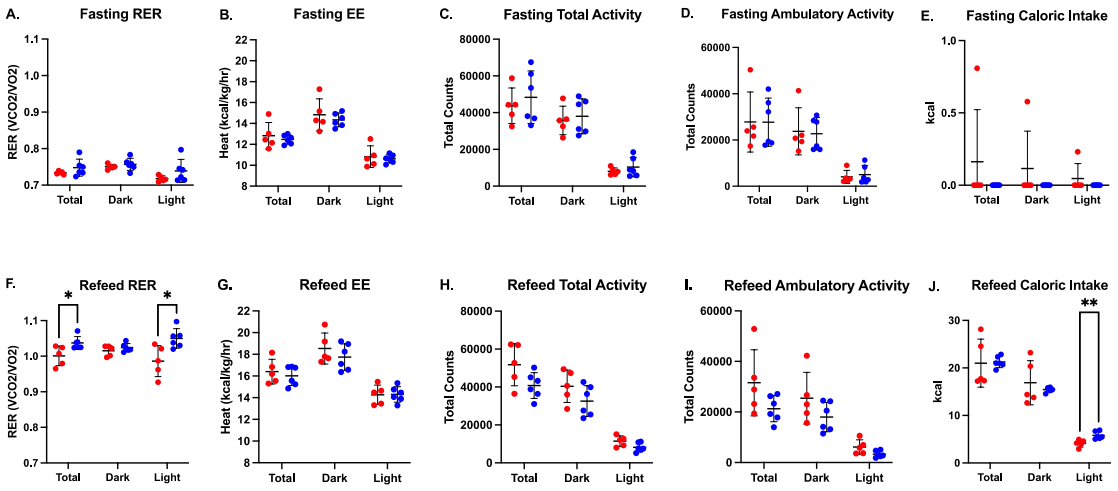

Figure A.1. CLAMS data for fasting and refeed conditions in males following low-fat diet intervention.

Fasting and refeed conditions of male *Crym*-tg and WT mice on LFD mice show significant changes only during refeed. Male *Crym*-tg on LFD have no significant differences compared to WT during a fasting/refeed period in (A) respiratory exchange ratio (RER), (B) energy expenditure (EE), (C) total activity, (D) ambulatory activity, (E) caloric intake during fasting conditions. Male *Crym*-tg on LFD have no significant differences compared to WT during the refeed period in (F) respiratory exchange ratio, (G) energy expenditure, (H) total activity, (I) ambulatory activity, (J) caloric intake. N = 6 for all groups ($p < 0.05$). Data for *Crym*-tg are in red and for WT in blue.

Figure A.2. CLAMS data for fasting and refeed conditions in females following low-fat diet intervention.

Female *Crym*-tg and WT mice show minimal changes in metabolic parameters following fasting/refeed on LFD. Fasting indirect calorimetry measurements in female *Crym*-tg and WT mice during fasting period of (A) respiratory exchange ratio, (B) energy expenditure, (C) total activity, (D) ambulatory activity, (E) caloric intake during fasting conditions only show significant changes in EE. Female *Crym*-tg on LFD have no significant differences compared to WT during a refeeding period in (F) respiratory exchange ratio, (G) energy expenditure, (H) total activity, (I) ambulatory activity, (J) caloric intake. N = 6 for all groups. Data for *Crym*-tg are in red and for WT in blue.

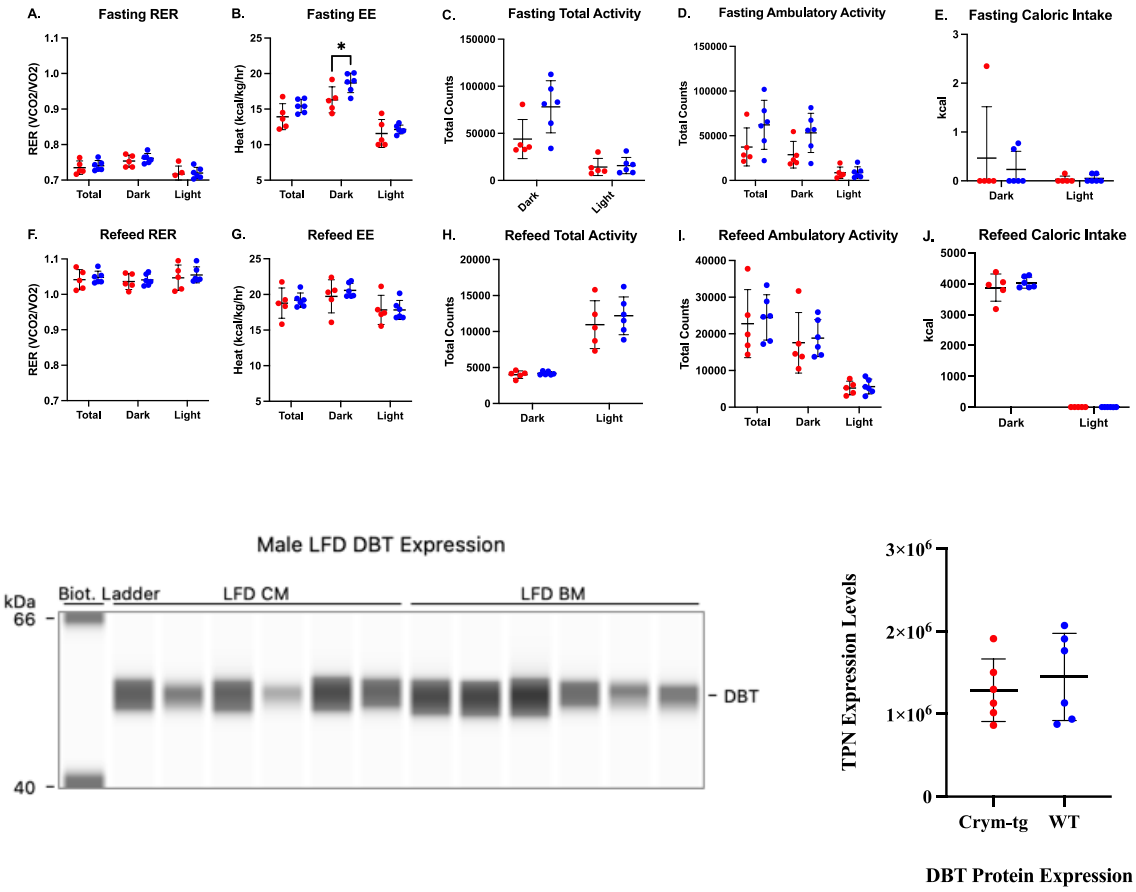

Figure A.3. Protein Expression Levels of Dbt *in LFD Males.*
Dbt protein expression as measured via capillary-based immunoassay shows no significant differences in males on LFD.

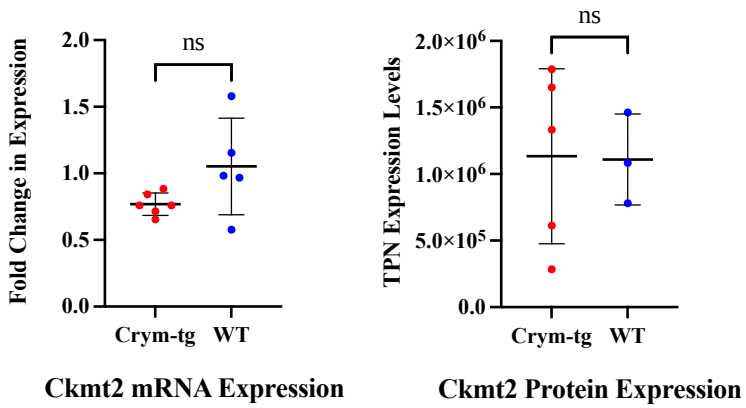

Figure A.4. mRNA and Protein Expression Levels of Ckmt2 *in LFD Males.*
Ckmt2 protein expression as measured via capillary-based immunoassay shows no significant differences in males on LFD.

High-Fat Diet Data

Table A.A. Complete CLAMS calorimetry data for all HFD experiments.
Indirect calorimetry analyses of male and female *Crym*-tg and WT littermates following 16 weeks of HFD. All data are expressed as means + SD. All significant data ($p < 0.05$) are noted by being bolded and underlined and trending values ($p < 0.09$) *italicized*. Key: WT, wildtype; VO2, rate of oxygen consumption; VCO2, rate of carbon dioxide production; RER, respiratory exchange ratio; EE, energy expenditure.

	WT		Crym-tg		p-value	WT		Crym-tg		p-value	WT		Crym-tg		p-value
	Mean	St Dev	Mean	St Dev		Mean	St Dev	Mean	St Dev		Mean	St Dev	Mean	St Dev	
Male, High Fat diet	*Ad libitum, dark cycle*					*Ad libitum, light cycle*					*Ad libitum, 24 h*				
n	5		8			5		8			5		8		
Body weight, g											47.6940	5.4289	49.7988	4.1569	0.4449
Food Intake, kcal	10.9097	1.9924	8.7882	1.4767	*0.0591*	4.3597	1.4227	1.7966	0.8464	**0.0028**	15.2694	3.3278	10.6634	2.1037	**0.0103**
VO2, ml/kgLM/h	2608.8197	246.1511	2310.9612	164.6271	**0.0231**	2152.7586	240.5143	1948.0474	167.0450	0.0955	2382.8772	242.8667	2129.5043	164.7972	**0.0452**
VCO2, mg/kg/LM/h	2061.5116	204.9080	1805.7716	137.7344	**0.0202**	1709.4894	205.5971	1507.9224	127.7029	**0.0498**	1887.1123	205.1271	1656.8470	131.3969	**0.0300**
RER, VCO2/VO2	0.7898	0.0090	0.7800	0.0163	0.2514	0.7930	0.0111	0.7735	0.0125	**0.0159**	0.7914	0.0099	0.7768	0.0139	*0.0671*
EE, kcal/kgLM/h	12.4924	0.3802	11.0422	0.7897	**0.0220**	10.3193	0.2715	9.2888	0.7942	*0.0832*	11.4158	0.6351	10.1655	0.7866	**0.0411**
Total activity, beam breaks	23912.0000	2956.4745	23487.5000	4114.3587	0.8456	7264.2000	1588.9282	6495.8750	1722.7314	0.4382	31176.2000	4155.4767	29983.3750	5486.8039	0.6862
Ambulatory Activity, counts	11116.6000	2193.9698	10842.8750	2948.8077	0.8620	2562.0000	1131.2805	1774.0000	799.2861	0.1669	13678.6000	2976.2583	12616.8750	3585.3837	0.5923
	Fasting, dark cycle					*Fasting, light cycle*					*Fasting, 24 h*				
Food Intake, kcal	0.0000	0.0000	0.0000	0.0000		0.0000	0.0000	0.0000	0.0000		0.0000	0.0000	0.0000	0.0000	
VO2, ml/kgLM/h	2358.6414	293.5440	2056.0627	180.7139	**0.0402**	1858.7103	213.5274	1730.0685	163.2586	0.2436	2108.6759	253.3843	1892.6096	165.0236	*0.0870*
VCO2, mg/kg/LM/h	1742.3931	205.2091	1516.5737	130.3213	**0.0322**	1382.3379	146.9897	1286.4978	115.0500	0.2144	1562.3655	175.7870	1401.2105	117.5412	*0.0711*
RER, VCO2/VO2	0.7384	0.0069	0.7374	0.0034	0.7201	0.7453	0.0123	0.7440	0.0056	0.8018	0.7419	0.0094	0.7407	0.0044	0.7672
EE, kcal/kgLM/h	11.1476	0.0000	9.7130	0.8531	**0.0385**	8.7945	0.0000	8.1833	0.7679	0.2362	9.9710	0.0000	8.9461	0.7775	*0.0833*
Total activity, beam breaks	25752.0000	3499.5136	21231.2500	5822.4748	0.1484	7693.0000	1532.2247	6142.7500	1312.1732	*0.0774*	33445.0000	4827.2902	27374.0000	6310.8692	0.0943
Ambulatory Activity, counts	13516.2000	2612.3029	10481.0000	4182.7341	0.1769	3102.8000	1012.4449	1993.0000	938.3858	*0.0690*	16619.0000	3522.7462	12474.0000	4709.3941	0.1202
	Refeed, dark cycle					*Refeed, light cycle*					*Refeed, 24 h*				
Food Intake, kcal	11.3498	1.4628	9.9785	2.6093	0.3168	4.6846	1.9015	2.7023	1.0119	**0.0401**	16.0344	2.9486	12.6808	3.2182	0.0956
VO2, ml/kgLM/h	2535.0815	279.0721	2327.2269	221.6663	0.1634	2143.0071	214.1433	1949.9286	181.1481	0.1084	2335.4800	241.2346	2135.1477	198.1485	0.1301
VCO2, mg/kg/LM/h	1971.8963	216.0653	1781.0602	169.2347	0.1020	1695.2714	184.2583	1518.5848	154.0834	*0.0882*	1831.0691	196.1409	1647.4364	158.4716	*0.0897*
RER, VCO2/VO2	0.7783	0.0165	0.7657	0.0078	*0.0855*	0.7901	0.0147	0.7780	0.0162	0.2009	0.7843	0.0153	0.7719	0.0112	0.1192
EE, kcal/kgLM/h	12.1015	0.2792	11.0727	1.0560	0.1487	10.2629	0.3629	9.3054	0.8787	0.1012	11.1655	0.5627	10.1730	0.9511	0.1192
Total activity, beam breaks	22176.0000	4865.5906	24089.7500	4064.8880	0.4589	7978.2000	957.4000	7819.5000	2104.3472	0.8782	30154.2000	5033.5076	31909.2500	4650.8418	0.5339
Ambulatory Activity, counts	10849.0000	3505.3721	11662.7500	3181.4452	0.6740	3060.0000	798.1905	2927.8750	1207.3567	0.8335	13909.0000	4056.5832	14590.6250	3636.9300	0.7586
	Wheel, dark cycle					*Wheel, light cycle*					*Wheel, 24 h*				
Food Intake, kcal	11.1298	3.4242	10.8169	1.4799	0.8317	16.0658	5.0764	13.6044	0.9763	0.1989	16.0658	5.0764	13.6044	0.9763	0.1989
VO2, ml/kgLM/h	2463.1172	342.4687	2170.4135	219.7815	*0.0846*	2262.7393	327.0603	1984.9752	209.0781	*0.0859*	2262.7393	327.0603	1984.9752	209.0781	*0.0859*
VCO2, mg/kg/LM/h	1966.8414	256.8407	1748.0111	154.4711	*0.0785*	1800.6143	245.3758	1585.2092	150.4472	*0.0729*	1800.6143	245.3758	1585.2092	150.4472	*0.0729*
RER, VCO2/VO2	0.7998	0.0246	0.8064	0.0203	0.6080	0.7966	0.0234	0.7986	0.0174	0.8645	0.7966	0.0234	0.7986	0.0174	0.8645
EE, kcal/kgLM/h	11.8193	0.6535	10.4347	1.0253	0.0829	9.8104	0.3304	8.5593	0.9589	*0.0884*	10.8507	0.9688	9.5248	0.9801	*0.0821*
Total activity, beam breaks	22476.8000	5971.6216	20125.3750	3802.8758	0.3998	28538.2000	6306.2512	25988.3750	4331.0358	0.4026	28538.2000	6306.2512	25988.3750	4331.0358	0.4026
Ambulatory Activity, counts	8005.6000	759.1484	8309.5000	2342.5082	0.7869	9784.4000	636.6253	10084.8750	2841.0292	0.8228	9784.4000	636.6253	10084.8750	2841.0292	0.8228
Wheel Activity, counts	884.2000	621.3169	441.8000	376.1007	0.2103	923.8000	630.7184	472.4000	370.1348	0.2049	923.8000	630.7184	472.4000	370.1348	0.2049
Female, High Fat diet	*Ad libitum, dark cycle*					*Ad libitum, light cycle*					*Ad libitum, 24 h*				
n	5		6			5		6			5		6		
Body weight, g											34.3460	3.2015	28.7533	3.1905	**0.0179**
Food Intake, kcal	9.2538	3.5226	12.4083	3.7570	0.2080	2.6619	1.0271	2.4104	0.8610	0.6858	11.9158	3.9725	14.2441	3.5514	0.3313
VO2, ml/kgLM/h	2955.8897	197.5050	3337.3013	289.8698	**0.0345**	2505.2345	101.3094	2714.1207	189.1807	*0.0548*	2730.5621	140.3959	3020.9628	231.9885	**0.0374**
VCO2, mg/kg/LM/h	2319.7379	127.4577	2610.8126	191.9372	**0.0179**	1939.4069	68.9719	2114.1494	165.2342	*0.0558*	2129.5724	90.3079	2358.7609	173.7780	**0.0265**
RER, VCO2/VO2	0.7837	0.0171	0.7830	0.0254	0.9596	0.7732	0.0066	0.7780	0.0163	0.5517	0.7785	0.0112	0.7805	0.0182	0.8324
EE, kcal/kgLM/h	14.1345	0.9032	15.9467	1.3273	**0.0295**	11.9434	0.4718	12.9575	0.9201	*0.0536*	13.0390	0.6437	14.4294	1.0900	**0.0339**
Total activity, beam breaks	31044.0000	12727.3350	39790.3333	9028.4372	0.2150	9474.8000	4474.2287	12176.6667	2643.6463	0.2435	40518.8000	15163.6809	51967.0000	11263.7520	0.1841
Ambulatory Activity, counts	19129.4000	11692.1865	19955.1667	5869.5467	0.8821	4601.0000	1002.0192	4631.1667	1477.8279	0.9700	23730.4000	12380.3695	24586.3333	7242.8721	0.8892
	Fasting, dark cycle					*Fasting, light cycle*					*Fasting, 24 h*				
Food Intake, kcal	0.0000	0.0000	0.0000	0.0000		0.0000	0.0000	0.0000	0.0000		0.0000	0.0000	0.0000	0.0000	
VO2, ml/kgLM/h	2701.2414	277.7272	3057.0402	248.7328	*0.0516*	2074.6756	131.6030	2252.2529	236.3392	0.1704	2389.2416	184.1330	2654.6466	225.2888	*0.0644*
VCO2, mg/kg/LM/h	1971.9724	204.2016	2291.3966	254.5679	*0.0503*	1538.6862	98.3290	1706.8506	212.1959	0.1392	1756.2062	138.0202	1999.1236	225.8794	*0.0661*
RER, VCO2/VO2	0.7306	0.0068	0.7490	0.0277	0.1846	0.7419	0.0056	0.7571	0.0158	*0.0722*	0.7362	0.0059	0.7530	0.0216	0.1280
EE, kcal/kgLM/h	12.7352	1.3098	14.4902	1.2556	**0.0498**	9.8142	0.6197	10.6966	1.1614	0.1630	11.2807	0.8698	12.5934	1.1350	*0.0637*
Total activity, beam breaks	40592.6000	16136.0270	50618.0000	16173.7122	0.3322	8563.2000	2173.0252	12815.0000	6177.7424	0.1797	49155.8000	17920.3545	63433.0000	21343.7033	0.2663
Ambulatory Activity, counts	28269.2000	14288.5615	29488.6667	12082.9943	0.8813	4834.4000	1876.4339	6396.8333	4570.0561	0.4951	33103.6000	15878.1578	35885.5000	16094.0675	0.7805
	Refeed, dark cycle					*Refeed, light cycle*					*Refeed, 24 h*				
Food Intake, kcal	11.7690	2.4987	13.6135	2.6353	0.2890	4.1710	0.8773	3.8986	1.5117	0.7364	15.9401	3.3348	17.5121	3.4519	0.4848
VO2, ml/kgLM/h	2840.0425	263.4236	3080.7693	324.1538	0.2159	2533.2345	222.3944	2792.2976	185.6041	*0.0641*	2675.7851	226.0656	2931.1998	223.3978	0.0931
VCO2, mg/kg/LM/h	2259.5280	212.7250	2500.9002	215.5761	0.0958	1949.1862	191.0743	2227.7321	164.2609	**0.0286**	2093.3777	188.2296	2359.1859	148.1667	**0.0275**
RER, VCO2/VO2	0.7949	0.0159	0.8135	0.0258	0.1948	0.7694	0.0128	0.8002	0.0341	0.0909	0.7812	0.0139	0.8066	0.0300	0.1183
EE, kcal/kgLM/h	13.6210	1.2672	14.8337	1.4939	0.1857	12.0669	1.0788	13.3969	0.8822	*0.0507*	12.7890	1.0907	14.0886	1.0162	*0.0713*
Total activity, beam breaks	28215.8000	9508.8070	30688.3333	5505.5757	0.6018	13253.8000	2064.8988	14497.6667	2882.2993	0.4415	41469.6000	10665.4760	45186.0000	5825.5758	0.4801
Ambulatory Activity, counts	17307.4000	8835.9714	15261.5000	2695.0104	0.6004	7648.4000	2273.2811	6033.0000	1854.6126	0.2257	24955.8000	10450.4886	21294.5000	3523.8525	0.4377
	Wheel, dark cycle					*Wheel, light cycle*					*Wheel, 24 h*				
Food Intake, kcal	12.5550	1.9418	13.1629	5.3775	0.8181	3.0182	0.4768	3.6156	1.2466	0.3462	15.5733	1.9924	16.2091	5.6844	0.8184
VO2, ml/kgLM/h	3164.3692	313.8547	3573.1667	500.9351	0.1492	2561.6778	164.2551	2767.5000	312.8166	0.2196	2871.7750	242.7022	3184.7202	399.1551	0.1613
VCO2, mg/kg/LM/h	2550.2643	227.4269	2875.8966	343.6900	0.1043	2003.0299	133.1848	2189.3889	242.2679	0.1605	2284.7143	182.8552	2544.9018	285.8550	0.1140
RER, VCO2/VO2	0.8051	0.0121	0.8071	0.0306	0.8938	0.7804	0.0031	0.7906	0.0237	0.3688	0.7931	0.0053	0.7991	0.0270	0.6396
EE, kcal/kgLM/h	15.2134	1.4741	17.1724	2.3235	0.1387	12.2392	0.7899	13.2549	1.4851	0.2043	13.7696	1.1498	15.2836	1.8658	0.1498
Total activity, beam breaks	38728.2000	7903.9669	63062.0000	32024.5602	0.1346	13359.6000	3250.3313	13778.0000	7909.0755	0.9148	52087.8000	10581.6672	76840.0000	37955.0478	0.1945
Ambulatory Activity, counts	23166.6000	12766.8871	28315.8333	23409.4707	0.6717	7828.2000	4322.2612	5612.3333	4972.9645	0.4557	30994.8000	17006.5321	33928.1667	27525.3647	0.8409
Wheel Activity, counts	6036.7500	5317.9189	9781.1667	7009.0076	0.3931	640.7500	591.0975	655.3333	802.2660	0.9761	6677.5000	5833.5977	10436.5000	7569.9330	0.4277

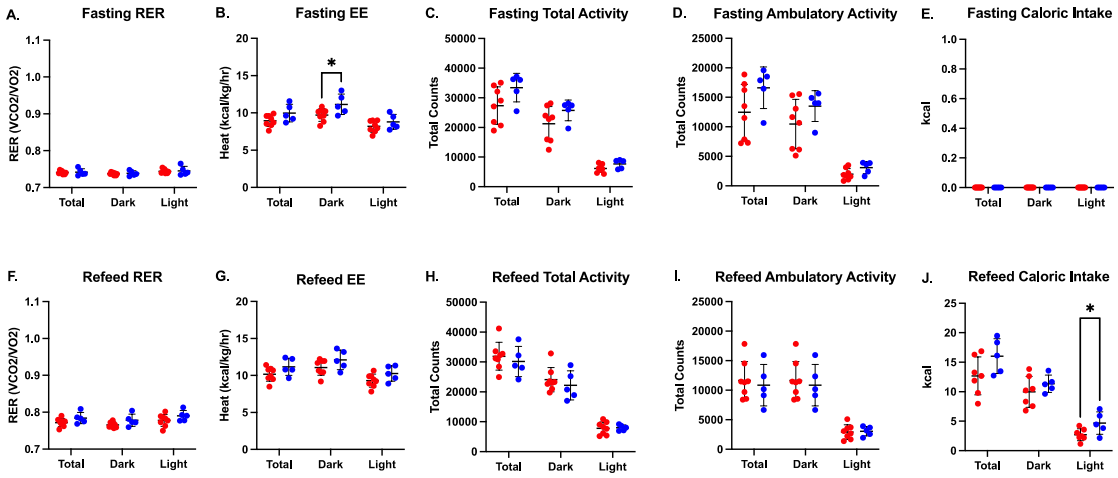

Figure A.5. CLAMS data for fasting and refeed conditions in males following high-fat diet intervention.

Male *Crym*-tg on HFD fast show a (B) decreased EE throughout the dark cycle compared to WT, with no significant changes in (A) RER, (C) total activity, (D) ambulatory activity and (E) caloric intake. During refeeding, male *Crym*-tg mice on HFD show (J) a decreased caloric intake during the light cycle refeeding after fasting with no changes in (F) refeed RER, (G) refeed EE, (H) refeed total activity, (I) ambulatory activity. ($p < 0.05$) *Crym*-tg are labeled in red and WT in blue.

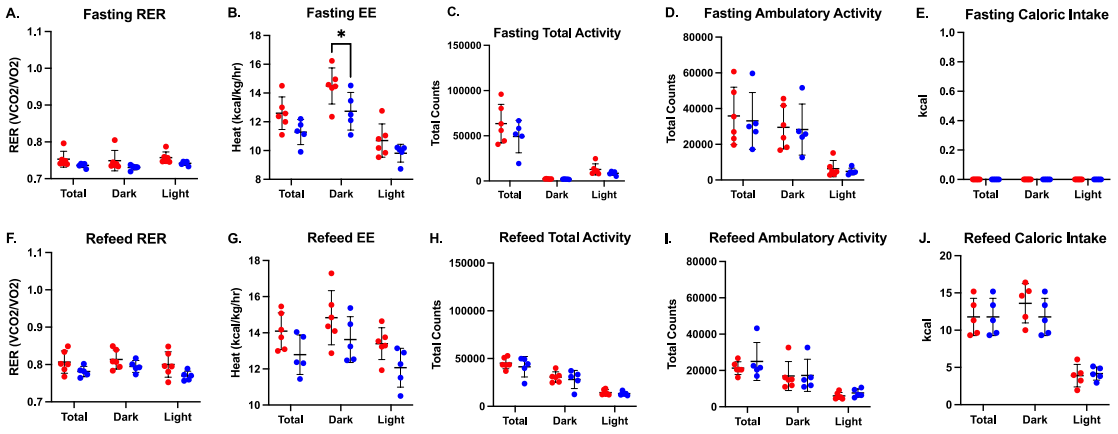

Figure A.6. CLAMS data for fasting and refeed conditions in females following high-fat diet intervention.

During fasting conditions female *Crym*-tg on HFD show (B) an increased EE throughout the light cycle compared to WT, with no changes in (A) fasting RER, (C) total activity, (D) ambulatory activity or (E) caloric intake. There are no significant differences during the refeeding period in (F) RER, (G) EE, (H) total activity, (I) ambulatory activity, and (J) caloric intake. ($p < 0.05$). *Crym*-tg are labeled in red and WT in blue.

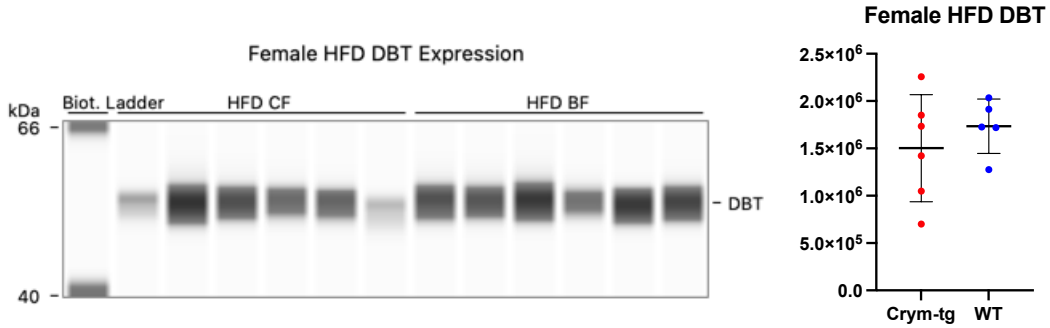

Figure A.7. Total protein normalized expression of Dbt *in HFD females.*
Protein expression levels of *Dbt* in HFD female mice does not significantly differ between *Crym*-tg and WT mice.

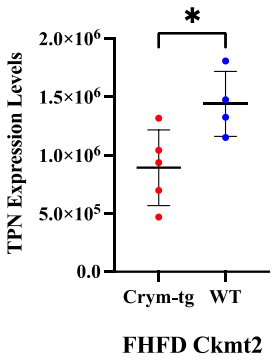

Figure A.8. Ckmt2 *Protein Expression in FHFD.*
Mitochondrial creatine kinase 2 protein expression is statistically significantly decreased HFD female *Crym*-tg mice.

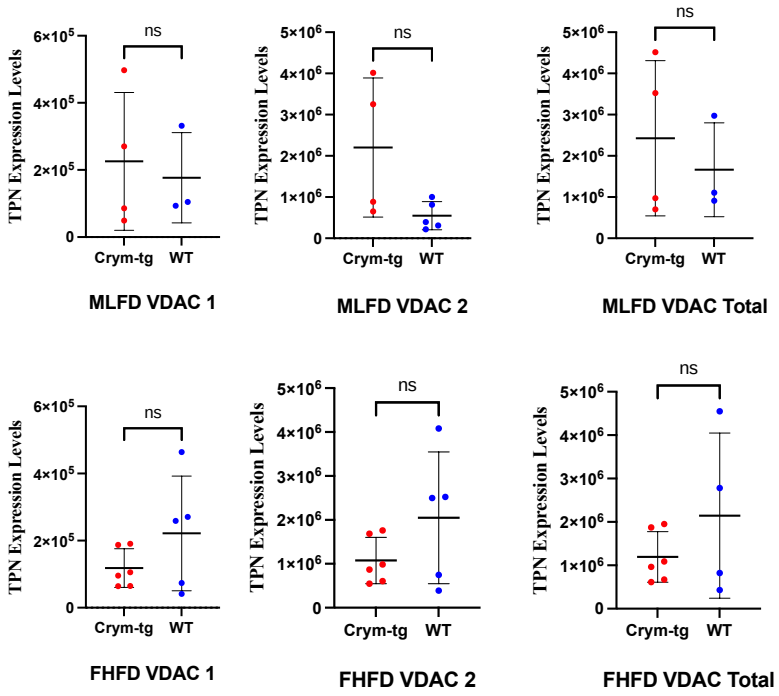

Figure A.9. VDAC protein expression in males on LFD and females on HFD.
There are no significant differences in protein level expression of *VDAC* in either LFD males or HFD females.

Gene Symbol	Gene Name	Ensembl ID	Unique Assay Id	Splice Variant(s) Targeted
Ube2d1	Ubiquitin-conjugating enzyme E2D 1, UBC4/5 homolog (yeast)	ENSMUSG00000019927	qMmuCID0006128	ENSMUST00000020085
Esr1	Estrogen receptor 1 (alpha)	ENSMUSG00000019768	qMmuCID0018069	ENSMUST00000105590 ENSMUST00000067086 ENSMUST00000105589
Calm3	Calmodulin 3	ENSMUSG00000019370	qMmuCED0045370	ENSMUST00000019514
Ppargc1a	Peroxisome proliferative activated receptor, gamma, coactivator 1 alpha	ENSMUSG00000029167	qMmuCID0006032	ENSMUST00000132734 ENSMUST00000151104 ENSMUST00000127135
Pik3r1	Phosphatidylinositol 3-kinase, regulatory subunit, polypeptide 1 (p85 alpha)	ENSMUSG00000041417	qMmuCID0005532	ENSMUST00000055518 ENSMUST00000035532
Mib1	Mindbomb homolog 1 (Drosophila)	ENSMUSG00000024294	qMmuCID0023135	ENSMUST00000052838 ENSMUST00000124288 ENSMUST00000165555
Ckmt2	Creatine kinase, mitochondrial 2	ENSMUSG00000021622	qMmuCID0018183	ENSMUST00000022122
Eif4ebp1	Eukaryotic translation initiation factor 4E binding protein 1	ENSMUSG00000031490	qMmuCID0006526	ENSMUST00000033880
Eif4ebp1	Eukaryotic translation initiation factor 4E binding protein 1	ENSMUSG00000031490	qMmuCID0006526	ENSMUST00000033880
Psme4	Proteasome (prosome, macropain) activator subunit 4	ENSMUSG00000040850	qMmuCID0014819	ENSMUST00000041231 ENSMUST00000154757
Irs2	Insulin receptor substrate 2	ENSMUSG00000038894	qMmuCID0021072	ENSMUST00000125544 ENSMUST00000006587 ENSMUST00000040514
Ppara	Peroxisome proliferator activated receptor alpha	ENSMUSG00000022383	qMmuCID0005156	ENSMUST00000109423 ENSMUST00000057979
Nom1	Nucleolar protein with MIF4G domain 1	ENSMUSG00000001569	qMmuCID0012631	ENSMUST00000001611
Deptor	DEP domain containing MTOR-interacting protein	ENSMUSG00000022419	qMmuCID0021861	ENSMUST00000096433 ENSMUST00000100660 ENSMUST00000023056
Stat5b	Signal transducer and activator of transcription 5B	ENSMUSG00000020919	qMmuCED0039632	ENSMUST00000004143 ENSMUST00000107358
Nfkbia	Nuclear factor of kappa light polypeptide gene enhancer in B cells inhibitor, alpha	ENSMUSG00000021025	qMmuCED0045043	ENSMUST00000021413
Crym	Crystallin, mu	ENSMUSG00000030905	qMmuCID0007165	ENSMUST00000033198

Table A.B. Table of Assays used for PrimePCR.

Bibliography

1 Dong, H. & Tsai, S. Y. Mitochondrial Properties in Skeletal Muscle Fiber. *Cells* 12 (2023). https://doi.org:10.3390/cells12172183

2 Huang, T. Y. *et al.* Combined effects of a ketogenic diet and exercise training alter mitochondrial and peroxisomal substrate oxidative capacity in skeletal muscle. *Am J Physiol Endocrinol Metab* 320, E1053-E1067 (2021). https://doi.org:10.1152/ajpendo.00410.2020

3 Liao, B. & Xu, Y. Exercise improves skeletal muscle insulin resistance without reduced basal mTOR/S6K1 signaling in rats fed a high-fat diet. *Eur J Appl Physiol* 111, 2743-2752 (2011). https://doi.org:10.1007/s00421-011-1892-5

4 Pattanakuhar, S., Pongchaidecha, A., Chattipakorn, N. & Chattipakorn, S. C. The effect of exercise on skeletal muscle fibre type distribution in obesity: From cellular levels to clinical application. *Obes Res Clin Pract* 11, 112-132 (2017). https://doi.org:10.1016/j.orcp.2016.09.012

5 Kwak, H. B. Exercise and obesity-induced insulin resistance in skeletal muscle. *Integr Med Res* 2, 131-138 (2013). https://doi.org:10.1016/j.imr.2013.09.004

6 Stanford, K. I. & Goodyear, L. J. Exercise and type 2 diabetes: molecular mechanisms regulating glucose uptake in skeletal muscle. *Adv Physiol Educ* 38, 308-314 (2014). https://doi.org:10.1152/advan.00080.2014

7 Plotkin, D. L., Roberts, M. D., Haun, C. T. & Schoenfeld, B. J. Muscle Fiber Type Transitions with Exercise Training: Shifting Perspectives. *Sports (Basel)* 9 (2021). https://doi.org:10.3390/sports9090127

8 Miro, C. *et al.* Thyroid Hormone Regulates the Lipid Content of Muscle Fibers, Thus Affecting Physical Exercise Performance. *Int J Mol Sci* 24 (2023). https://doi.org:10.3390/ijms241512074

9 Churchward-Venne, T. A., Burd, N. A. & Phillips, S. M. Nutritional regulation of muscle protein synthesis with resistance exercise: strategies to enhance anabolism. *Nutr Metab (Lond)* 9, 40 (2012). https://doi.org:10.1186/1743-7075-9-40

10 Herrenbruck, A. R. & Bollinger, L. M. Role of skeletal muscle autophagy in high-fat-diet-induced obesity and exercise. *Nutr Rev* 78, 56-64 (2020). https://doi.org:10.1093/nutrit/nuz044

11 Hua, N. *et al.* Influence of muscle fiber type composition on early fat accumulation under high-fat diet challenge. *PLoS One* 12, e0182430 (2017). https://doi.org:10.1371/journal.pone.0182430

12 Ishida, A., Kyoya, T., Nakashima, K. & Katsumata, M. Muscle protein metabolism during compensatory growth with changing dietary lysine levels from deficient to sufficient in growing rats. *J Nutr Sci Vitaminol (Tokyo)* 57, 401-408 (2011). https://doi.org:10.3177/jnsv.57.401

13 Jun, L., Robinson, M., Geetha, T., Broderick, T. L. & Babu, J. R. Prevalence and Mechanisms of Skeletal Muscle Atrophy in Metabolic Conditions. *Int J Mol Sci* 24 (2023). https://doi.org:10.3390/ijms24032973

14 Millward, D. J. Interactions between Growth of Muscle and Stature: Mechanisms Involved and Their Nutritional Sensitivity to Dietary Protein: The Protein-Stat Revisited. *Nutrients* 13 (2021). https://doi.org:10.3390/nu13030729

15 Oh, T. S. *et al.* Gender dimorphism in skeletal muscle proteome between lean and diet-induced obese rats. *Cell Physiol Biochem* 28, 981-996 (2011). https://doi.org:10.1159/000335811

16 Pinho, R. A. *et al.* High-fat diet induces skeletal muscle oxidative stress in a fiber type-dependent manner in rats. *Free Radic Biol Med* 110, 381-389 (2017). https://doi.org:10.1016/j.freeradbiomed.2017.07.005

17 Tagawa, T. *et al.* A chronic high-fat diet does not exacerbate muscle atrophy in fast-twitch skeletal muscle of aged mice. *Exp Physiol* 108, 940-945 (2023). https://doi.org:10.1113/EP091106

18 Trajcevski, K. E. *et al.* Enhanced lipid oxidation and maintenance of muscle insulin sensitivity despite glucose intolerance in a diet-induced obesity mouse model. *PLoS One* 8, e71747 (2013). https://doi.org:10.1371/journal.pone.0071747

19 Warfel, J. D. *et al.* A low fat diet ameliorates pathology but retains beneficial effects associated with CPT1b knockout in skeletal muscle. *PLoS One* 12, e0188850 (2017). https://doi.org:10.1371/journal.pone.0188850

20 Bloise, F. F., Cordeiro, A. & Ortiga-Carvalho, T. M. Role of thyroid hormone in skeletal muscle physiology. *J Endocrinol* 236, R57-R68 (2018). https://doi.org:10.1530/JOE-16-0611

21 Brettle, H. *et al.* Sex hormones, intestinal inflammation, and the gut microbiome: Major influencers of the sexual dimorphisms in obesity. *Front Immunol* 13, 971048 (2022). https://doi.org:10.3389/fimmu.2022.971048

22 Gambke, B., Lyons, G. E., Haselgrove, J., Kelly, A. M. & Rubinstein, N. A. Thyroidal and neural control of myosin transitions during development of rat fast and slow muscles. *FEBS Lett* 156, 335-339 (1983). https://doi.org:10.1016/0014-5793(83)80524-9

23 Izumo, S., Nadal-Ginard, B. & Mahdavi, V. All members of the MHC multigene family respond to thyroid hormone in a highly tissue-specific manner. *Science* 231, 597-600 (1986). https://doi.org:10.1126/science.3945800

24 Klover, P., Chen, W., Zhu, B. M. & Hennighausen, L. Skeletal muscle growth and fiber composition in mice are regulated through the transcription factors STAT5a/b: linking growth hormone to the androgen receptor. *FASEB J* 23, 3140-3148 (2009). https://doi.org:10.1096/fj.08-128215

25 Nicolaisen, T. S. *et al.* Thyroid hormone receptor α in skeletal muscle is essential for T3-mediated increase in energy expenditure. *Faseb j* 34, 15480-15491 (2020). https://doi.org:10.1096/fj.202001258RR

26 Simonides, W. S. & van Hardeveld, C. Thyroid hormone as a determinant of metabolic and contractile phenotype of skeletal muscle. *Thyroid* 18, 205-216 (2008). https://doi.org:10.1089/thy.2007.0256

27 Soukup, T. & Smerdu, V. Effect of altered innervation and thyroid hormones on myosin heavy chain expression and fiber type transitions: a mini-review. *Histochem Cell Biol* 143, 123-130 (2015). https://doi.org:10.1007/s00418-014-1276-0

28 Yu, F., Degens, H. & Larsson, L. The influence of thyroid hormone on myosin isoform composition and shortening velocity of single skeletal muscle fibres with special reference to ageing and gender. *Acta Physiol Scand* 167, 313-316 (1999). https://doi.org:10.1046/j.1365-201x.1999.00620.x

29 Zhang, D. *et al.* Thyroid hormone regulates muscle fiber type conversion via miR-133a1. *J Cell Biol* 207, 753-766 (2014). https://doi.org:10.1083/jcb.201406068

30 Zhou, J. *et al.* Thyroid Hormone Status Regulates Skeletal Muscle Response to Chronic Motor Nerve Stimulation. *Front Physiol* 10, 1363 (2019). https://doi.org:10.3389/fphys.2019.01363

31 Frontera, W. R. & Ochala, J. Skeletal muscle: a brief review of structure and function. *Calcif Tissue Int* 96, 183-195 (2015). https://doi.org:10.1007/s00223-014-9915-y

32 Bassel-Duby, R. & Olson, E. N. Signaling pathways in skeletal muscle remodeling. *Annu Rev Biochem* 75, 19-37 (2006). https://doi.org:10.1146/annurev.biochem.75.103004.142622

33 Rogeri, P. S. *et al.* Crosstalk Between Skeletal Muscle and Immune System: Which Roles Do IL-6 and Glutamine Play? *Front Physiol* 11, 582258 (2020). https://doi.org:10.3389/fphys.2020.582258

34 Stanford, K. I. & Goodyear, L. J. Muscle-Adipose Tissue Cross Talk. *Cold Spring Harb Perspect Med* 8 (2018). https://doi.org:10.1101/cshperspect.a029801

35 Periasamy, M., Herrera, J. L. & Reis, F. C. G. Skeletal Muscle Thermogenesis and Its Role in Whole Body Energy Metabolism. *Diabetes Metab J* 41, 327-336 (2017). https://doi.org:10.4093/dmj.2017.41.5.327

36 Luijten, I. H. N., Feldmann, H. M., von Essen, G., Cannon, B. & Nedergaard, J. In the absence of UCP1-mediated diet-induced thermogenesis, obesity is augmented even in the obesity-resistant 129S mouse strain. *Am J Physiol Endocrinol Metab* 316, E729-E740 (2019). https://doi.org:10.1152/ajpendo.00020.2019

37 Allard, C., Miralpeix, C., Lopez-Gambero, A. J. & Cota, D. mTORC1 in energy expenditure: consequences for obesity. *Nat Rev Endocrinol* (2024). https://doi.org:10.1038/s41574-023-00934-0

38 Yakupova, E. I., Bocharnikov, A. D. & Plotnikov, E. Y. Effects of Ketogenic Diet on Muscle Metabolism in Health and Disease. *Nutrients* 14 (2022). https://doi.org:10.3390/nu14183842

39 Argiles, J. M., Campos, N., Lopez-Pedrosa, J. M., Rueda, R. & Rodriguez-Manas, L. Skeletal Muscle Regulates Metabolism via Interorgan Crosstalk: Roles in Health and Disease. *J Am Med Dir Assoc* 17, 789-796 (2016). https://doi.org:10.1016/j.jamda.2016.04.019

40 Essen, B., Jansson, E., Henriksson, J., Taylor, A. W. & Saltin, B. Metabolic characteristics of fibre types in human skeletal muscle. *Acta Physiol Scand* 95, 153-165 (1975). https://doi.org:10.1111/j.1748-1716.1975.tb10038.x

41 Glancy, B. & Balaban, R. S. Energy metabolism design of the striated muscle cell. *Physiol Rev* 101, 1561-1607 (2021). https://doi.org:10.1152/physrev.00040.2020

42 Groeneveld, K. Muscle physiology and its relations to the whole body in health and disease. *Acta Physiol (Oxf)*, e14131 (2024). https://doi.org:10.1111/apha.14131

43 Imbesi, R., D'Agata, V., Musumeci, G. & Castrogiovanni, P. [Skeletal muscle: from development to function]. *Clin Ter* 165, 47-56 (2014). https://doi.org:10.7471/CT.2014.1661

44 Stump, C. S., Henriksen, E. J., Wei, Y. & Sowers, J. R. The metabolic syndrome: role of skeletal muscle metabolism. *Ann Med* 38, 389-402 (2006). https://doi.org:10.1080/07853890600888413

45 Purslow, P. P. The Structure and Role of Intramuscular Connective Tissue in Muscle Function. *Front Physiol* 11, 495 (2020). https://doi.org:10.3389/fphys.2020.00495

46 Schiaffino, S. & Reggiani, C. Fiber types in mammalian skeletal muscles. *Physiol Rev* 91, 1447-1531 (2011). https://doi.org:10.1152/physrev.00031.2010

47 Pette, D. & Staron, R. S. Mammalian skeletal muscle fiber type transitions. *Int Rev Cytol* 170, 143-223 (1997). https://doi.org:10.1016/s0074-7696(08)61622-8

48 Staron, R. S. Human skeletal muscle fiber types: delineation, development, and distribution. *Can J Appl Physiol* 22, 307-327 (1997). https://doi.org:10.1139/h97-020

49 Hilber, K., Galler, S., Gohlsch, B. & Pette, D. Kinetic properties of myosin heavy chain isoforms in single fibers from human skeletal muscle. *FEBS Lett* 455, 267-270 (1999). https://doi.org:10.1016/s0014-5793(99)00903-5

50 Holloszy, J. O. Biochemical adaptations in muscle. Effects of exercise on mitochondrial oxygen uptake and respiratory enzyme activity in skeletal muscle. *J Biol Chem* 242, 2278-2282 (1967).

51 Larsson, L., Edstrom, L., Lindegren, B., Gorza, L. & Schiaffino, S. MHC composition and enzyme-histochemical and physiological properties of a novel fast-twitch motor unit type. *Am J Physiol* 261, C93-101 (1991). https://doi.org:10.1152/ajpcell.1991.261.1.C93

52 Pette, D. & Staron, R. S. Myosin isoforms, muscle fiber types, and transitions. *Microsc Res Tech* 50, 500-509 (2000). https://doi.org:10.1002/1097-0029(20000915)50:6<500::AID-JEMT7>3.0.CO;2-7

53 Schiaffino, S. Muscle fiber type diversity revealed by anti-myosin heavy chain antibodies. *FEBS J* 285, 3688-3694 (2018). https://doi.org:10.1111/febs.14502

54 Scott, W., Stevens, J. & Binder-Macleod, S. A. Human skeletal muscle fiber type classifications. *Phys Ther* 81, 1810-1816 (2001).

55 Vasileiadou, O. *et al.* Redox Profile of Skeletal Muscles: Implications for Research Design and Interpretation. *Antioxidants (Basel)* 12 (2023). https://doi.org:10.3390/antiox12091738

56 Barany, M. ATPase activity of myosin correlated with speed of muscle shortening. *J Gen Physiol* 50, Suppl:197-218 (1967). https://doi.org:10.1085/jgp.50.6.197

57 Medler, S. Mixing it up: the biological significance of hybrid skeletal muscle fibers. *J Exp Biol* 222 (2019). https://doi.org:10.1242/jeb.200832

58 Murgia, M. *et al.* Protein profile of fiber types in human skeletal muscle: a single-fiber proteomics study. *Skelet Muscle* 11, 24 (2021). https://doi.org:10.1186/s13395-021-00279-0

59 Mukund, K. & Subramaniam, S. Skeletal muscle: A review of molecular structure and function, in health and disease. *Wiley Interdiscip Rev Syst Biol Med* 12, e1462 (2020). https://doi.org:10.1002/wsbm.1462

60 Serrano, N., Hyatt, J. K., Houmard, J. A., Murgia, M. & Katsanos, C. S. Muscle fiber phenotype: a culprit of abnormal metabolism and function in skeletal muscle of humans with obesity. *Am J Physiol Endocrinol Metab* 325, E723-E733 (2023). https://doi.org:10.1152/ajpendo.00190.2023

61 Graziotti, G. H., Rios, C. M. & Rivero, J. L. Evidence for three fast myosin heavy chain isoforms in type II skeletal muscle fibers in the adult llama (Lama glama). *J Histochem Cytochem* 49, 1033-1044 (2001). https://doi.org:10.1177/002215540104900811

62 Lefaucheur, L. *et al.* Evidence for three adult fast myosin heavy chain isoforms in type II skeletal muscle fibers in pigs. *J Anim Sci* 76, 1584-1593 (1998). https://doi.org:10.2527/1998.7661584x

63 Schiaffino, S. *et al.* Three myosin heavy chain isoforms in type 2 skeletal muscle fibres. *J Muscle Res Cell Motil* 10, 197-205 (1989). https://doi.org:10.1007/BF01739810

64 Schiaffino, S. *et al.* Myosin heavy chain isoforms and velocity of shortening of type 2 skeletal muscle fibres. *Acta Physiol Scand* 134, 575-576 (1988). https://doi.org:10.1111/j.1748-1716.1998.tb08539.x

65 Bottinelli, R., Schiaffino, S. & Reggiani, C. Force-velocity relations and myosin heavy chain isoform compositions of skinned fibres from rat skeletal muscle. *J Physiol* 437, 655-672 (1991). https://doi.org:10.1113/jphysiol.1991.sp018617

66 Bottinelli, R., Betto, R., Schiaffino, S. & Reggiani, C. Maximum shortening velocity and coexistence of myosin heavy chain isoforms in single skinned fast fibres of rat skeletal muscle. *J Muscle Res Cell Motil* 15, 413-419 (1994). https://doi.org:10.1007/BF00122115

67 DeNardi, C. *et al.* Type 2X-myosin heavy chain is coded by a muscle fiber type-specific and developmentally regulated gene. *J Cell Biol* 123, 823-835 (1993). https://doi.org:10.1083/jcb.123.4.823

68 Talmadge, R. J., Roy, R. R. & Edgerton, V. R. Muscle fiber types and function. *Curr Opin Rheumatol* 5, 695-705 (1993). https://doi.org:10.1097/00002281-199305060-00002

69 Needham, D. M. Red and White Muscle. *Physiological Reviews* 6, 1-27 (1926).

70 Nemeth, P. M. & Lowry, O. H. Myoglobin levels in individual human skeletal muscle fibers of different types. *J Histochem Cytochem* 32, 1211-1216 (1984). https://doi.org:10.1177/32.11.6491255

71 Edstrom, L. & Kugelberg, E. Histochemical composition, distribution of fibres and fatiguability of single motor units. Anterior tibial muscle of the rat. *J Neurol Neurosurg Psychiatry* 31, 424-433 (1968). https://doi.org:10.1136/jnnp.31.5.424

72 Schiaffino, S., Hanzlikova, V. & Pierobon, S. Relations between structure and function in rat skeletal muscle fibers. *J Cell Biol* 47, 107-119 (1970). https://doi.org:10.1083/jcb.47.1.107

73 Baldwin, K. M., Winder, W. W., Terjung, R. L. & Holloszy, J. O. Glycolytic enzymes in different types of skeletal muscle: adaptation to exercise. *Am J Physiol* 225, 962-966 (1973). https://doi.org:10.1152/ajplegacy.1973.225.4.962

74 Miyabara, E. H. *et al.* Thyroid hormone receptor-beta-selective agonist GC-24 spares skeletal muscle type I to II fiber shift. *Cell Tissue Res* 321, 233-241 (2005). https://doi.org:10.1007/s00441-005-1119-3

75 Zumbaugh, M. D., Johnson, S. E., Shi, T. H. & Gerrard, D. E. Molecular and biochemical regulation of skeletal muscle metabolism. *Journal of Animal Science* 100 (2022). https://doi.org:10.1093/jas/skac035

76 Evans, P. L., McMillin, S. L., Weyrauch, L. A. & Witczak, C. A. Regulation of Skeletal Muscle Glucose Transport and Glucose Metabolism by Exercise Training. *Nutrients* 11 (2019). https://doi.org:10.3390/nu11102432

77 Hulett, N. A., Scalzo, R. L. & Reusch, J. E. B. Glucose Uptake by Skeletal Muscle within the Contexts of Type 2 Diabetes and Exercise: An Integrated Approach. *Nutrients* 14 (2022). https://doi.org:10.3390/nu14030647

78 Kjobsted, R. *et al.* AMPK in skeletal muscle function and metabolism. *FASEB J* 32, 1741-1777 (2018). https://doi.org:10.1096/fj.201700442R

79 Merz, K. E. & Thurmond, D. C. Role of Skeletal Muscle in Insulin Resistance and Glucose Uptake. *Compr Physiol* 10, 785-809 (2020). https://doi.org:10.1002/cphy.c190029

80 Ploug, T., van Deurs, B., Ai, H., Cushman, S. W. & Ralston, E. Analysis of GLUT4 distribution in whole skeletal muscle fibers: identification of distinct storage compartments that are recruited by insulin and muscle contractions. *J Cell Biol* 142, 1429-1446 (1998). https://doi.org:10.1083/jcb.142.6.1429

81 Wang, J. *et al.* BCAA Catabolic Defect Alters Glucose Metabolism in Lean Mice. *Front Physiol* 10, 1140 (2019). https://doi.org:10.3389/fphys.2019.01140

82 Wright, D. C., Hucker, K. A., Holloszy, J. O. & Han, D. H. Ca2+ and AMPK both mediate stimulation of glucose transport by muscle contractions. *Diabetes* 53, 330-335 (2004). https://doi.org:10.2337/diabetes.53.2.330

83 Brooks, D. C., Bessey, P. Q., Black, P. R., Aoki, T. T. & Wilmore, D. W. Insulin stimulates branched chain amino acid uptake and diminishes nitrogen flux from skeletal muscle of injured patients. *J Surg Res* 40, 395-405 (1986). https://doi.org:10.1016/0022-4804(86)90205-2

84 Ishikawa, T. *et al.* Muscle-specific deletion of BDK amplifies loss of myofibrillar protein during protein undernutrition. *Sci Rep* 7, 39825 (2017). https://doi.org:10.1038/srep39825

85 Mann, G., Mora, S., Madu, G. & Adegoke, O. A. J. Branched-chain Amino Acids: Catabolism in Skeletal Muscle and Implications for Muscle and Whole-body Metabolism. *Front Physiol* 12, 702826 (2021). https://doi.org:10.3389/fphys.2021.702826

86 May, M. E. & Buse, M. G. Effects of branched-chain amino acids on protein turnover. *Diabetes Metab Rev* 5, 227-245 (1989). https://doi.org:10.1002/dmr.5610050303

87 She, P. *et al.* Disruption of BCAA metabolism in mice impairs exercise metabolism and endurance. *J Appl Physiol (1985)* 108, 941-949 (2010). https://doi.org:10.1152/japplphysiol.01248.2009

88 Beaudry, K. M. & Devries, M. C. Sex-based differences in hepatic and skeletal muscle triglyceride storage and metabolism (1). *Appl Physiol Nutr Metab* 44, 805-813 (2019). https://doi.org:10.1139/apnm-2018-0635

89 Biral, D. *et al.* Gender- and thyroid hormone-related transitions of essential myosin light chain isoform expression in rat soleus muscle during ageing. *Acta Physiol Scand* 167, 317-323 (1999). https://doi.org:10.1046/j.1365-201x.1999.00621.x

90 Haizlip, K. M., Harrison, B. C. & Leinwand, L. A. Sex-based differences in skeletal muscle kinetics and fiber-type composition. *Physiology (Bethesda)* 30, 30-39 (2015). https://doi.org:10.1152/physiol.00024.2014

91 Lundsgaard, A. M. & Kiens, B. Gender differences in skeletal muscle substrate metabolism - molecular mechanisms and insulin sensitivity. *Front Endocrinol (Lausanne)* 5, 195 (2014). https://doi.org:10.3389/fendo.2014.00195

92 McGowan, E. M., Ehrlicher, S. E., Stierwalt, H. D., Robinson, M. M. & Newsom, S. A. Impact of 4 weeks of western diet and aerobic exercise training on whole-body phenotype and skeletal muscle mitochondrial respiration in male and female mice. *Physiol Rep* 10, e15543 (2022). https://doi.org:10.14814/phy2.15543

93 Nuzzo, J. L. Sex differences in skeletal muscle fiber types: A meta-analysis. *Clin Anat* 37, 81-91 (2024). https://doi.org:10.1002/ca.24091

94 Ryan, A. S., Li, G., McMillin, S. & Ortmeyer, H. K. Sex differences in insulin regulation of skeletal muscle glycogen synthase and changes during weight loss and exercise in adults. *Obesity (Silver Spring)* (2024). https://doi.org:10.1002/oby.23987

95 Welle, S., Tawil, R. & Thornton, C. A. Sex-related differences in gene expression in human skeletal muscle. *PLoS One* 3, e1385 (2008). https://doi.org:10.1371/journal.pone.0001385

96 Egan, B. & Zierath, J. R. Exercise metabolism and the molecular regulation of skeletal muscle adaptation. *Cell Metab* 17, 162-184 (2013). https://doi.org:10.1016/j.cmet.2012.12.012

97 Samuel, V. T. & Shulman, G. I. Mechanisms for insulin resistance: common threads and missing links. *Cell* 148, 852-871 (2012). https://doi.org:10.1016/j.cell.2012.02.017

98 Chang, L., Chiang, S. H. & Saltiel, A. R. Insulin signaling and the regulation of glucose transport. *Mol Med* 10, 65-71 (2004). https://doi.org:10.2119/2005-00029.Saltiel

99 Handberg, A., Kayser, L., Hoyer, P. E. & Vinten, J. A substantial part of GLUT-1 in crude membranes from muscle originates from perineurial sheaths. *Am J Physiol* 262, E721-727 (1992). https://doi.org:10.1152/ajpendo.1992.262.5.E721

100 Alam, Y. H., Kim, R. & Jang, C. Metabolism and Health Impacts of Dietary Sugars. *J Lipid Atheroscler* 11, 20-38 (2022). https://doi.org:10.12997/jla.2022.11.1.20

101 Meijer, A. E. The pentose phosphate pathway in skeletal muscle under patho-physiological conditions. A combined histochemical and biochemical study. *Prog*

Histochem Cytochem 22, 1-118 (1991). https://doi.org:10.1016/s0079-6336(11)80052-5

102 Love, D. C. & Hanover, J. A. The hexosamine signaling pathway: deciphering the "O-GlcNAc code". *Sci STKE* 2005, re13 (2005). https://doi.org:10.1126/stke.3122005re13

103 Petersen, K. F. *et al.* The role of skeletal muscle insulin resistance in the pathogenesis of the metabolic syndrome. *Proc Natl Acad Sci U S A* 104, 12587-12594 (2007). https://doi.org:10.1073/pnas.0705408104

104 Baldwin, K. M. & Haddad, F. Effects of different activity and inactivity paradigms on myosin heavy chain gene expression in striated muscle. *J Appl Physiol (1985)* 90, 345-357 (2001). https://doi.org:10.1152/jappl.2001.90.1.345

105 Bell, R. A., Al-Khalaf, M. & Megeney, L. A. The beneficial role of proteolysis in skeletal muscle growth and stress adaptation. *Skelet Muscle* 6, 16 (2016). https://doi.org:10.1186/s13395-016-0086-6

106 Bechet, D., Tassa, A., Combaret, L., Taillandier, D. & Attaix, D. Regulation of skeletal muscle proteolysis by amino acids. *J Ren Nutr* 15, 18-22 (2005). https://doi.org:10.1053/j.jrn.2004.09.005

107 Mammucari, C. *et al.* FoxO3 controls autophagy in skeletal muscle in vivo. *Cell Metab* 6, 458-471 (2007). https://doi.org:10.1016/j.cmet.2007.11.001

108 Sandri, M. Protein breakdown in muscle wasting: role of autophagy-lysosome and ubiquitin-proteasome. *Int J Biochem Cell Biol* 45, 2121-2129 (2013). https://doi.org:10.1016/j.biocel.2013.04.023

109 Jackman, R. W. & Kandarian, S. C. The molecular basis of skeletal muscle atrophy. *Am J Physiol Cell Physiol* 287, C834-843 (2004). https://doi.org:10.1152/ajpcell.00579.2003

110 Zizzo, J. Muscle Atrophy Classification: The Need for a Pathway-Driven Approach. *Curr Pharm Des* 27, 3012-3019 (2021). https://doi.org:10.2174/1381612824666210316102413

111 Bonaldo, P. & Sandri, M. Cellular and molecular mechanisms of muscle atrophy. *Dis Model Mech* 6, 25-39 (2013). https://doi.org:10.1242/dmm.010389

112 Schiaffino, S., Dyar, K. A., Ciciliot, S., Blaauw, B. & Sandri, M. Mechanisms regulating skeletal muscle growth and atrophy. *FEBS J* 280, 4294-4314 (2013). https://doi.org:10.1111/febs.12253

113 Chen, X. *et al.* Mitochondrial dysfunction: roles in skeletal muscle atrophy. *J Transl Med* 21, 503 (2023). https://doi.org:10.1186/s12967-023-04369-z

114 Franch, H. A. & Price, S. R. Molecular signaling pathways regulating muscle proteolysis during atrophy. *Curr Opin Clin Nutr Metab Care* 8, 271-275 (2005). https://doi.org:10.1097/01.mco.0000165005.01331.45

115 Haddad, F., Roy, R. R., Zhong, H., Edgerton, V. R. & Baldwin, K. M. Atrophy responses to muscle inactivity. I. Cellular markers of protein deficits. *J Appl Physiol (1985)* 95, 781-790 (2003). https://doi.org:10.1152/japplphysiol.00317.2003

116 Haddad, F., Roy, R. R., Zhong, H., Edgerton, V. R. & Baldwin, K. M. Atrophy responses to muscle inactivity. II. Molecular markers of protein deficits. *J Appl Physiol (1985)* 95, 791-802 (2003). https://doi.org:10.1152/japplphysiol.01113.2002

117 Kubat, G. B. *et al.* Mitochondrial dysfunction and skeletal muscle atrophy: Causes, mechanisms, and treatment strategies. *Mitochondrion* 72, 33-58 (2023). https://doi.org:10.1016/j.mito.2023.07.003

118 Holecek, M. Why Are Branched-Chain Amino Acids Increased in Starvation and Diabetes? *Nutrients* 12 (2020). https://doi.org:10.3390/nu12103087

119 She, P. *et al.* Disruption of BCATm in mice leads to increased energy expenditure associated with the activation of a futile protein turnover cycle. *Cell Metab* 6, 181-194 (2007). https://doi.org:10.1016/j.cmet.2007.08.003

120 Shimomura, Y., Obayashi, M., Murakami, T. & Harris, R. A. Regulation of branched-chain amino acid catabolism: nutritional and hormonal regulation of activity and expression of the branched-chain alpha-keto acid dehydrogenase kinase. *Curr Opin Clin Nutr Metab Care* 4, 419-423 (2001). https://doi.org:10.1097/00075197-200109000-00013

121 Xu, M. *et al.* Endurance performance and energy metabolism during exercise in mice with a muscle-specific defect in the control of branched-chain amino acid catabolism. *PLoS One* 12, e0180989 (2017). https://doi.org:10.1371/journal.pone.0180989

122 Suryawan, A. *et al.* A molecular model of human branched-chain amino acid metabolism. *Am J Clin Nutr* 68, 72-81 (1998). https://doi.org:10.1093/ajcn/68.1.72

123 Biswas, D., Duffley, L. & Pulinilkunnil, T. Role of branched-chain amino acid-catabolizing enzymes in intertissue signaling, metabolic remodeling, and energy homeostasis. *FASEB J* 33, 8711-8731 (2019). https://doi.org:10.1096/fj.201802842RR

124 Paul, H. S., Liu, W. Q. & Adibi, S. A. Alteration in gene expression of branched-chain keto acid dehydrogenase kinase but not in gene expression of its substrate in the liver of clofibrate-treated rats. *Biochem J* 317 (Pt 2), 411-417 (1996). https://doi.org:10.1042/bj3170411

125 Edozien, J. C., Niehaus, N., Mar, M. H., Makoui, T. & Switzer, B. R. Diet-hormone interrelationships in the rat. *J Nutr* 108, 1767-1776 (1978). https://doi.org:10.1093/jn/108.11.1767

126 Kobayashi, R., Shimomura, Y., Otsuka, M., Popov, K. M. & Harris, R. A. Experimental hyperthyroidism causes inactivation of the branched-chain alpha-

ketoacid dehydrogenase complex in rat liver. *Arch Biochem Biophys* 375, 55-61 (2000). https://doi.org:10.1006/abbi.1999.1635

127 Shimomura, Y. *et al.* Branched-chain amino acid catabolism in exercise and liver disease. *J Nutr* 136, 250S-253S (2006). https://doi.org:10.1093/jn/136.1.250S

128 Hallen, A., Jamie, J. F. & Cooper, A. J. Lysine metabolism in mammalian brain: an update on the importance of recent discoveries. *Amino Acids* 45, 1249-1272 (2013). https://doi.org:10.1007/s00726-013-1590-1

129 Duan, Y. *et al.* The role of leucine and its metabolites in protein and energy metabolism. *Amino Acids* 48, 41-51 (2016). https://doi.org:10.1007/s00726-015-2067-1

130 Mechanick, J. I., Garber, A. J., Handelsman, Y. & Garvey, W. T. American Association of Clinical Endocrinologists' position statement on obesity and obesity medicine. *Endocr Pract* 18, 642-648 (2012). https://doi.org:10.4158/EP12160.PS

131 Adult Obesity Prevalence Maps. (Centers for Disease Control and Prevention. National Center for Chronic Disease Prevention and Health Promotion, Division of Nutrition, Physical Activity, and Obesity, https://www.cdc.gov/obesity/data/prevalence-maps.html, 2023).

132 *Obesity and Overweight*, <https://www.who.int/news-room/fact-sheets/detail/obesity-and-overweight> (2024).

133 Garvey, W. T. & Mechanick, J. I. Proposal for a Scientifically Correct and Medically Actionable Disease Classification System (ICD) for Obesity. *Obesity (Silver Spring)* 28, 484-492 (2020). https://doi.org:10.1002/oby.22727

134 Choquet, H. & Meyre, D. Genetics of Obesity: What have we Learned? *Curr Genomics* 12, 169-179 (2011). https://doi.org:10.2174/138920211795677895

135 Farooqi, I. S. Monogenic human obesity syndromes. *Handb Clin Neurol* 181, 301-310 (2021). https://doi.org:10.1016/B978-0-12-820683-6.00022-1

136 Haspula, D. & Cui, Z. Neurochemical Basis of Inter-Organ Crosstalk in Health and Obesity: Focus on the Hypothalamus and the Brainstem. *Cells* 12 (2023). https://doi.org:10.3390/cells12131801

137 Heindel, J. J., Lustig, R. H., Howard, S. & Corkey, B. E. Obesogens: a unifying theory for the global rise in obesity. *Int J Obes (Lond)* (2024). https://doi.org:10.1038/s41366-024-01460-3

138 Keller, M., Svensson, S. I. A., Rohde-Zimmermann, K., Kovacs, P. & Bottcher, Y. Genetics and Epigenetics in Obesity: What Do We Know so Far? *Curr Obes Rep* 12, 482-501 (2023). https://doi.org:10.1007/s13679-023-00526-z

139 Koenen, M., Hill, M. A., Cohen, P. & Sowers, J. R. Obesity, Adipose Tissue and Vascular Dysfunction. *Circ Res* 128, 951-968 (2021). https://doi.org:10.1161/CIRCRESAHA.121.318093

140 Koerber-Rosso, I. *et al.* A fresh look to the phenotype in mono-allelic likely pathogenic variants of the leptin and the leptin receptor gene. *Mol Cell Pediatr* 8, 10 (2021). https://doi.org:10.1186/s40348-021-00119-7

141 Kuhnen, P., Krude, H. & Biebermann, H. Melanocortin-4 Receptor Signalling: Importance for Weight Regulation and Obesity Treatment. *Trends Mol Med* 25, 136-148 (2019). https://doi.org:10.1016/j.molmed.2018.12.002

142 Loos, R. J. F. & Yeo, G. S. H. The genetics of obesity: from discovery to biology. *Nat Rev Genet* 23, 120-133 (2022). https://doi.org:10.1038/s41576-021-00414-z

143 Mahmoud, R., Kimonis, V. & Butler, M. G. Genetics of Obesity in Humans: A Clinical Review. *Int J Mol Sci* 23 (2022). https://doi.org:10.3390/ijms231911005

144 Park, H. K. & Ahima, R. S. Endocrine disorders associated with obesity. *Best Pract Res Clin Obstet Gynaecol* 90, 102394 (2023). https://doi.org:10.1016/j.bpobgyn.2023.102394

145 Petito, G. *et al.* Adipose Tissue Remodeling in Obesity: An Overview of the Actions of Thyroid Hormones and Their Derivatives. *Pharmaceuticals (Basel)* 16 (2023). https://doi.org:10.3390/ph16040572

146 Stienstra, R., Duval, C., Muller, M. & Kersten, S. PPARs, Obesity, and Inflammation. *PPAR Res* 2007, 95974 (2007). https://doi.org:10.1155/2007/95974

147 Tschop, M. H. & Friedman, J. M. Seeking satiety: From signals to solutions. *Sci Transl Med* 15, eadh4453 (2023). https://doi.org:10.1126/scitranslmed.adh4453

148 Walley, A. J., Asher, J. E. & Froguel, P. The genetic contribution to non-syndromic human obesity. *Nat Rev Genet* 10, 431-442 (2009). https://doi.org:10.1038/nrg2594

149 Wang, C. Y. & Liao, J. K. A mouse model of diet-induced obesity and insulin resistance. *Methods Mol Biol* 821, 421-433 (2012). https://doi.org:10.1007/978-1-61779-430-8_27

150 West, D. B., Boozer, C. N., Moody, D. L. & Atkinson, R. L. Dietary obesity in nine inbred mouse strains. *Am J Physiol* 262, R1025-1032 (1992). https://doi.org:10.1152/ajpregu.1992.262.6.R1025

151 West, D. B., Waguespack, J. & McCollister, S. Dietary obesity in the mouse: interaction of strain with diet composition. *Am J Physiol* 268, R658-665 (1995). https://doi.org:10.1152/ajpregu.1995.268.3.R658

152 Zhou, F., Tian, G., Cui, Y., He, S. & Yan, Y. Development of genome-wide association studies on childhood obesity and its indicators: A scoping review and enrichment analysis. *Pediatr Obes* 18, e13077 (2023). https://doi.org:10.1111/ijpo.13077

153 Friedman, J. 20 years of leptin: leptin at 20: an overview. *J Endocrinol* 223, T1-8 (2014). https://doi.org:10.1530/JOE-14-0405

154 Friedman, J. M. & Halaas, J. L. Leptin and the regulation of body weight in mammals. *Nature* 395, 763-770 (1998). https://doi.org:10.1038/27376

155 Montague, C. T. *et al.* Congenital leptin deficiency is associated with severe early-onset obesity in humans. *Nature* 387, 903-908 (1997). https://doi.org:10.1038/43185

156 Liu, J., Lai, F., Hou, Y. & Zheng, R. Leptin signaling and leptin resistance. *Med Rev (2021)* 2, 363-384 (2022). https://doi.org:10.1515/mr-2022-0017

157 Malik, N. M. *et al.* Leptin requirement for conception, implantation, and gestation in the mouse. *Endocrinology* 142, 5198-5202 (2001). https://doi.org:10.1210/endo.142.12.8535

158 Metlakunta, A. S., Sahu, M. & Sahu, A. Hypothalamic phosphatidylinositol 3-kinase pathway of leptin signaling is impaired during the development of diet-induced obesity in FVB/N mice. *Endocrinology* 149, 1121-1128 (2008). https://doi.org:10.1210/en.2007-1307

159 Jackson, R. S. *et al.* Obesity and impaired prohormone processing associated with mutations in the human prohormone convertase 1 gene. *Nat Genet* 16, 303-306 (1997). https://doi.org:10.1038/ng0797-303

160 Amin, R. H., Mathews, S. T., Camp, H. S., Ding, L. & Leff, T. Selective activation of PPARgamma in skeletal muscle induces endogenous production of adiponectin and protects mice from diet-induced insulin resistance. *Am J Physiol Endocrinol Metab* 298, E28-37 (2010). https://doi.org:10.1152/ajpendo.00446.2009

161 Ma, X., Wang, D., Zhao, W. & Xu, L. Deciphering the Roles of PPARγ in Adipocytes via Dynamic Change of Transcription Complex. *Frontiers in Endocrinology* 9 (2018). https://doi.org:10.3389/fendo.2018.00473

162 Ohkubo, Y. *et al.* Loss of mu-crystallin causes PPARgamma activation and obesity in high-fat diet-fed mice. *Biochem Biophys Res Commun* 508, 914-920 (2019). https://doi.org:10.1016/j.bbrc.2018.12.038

163 Straczkowski, M. *et al.* Adipose Tissue and Skeletal Muscle Expression of Genes Associated with Thyroid Hormone Action in Obesity and Insulin Resistance. *Thyroid* 32, 206-214 (2022). https://doi.org:10.1089/thy.2021.0351

164 Tyagi, S., Gupta, P., Saini, A. S., Kaushal, C. & Sharma, S. The peroxisome proliferator-activated receptor: A family of nuclear receptors role in various diseases. *J Adv Pharm Technol Res* 2, 236-240 (2011). https://doi.org:10.4103/2231-4040.90879

165 Flores-Dorantes, M. T., Diaz-Lopez, Y. E. & Gutierrez-Aguilar, R. Environment and Gene Association With Obesity and Their Impact on Neurodegenerative and Neurodevelopmental Diseases. *Front Neurosci* 14, 863 (2020). https://doi.org:10.3389/fnins.2020.00863

166 Fisman, E. Z. & Tenenbaum, A. The dual glucose-dependent insulinotropic polypeptide (GIP) and glucagon-like peptide-1 (GLP-1) receptor agonist tirzepatide: a novel cardiometabolic therapeutic prospect. *Cardiovasc Diabetol* 20, 225 (2021). https://doi.org:10.1186/s12933-021-01412-5

167 Ahima, R. S. & Osei, S. Y. Molecular regulation of eating behavior: new insights and prospects for therapeutic strategies. *Trends Mol Med* 7, 205-213 (2001). https://doi.org:10.1016/s1471-4914(01)01989-x

168 Vettor, R., Di Vincenzo, A., Maffei, P. & Rossato, M. Regulation of energy intake and mechanisms of metabolic adaptation or maladaptation after caloric restriction. *Rev Endocr Metab Disord* 21, 399-409 (2020). https://doi.org:10.1007/s11154-020-09565-6

169 Watts, A. G., Kanoski, S. E., Sanchez-Watts, G. & Langhans, W. The physiological control of eating: signals, neurons, and networks. *Physiol Rev* 102, 689-813 (2022). https://doi.org:10.1152/physrev.00028.2020

170 Bairqdar, A., Ivanoshchuk, D. & Shakhtshneider, E. Functionally Significant Variants in Genes Associated with Abdominal Obesity: A Review. *J Pers Med* 13 (2023). https://doi.org:10.3390/jpm13030460

171 Kisielnicka, A. *et al.* The Analysis of a Genome-Wide Association Study (GWAS) of Overweight and Obesity in Psoriasis. *Int J Mol Sci* 23 (2022). https://doi.org:10.3390/ijms23137396

172 Carvalho, L. M. L., Jorge, A. A. L., Bertola, D. R., Krepischi, A. C. V. & Rosenberg, C. A Comprehensive Review of Syndromic Forms of Obesity: Genetic Etiology, Clinical Features and Molecular Diagnosis. *Curr Obes Rep* (2024). https://doi.org:10.1007/s13679-023-00543-y

173 Koves, I. H. & Roth, C. Genetic and Syndromic Causes of Obesity and its Management. *Indian J Pediatr* 85, 478-485 (2018). https://doi.org:10.1007/s12098-017-2502-2

174 Kalinderi, K., Goula, V., Sapountzi, E., Tsinopoulou, V. R. & Fidani, L. Syndromic and Monogenic Obesity: New Opportunities Due to Genetic-Based Pharmacological Treatment. *Children (Basel)* 11 (2024). https://doi.org:10.3390/children11020153

175 Cassidy, S. B., Schwartz, S., Miller, J. L. & Driscoll, D. J. Prader-Willi syndrome. *Genet Med* 14, 10-26 (2012). https://doi.org:10.1038/gim.0b013e31822bead0

176 Khan, M. J., Gerasimidis, K., Edwards, C. A. & Shaikh, M. G. Mechanisms of obesity in Prader-Willi syndrome. *Pediatr Obes* 13, 3-13 (2018). https://doi.org:10.1111/ijpo.12177

177 Khan, S. A. *et al.* Genetics of human Bardet-Biedl syndrome, an updates. *Clin Genet* 90, 3-15 (2016). https://doi.org:10.1111/cge.12737

178 Florea, L., Caba, L. & Gorduza, E. V. Bardet-Biedl Syndrome-Multiple Kaleidoscope Images: Insight into Mechanisms of Genotype-Phenotype Correlations. *Genes (Basel)* 12 (2021). https://doi.org:10.3390/genes12091353

179 Bilezikian, J. P. Hypoparathyroidism. *J Clin Endocrinol Metab* 105, 1722-1736 (2020). https://doi.org:10.1210/clinem/dgaa113

180 Juppner, H. Molecular Definition of Pseudohypoparathyroidism Variants. *J Clin Endocrinol Metab* 106, 1541-1552 (2021). https://doi.org:10.1210/clinem/dgab060

181 Holder, J. L., Jr., Butte, N. F. & Zinn, A. R. Profound obesity associated with a balanced translocation that disrupts the SIM1 gene. *Hum Mol Genet* 9, 101-108 (2000). https://doi.org:10.1093/hmg/9.1.101

182 Ramachandrappa, S. *et al.* Rare variants in single-minded 1 (SIM1) are associated with severe obesity. *J Clin Invest* 123, 3042-3050 (2013). https://doi.org:10.1172/JCI68016

183 Vague, J. Sexual differentiation. A determinant factor of the forms of obesity. 1947. *Obes Res* 4, 201-203 (1996). https://doi.org:10.1002/j.1550-8528.1996.tb00535.x

184 Stubbins, R. E., Holcomb, V. B., Hong, J. & Nunez, N. P. Estrogen modulates abdominal adiposity and protects female mice from obesity and impaired glucose tolerance. *Eur J Nutr* 51, 861-870 (2012). https://doi.org:10.1007/s00394-011-0266-4

185 Clegg, D. J., Brown, L. M., Woods, S. C. & Benoit, S. C. Gonadal hormones determine sensitivity to central leptin and insulin. *Diabetes* 55, 978-987 (2006). https://doi.org:10.2337/diabetes.55.04.06.db05-1339

186 Geary, N. Estradiol, CCK and satiation. *Peptides* 22, 1251-1263 (2001). https://doi.org:10.1016/s0196-9781(01)00449-1

187 Shen, L. *et al.* Estradiol increases the anorectic effect of central apolipoprotein A-IV. *Endocrinology* 151, 3163-3168 (2010). https://doi.org:10.1210/en.2010-0203

188 Zhu, Z., Liu, X., Senthil Kumar, S. P., Zhang, J. & Shi, H. Central expression and anorectic effect of brain-derived neurotrophic factor are regulated by circulating estradiol levels. *Horm Behav* 63, 533-542 (2013). https://doi.org:10.1016/j.yhbeh.2013.01.009

189 Messina, M. M., Boersma, G., Overton, J. M. & Eckel, L. A. Estradiol decreases the orexigenic effect of melanin-concentrating hormone in ovariectomized rats. *Physiol Behav* 88, 523-528 (2006). https://doi.org:10.1016/j.physbeh.2006.05.002

190 Gambacciani, M. *et al.* Body weight, body fat distribution, and hormonal replacement therapy in early postmenopausal women. *J Clin Endocrinol Metab* 82, 414-417 (1997). https://doi.org:10.1210/jcem.82.2.3735

191 Abildgaard, J. *et al.* Menopause is associated with decreased whole body fat oxidation during exercise. *Am J Physiol Endocrinol Metab* 304, E1227-1236 (2013). https://doi.org:10.1152/ajpendo.00492.2012

192 Lovejoy, J. C., Champagne, C. M., de Jonge, L., Xie, H. & Smith, S. R. Increased visceral fat and decreased energy expenditure during the menopausal transition. *Int J Obes (Lond)* 32, 949-958 (2008). https://doi.org:10.1038/ijo.2008.25

193 Musatov, S. *et al.* Silencing of estrogen receptor alpha in the ventromedial nucleus of hypothalamus leads to metabolic syndrome. *Proc Natl Acad Sci U S A* 104, 2501-2506 (2007). https://doi.org:10.1073/pnas.0610787104

194 Xu, Y. *et al.* Distinct hypothalamic neurons mediate estrogenic effects on energy homeostasis and reproduction. *Cell Metab* 14, 453-465 (2011). https://doi.org:10.1016/j.cmet.2011.08.009

195 Palmer, B. F. & Clegg, D. J. The sexual dimorphism of obesity. *Mol Cell Endocrinol* 402, 113-119 (2015). https://doi.org:10.1016/j.mce.2014.11.029

196 Ramirez, M. E. *et al.* Evidence for sex steroid inhibition of lipoprotein lipase in men: comparison of abdominal and femoral adipose tissue. *Metabolism* 46, 179-185 (1997). https://doi.org:10.1016/s0026-0495(97)90299-7

197 Arner, P., Lithell, H., Wahrenberg, H. & Bronnegard, M. Expression of lipoprotein lipase in different human subcutaneous adipose tissue regions. *J Lipid Res* 32, 423-429 (1991).

198 Gavin, K. M., Cooper, E. E. & Hickner, R. C. Estrogen receptor protein content is different in abdominal than gluteal subcutaneous adipose tissue of overweight-to-obese premenopausal women. *Metabolism* 62, 1180-1188 (2013). https://doi.org:10.1016/j.metabol.2013.02.010

199 Cypess, A. M. *et al.* Identification and importance of brown adipose tissue in adult humans. *N Engl J Med* 360, 1509-1517 (2009). https://doi.org:10.1056/NEJMoa0810780

200 Nookaew, I. *et al.* Adipose tissue resting energy expenditure and expression of genes involved in mitochondrial function are higher in women than in men. *J Clin Endocrinol Metab* 98, E370-378 (2013). https://doi.org:10.1210/jc.2012-2764

201 Richelsen, B. Increased alpha 2- but similar beta-adrenergic receptor activities in subcutaneous gluteal adipocytes from females compared with males. *Eur J Clin Invest* 16, 302-309 (1986). https://doi.org:10.1111/j.1365-2362.1986.tb01346.x

202 Despres, J. P. & Lemieux, I. Abdominal obesity and metabolic syndrome. *Nature* 444, 881-887 (2006). https://doi.org:10.1038/nature05488

203 Despres, J. P. *et al.* Role of deep abdominal fat in the association between regional adipose tissue distribution and glucose tolerance in obese women. *Diabetes* 38, 304-309 (1989). https://doi.org:10.2337/diab.38.3.304

204 Pouliot, M. C. *et al.* Visceral obesity in men. Associations with glucose tolerance, plasma insulin, and lipoprotein levels. *Diabetes* 41, 826-834 (1992). https://doi.org:10.2337/diab.41.7.826

205 Wajchenberg, B. L. Subcutaneous and visceral adipose tissue: their relation to the metabolic syndrome. *Endocr Rev* 21, 697-738 (2000). https://doi.org:10.1210/edrv.21.6.0415

206 Janssen, I., Katzmarzyk, P. T. & Ross, R. Waist circumference and not body mass index explains obesity-related health risk. *Am J Clin Nutr* 79, 379-384 (2004). https://doi.org:10.1093/ajcn/79.3.379

207 Zhang, C., Rexrode, K. M., van Dam, R. M., Li, T. Y. & Hu, F. B. Abdominal obesity and the risk of all-cause, cardiovascular, and cancer mortality: sixteen years of follow-up in US women. *Circulation* 117, 1658-1667 (2008). https://doi.org:10.1161/CIRCULATIONAHA.107.739714

208 Balkau, B. *et al.* International Day for the Evaluation of Abdominal Obesity (IDEA): a study of waist circumference, cardiovascular disease, and diabetes mellitus in 168,000 primary care patients in 63 countries. *Circulation* 116, 1942-1951 (2007). https://doi.org:10.1161/CIRCULATIONAHA.106.676379

209 de Oliveira, M. *et al.* The roles of triiodothyronine and irisin in improving the lipid profile and directing the browning of human adipose subcutaneous cells. *Mol Cell Endocrinol* 506, 110744 (2020). https://doi.org:10.1016/j.mce.2020.110744

210 Duntas, L. H. & Brenta, G. A Renewed Focus on the Association Between Thyroid Hormones and Lipid Metabolism. *Front Endocrinol (Lausanne)* 9, 511 (2018). https://doi.org:10.3389/fendo.2018.00511

211 Salvatore, D., Simonides, W. S., Dentice, M., Zavacki, A. M. & Larsen, P. R. Thyroid hormones and skeletal muscle--new insights and potential implications. *Nat Rev Endocrinol* 10, 206-214 (2014). https://doi.org:10.1038/nrendo.2013.238

212 Shahid, M. A., Ashraf, M. A. & Sharma, S. in *StatPearls* (2024).

213 Sinha, R. A., Singh, B. K. & Yen, P. M. Thyroid hormone regulation of hepatic lipid and carbohydrate metabolism. *Trends Endocrinol Metab* 25, 538-545 (2014). https://doi.org:10.1016/j.tem.2014.07.001

214 van der Spek, A. H., Fliers, E. & Boelen, A. The classic pathways of thyroid hormone metabolism. *Mol Cell Endocrinol* 458, 29-38 (2017). https://doi.org:10.1016/j.mce.2017.01.025

215 Wiles, C. M., Young, A., Jones, D. A. & Edwards, R. H. Muscle relaxation rate, fibre-type composition and energy turnover in hyper- and hypo-thyroid patients. *Clin Sci (Lond)* 57, 375-384 (1979). https://doi.org:10.1042/cs0570375

216 Yen, P. M. Physiological and molecular basis of thyroid hormone action. *Physiol Rev* 81, 1097-1142 (2001). https://doi.org:10.1152/physrev.2001.81.3.1097

217 Silva, J. E. Thermogenic mechanisms and their hormonal regulation. *Physiol Rev* 86, 435-464 (2006). https://doi.org:10.1152/physrev.00009.2005

218 Mendoza, A. & Hollenberg, A. N. New insights into thyroid hormone action. *Pharmacol Ther* 173, 135-145 (2017). https://doi.org:10.1016/j.pharmthera.2017.02.012

219 Murolo, M., Di Vincenzo, O., Cicatiello, A. G., Scalfi, L. & Dentice, M. Cardiovascular and Neuronal Consequences of Thyroid Hormones Alterations in

the Ischemic Stroke. *Metabolites* 13 (2022). https://doi.org:10.3390/metabo13010022

220 Gagne, R., Green, J. R., Dong, H., Wade, M. G. & Yauk, C. L. Identification of thyroid hormone receptor binding sites in developing mouse cerebellum. *BMC Genomics* 14, 341 (2013). https://doi.org:10.1186/1471-2164-14-341

221 Gothie, J. D. *et al.* Adult neural stem cell fate is determined by thyroid hormone activation of mitochondrial metabolism. *Mol Metab* 6, 1551-1561 (2017). https://doi.org:10.1016/j.molmet.2017.08.003

222 Bernal, J. Thyroid hormone receptors in brain development and function. *Nat Clin Pract Endocrinol Metab* 3, 249-259 (2007). https://doi.org:10.1038/ncpendmet0424

223 Patel, J., Landers, K., Li, H., Mortimer, R. H. & Richard, K. Thyroid hormones and fetal neurological development. *J Endocrinol* 209, 1-8 (2011). https://doi.org:10.1530/JOE-10-0444

224 Costa-e-Sousa, R. H. & Hollenberg, A. N. Minireview: The neural regulation of the hypothalamic-pituitary-thyroid axis. *Endocrinology* 153, 4128-4135 (2012). https://doi.org:10.1210/en.2012-1467

225 Wu, Y. & Koenig, R. J. Gene regulation by thyroid hormone. *Trends Endocrinol Metab* 11, 207-211 (2000). https://doi.org:10.1016/s1043-2760(00)00263-0

226 Wu, Y., Xu, B. & Koenig, R. J. Thyroid hormone response element sequence and the recruitment of retinoid X receptors for thyroid hormone responsiveness. *J Biol Chem* 276, 3929-3936 (2001). https://doi.org:10.1074/jbc.M006743200

227 Zhang, J. & Lazar, M. A. The mechanism of action of thyroid hormones. *Annu Rev Physiol* 62, 439-466 (2000). https://doi.org:10.1146/annurev.physiol.62.1.439

228 Friesema, E. C. *et al.* Effective cellular uptake and efflux of thyroid hormone by human monocarboxylate transporter 10. *Mol Endocrinol* 22, 1357-1369 (2008). https://doi.org:10.1210/me.2007-0112

229 van Mullem, A. A. *et al.* Effects of thyroid hormone transporters MCT8 and MCT10 on nuclear activity of T3. *Mol Cell Endocrinol* 437, 252-260 (2016). https://doi.org:10.1016/j.mce.2016.07.037

230 Visser, T. J. in *Endotext* (eds K. R. Feingold *et al.*) (2000).

231 Sandler, B. *et al.* Thyroxine-thyroid hormone receptor interactions. *J Biol Chem* 279, 55801-55808 (2004). https://doi.org:10.1074/jbc.M410124200

232 Bianco, A. C. & Kim, B. W. Deiodinases: implications of the local control of thyroid hormone action. *J Clin Invest* 116, 2571-2579 (2006). https://doi.org:10.1172/JCI29812

233 Bianco, A. C. Minireview: cracking the metabolic code for thyroid hormone signaling. *Endocrinology* 152, 3306-3311 (2011). https://doi.org:10.1210/en.2011-1104

234 Gereben, B. *et al.* Cellular and molecular basis of deiodinase-regulated thyroid hormone signaling. *Endocr Rev* 29, 898-938 (2008). https://doi.org:10.1210/er.2008-0019

235 Peeters, R. P. & Visser, T. J. in *Endotext* (eds K. R. Feingold *et al.*) (2000).

236 Maia, A. L., Goemann, I. M., Meyer, E. L. & Wajner, S. M. Deiodinases: the balance of thyroid hormone: type 1 iodothyronine deiodinase in human physiology and disease. *J Endocrinol* 209, 283-297 (2011). https://doi.org:10.1530/JOE-10-0481

237 Schneider, M. J. *et al.* Targeted disruption of the type 1 selenodeiodinase gene (Dio1) results in marked changes in thyroid hormone economy in mice. *Endocrinology* 147, 580-589 (2006). https://doi.org:10.1210/en.2005-0739

238 Dentice, M., Marsili, A., Zavacki, A., Larsen, P. R. & Salvatore, D. The deiodinases and the control of intracellular thyroid hormone signaling during cellular differentiation. *Biochim Biophys Acta* 1830, 3937-3945 (2013). https://doi.org:10.1016/j.bbagen.2012.05.007

239 Deng, Y., Han, Y., Gao, S., Dong, W. & Yu, Y. The Physiological Functions and Polymorphisms of Type II Deiodinase. *Endocrinol Metab (Seoul)* 38, 190-202 (2023). https://doi.org:10.3803/EnM.2022.1599

240 Arrojo, E. D. R. & Bianco, A. C. Type 2 deiodinase at the crossroads of thyroid hormone action. *Int J Biochem Cell Biol* 43, 1432-1441 (2011). https://doi.org:10.1016/j.biocel.2011.05.016

241 Marsili, A. *et al.* Type 2 iodothyronine deiodinase levels are higher in slow-twitch than fast-twitch mouse skeletal muscle and are increased in hypothyroidism. *Endocrinology* 151, 5952-5960 (2010). https://doi.org:10.1210/en.2010-0631

242 Mahdavi, V., Izumo, S. & Nadal-Ginard, B. Developmental and hormonal regulation of sarcomeric myosin heavy chain gene family. *Circ Res* 60, 804-814 (1987). https://doi.org:10.1161/01.res.60.6.804

243 Gereben, B., Zeold, A., Dentice, M., Salvatore, D. & Bianco, A. C. Activation and inactivation of thyroid hormone by deiodinases: local action with general consequences. *Cell Mol Life Sci* 65, 570-590 (2008). https://doi.org:10.1007/s00018-007-7396-0

244 Martinez, M. E. & Hernandez, A. The Type 3 Deiodinase Is a Critical Modulator of Thyroid Hormone Sensitivity in the Fetal Brain. *Front Neurosci* 15, 703730 (2021). https://doi.org:10.3389/fnins.2021.703730

245 Fisher, D. A. Clinical review 19: Management of congenital hypothyroidism. *J Clin Endocrinol Metab* 72, 523-529 (1991). https://doi.org:10.1210/jcem-72-3-523

246 Ciavardelli, D., Bellomo, M., Crescimanno, C. & Vella, V. Type 3 deiodinase: role in cancer growth, stemness, and metabolism. *Front Endocrinol (Lausanne)* 5, 215 (2014). https://doi.org:10.3389/fendo.2014.00215

247 Visser, W. E., Friesema, E. C. & Visser, T. J. Minireview: thyroid hormone transporters: the knowns and the unknowns. *Mol Endocrinol* 25, 1-14 (2011). https://doi.org:10.1210/me.2010-0095

248 Shibusawa, N., Hollenberg, A. N. & Wondisford, F. E. Thyroid hormone receptor DNA binding is required for both positive and negative gene regulation. *J Biol Chem* 278, 732-738 (2003). https://doi.org:10.1074/jbc.M207264200

249 Wahlstrom, G. M., Sjoberg, M., Andersson, M., Nordstrom, K. & Vennstrom, B. Binding characteristics of the thyroid hormone receptor homo- and heterodimers to consensus AGGTCA repeat motifs. *Mol Endocrinol* 6, 1013-1022 (1992). https://doi.org:10.1210/mend.6.7.1324417

250 Tedeschi, L., Vassalle, C., Iervasi, G. & Sabatino, L. Main Factors Involved in Thyroid Hormone Action. *Molecules* 26 (2021). https://doi.org:10.3390/molecules26237337

251 Forman, B. M., Casanova, J., Raaka, B. M., Ghysdael, J. & Samuels, H. H. Half-site spacing and orientation determines whether thyroid hormone and retinoic acid receptors and related factors bind to DNA response elements as monomers, homodimers, or heterodimers. *Mol Endocrinol* 6, 429-442 (1992). https://doi.org:10.1210/mend.6.3.1316541

252 Naar, A. M. *et al.* The orientation and spacing of core DNA-binding motifs dictate selective transcriptional responses to three nuclear receptors. *Cell* 65, 1267-1279 (1991). https://doi.org:10.1016/0092-8674(91)90021-p

253 Kurokawa, R. *et al.* Differential orientations of the DNA-binding domain and carboxy-terminal dimerization interface regulate binding site selection by nuclear receptor heterodimers. *Genes Dev* 7, 1423-1435 (1993). https://doi.org:10.1101/gad.7.7b.1423

254 Lazar, M. A., Berrodin, T. J. & Harding, H. P. Differential DNA binding by monomeric, homodimeric, and potentially heteromeric forms of the thyroid hormone receptor. *Mol Cell Biol* 11, 5005-5015 (1991). https://doi.org:10.1128/mcb.11.10.5005-5015.1991

255 Hashimoto, K. *et al.* Cross-talk between thyroid hormone receptor and liver X receptor regulatory pathways is revealed in a thyroid hormone resistance mouse model. *J Biol Chem* 281, 295-302 (2006). https://doi.org:10.1074/jbc.M507877200

256 Liu, Y. Y. *et al.* A mutant thyroid hormone receptor alpha antagonizes peroxisome proliferator-activated receptor alpha signaling in vivo and impairs fatty acid oxidation. *Endocrinology* 148, 1206-1217 (2007). https://doi.org:10.1210/en.2006-0836

257 Cheng, S. Y., Leonard, J. L. & Davis, P. J. Molecular aspects of thyroid hormone actions. *Endocr Rev* 31, 139-170 (2010). https://doi.org:10.1210/er.2009-0007

258 Privalsky, M. L. *et al.* The p160 coactivator PAS-B motif stabilizes nuclear receptor binding and contributes to isoform-specific regulation by thyroid hormone receptors. *J Biol Chem* 284, 19554-19563 (2009). https://doi.org:10.1074/jbc.M109.007542

259 Schroeder, A. C. & Privalsky, M. L. Thyroid hormones, t3 and t4, in the brain. *Front Endocrinol (Lausanne)* 5, 40 (2014). https://doi.org:10.3389/fendo.2014.00040

260 Spencer, C. A. in *Endotext* (eds K. R. Feingold *et al.*) (2000).

261 Freitas, J. *et al.* Identification of thyroid hormone receptor active compounds using a quantitative high-throughput screening platform. *Curr Chem Genom Transl Med* 8, 36-46 (2014). https://doi.org:10.2174/2213988501408010036

262 Matsubara, K. *et al.* An improved thyroid hormone reporter assay to determine the thyroid hormone-like activity of amiodarone, bithionol, closantel and rafoxanide. *Toxicol Lett* 208, 30-35 (2012). https://doi.org:10.1016/j.toxlet.2011.10.004

263 Sirakov, M. & Plateroti, M. In Vitro Approaches to Identify Thyroid Hormone Receptor-Dependent Transcriptional Response. *Methods Mol Biol* 1801, 29-38 (2018). https://doi.org:10.1007/978-1-4939-7902-8_4

264 Lazar, M. A. Thyroid hormone receptors: multiple forms, multiple possibilities. *Endocr Rev* 14, 184-193 (1993). https://doi.org:10.1210/edrv-14-2-184

265 Wood, W. M., Ocran, K. W., Gordon, D. F. & Ridgway, E. C. Isolation and characterization of mouse complementary DNAs encoding alpha and beta thyroid hormone receptors from thyrotrope cells: the mouse pituitary-specific beta 2 isoform differs at the amino terminus from the corresponding species from rat pituitary tumor cells. *Mol Endocrinol* 5, 1049-1061 (1991). https://doi.org:10.1210/mend-5-8-1049

266 Chassande, O. *et al.* Identification of transcripts initiated from an internal promoter in the c-erbA alpha locus that encode inhibitors of retinoic acid receptor-alpha and triiodothyronine receptor activities. *Mol Endocrinol* 11, 1278-1290 (1997). https://doi.org:10.1210/mend.11.9.9972

267 Williams, G. R. Cloning and characterization of two novel thyroid hormone receptor beta isoforms. *Mol Cell Biol* 20, 8329-8342 (2000). https://doi.org:10.1128/MCB.20.22.8329-8342.2000

268 Vella, K. R. & Hollenberg, A. N. The actions of thyroid hormone signaling in the nucleus. *Mol Cell Endocrinol* 458, 127-135 (2017). https://doi.org:10.1016/j.mce.2017.03.001

269 Gauthier, K. *et al.* Different functions for the thyroid hormone receptors TRalpha and TRbeta in the control of thyroid hormone production and post-natal development. *EMBO J* 18, 623-631 (1999). https://doi.org:10.1093/emboj/18.3.623

270 Forhead, A. J. & Fowden, A. L. Thyroid hormones in fetal growth and prepartum maturation. *J Endocrinol* 221, R87-R103 (2014). https://doi.org:10.1530/JOE-14-0025

271 Duarte-Guterman, P., Navarro-Martin, L. & Trudeau, V. L. Mechanisms of crosstalk between endocrine systems: regulation of sex steroid hormone synthesis and action by thyroid hormones. *Gen Comp Endocrinol* 203, 69-85 (2014). https://doi.org:10.1016/j.ygcen.2014.03.015

272 Hapon, M. B., Simoncini, M., Via, G. & Jahn, G. A. Effect of hypothyroidism on hormone profiles in virgin, pregnant and lactating rats, and on lactation. *Reproduction* 126, 371-382 (2003). https://doi.org:10.1530/rep.0.1260371

273 Osorio, A., Ruiz, E. & Ortega, E. Possible role of GH/IGF-1 in the ovarian function of adult hypothyroid rats. *Mol Cell Biochem* 179, 7-11 (1998). https://doi.org:10.1023/a:1006867109759

274 Bjorntorp, P. The regulation of adipose tissue distribution in humans. *Int J Obes Relat Metab Disord* 20, 291-302 (1996).

275 Britton, K. A. *et al.* Body fat distribution, incident cardiovascular disease, cancer, and all-cause mortality. *J Am Coll Cardiol* 62, 921-925 (2013). https://doi.org:10.1016/j.jacc.2013.06.027

276 Mauvais-Jarvis, F. Sex differences in metabolic homeostasis, diabetes, and obesity. *Biol Sex Differ* 6, 14 (2015). https://doi.org:10.1186/s13293-015-0033-y

277 Moreira-Pais, A. *et al.* Sex differences on adipose tissue remodeling: from molecular mechanisms to therapeutic interventions. *J Mol Med (Berl)* 98, 483-493 (2020). https://doi.org:10.1007/s00109-020-01890-2

278 Kelly, D. M. & Jones, T. H. Testosterone and obesity. *Obes Rev* 16, 581-606 (2015). https://doi.org:10.1111/obr.12282

279 DeFronzo, R. A. *et al.* The effect of insulin on the disposal of intravenous glucose. Results from indirect calorimetry and hepatic and femoral venous catheterization. *Diabetes* 30, 1000-1007 (1981). https://doi.org:10.2337/diab.30.12.1000

280 Schiaffino, S., Reggiani, C., Kostrominova, T. Y., Mann, M. & Murgia, M. Mitochondrial specialization revealed by single muscle fiber proteomics: focus on the Krebs cycle. *Scand J Med Sci Sports* 25 Suppl 4, 41-48 (2015). https://doi.org:10.1111/sms.12606

281 Nolfi-Donegan, D., Braganza, A. & Shiva, S. Mitochondrial electron transport chain: Oxidative phosphorylation, oxidant production, and methods of measurement. *Redox Biol* 37, 101674 (2020). https://doi.org:10.1016/j.redox.2020.101674

282 Zhao, R. Z., Jiang, S., Zhang, L. & Yu, Z. B. Mitochondrial electron transport chain, ROS generation and uncoupling (Review). *Int J Mol Med* 44, 3-15 (2019). https://doi.org:10.3892/ijmm.2019.4188

283 Rabinowitz, J. D. & Enerback, S. Lactate: the ugly duckling of energy metabolism. *Nat Metab* 2, 566-571 (2020). https://doi.org:10.1038/s42255-020-0243-4

284 Gaitanos, G. C., Williams, C., Boobis, L. H. & Brooks, S. Human muscle metabolism during intermittent maximal exercise. *J Appl Physiol (1985)* 75, 712-719 (1993). https://doi.org:10.1152/jappl.1993.75.2.712

285 Andersen, P. & Saltin, B. Maximal perfusion of skeletal muscle in man. *J Physiol* 366, 233-249 (1985). https://doi.org:10.1113/jphysiol.1985.sp015794

286 Gibala, M. J., MacLean, D. A., Graham, T. E. & Saltin, B. Tricarboxylic acid cycle intermediate pool size and estimated cycle flux in human muscle during exercise. *Am J Physiol* 275, E235-242 (1998). https://doi.org:10.1152/ajpendo.1998.275.2.E235

287 Mullur, R., Liu, Y. Y. & Brent, G. A. Thyroid hormone regulation of metabolism. *Physiol Rev* 94, 355-382 (2014). https://doi.org:10.1152/physrev.00030.2013

288 Hashizume, K. *et al.* Evidence for the presence of two active forms of cytosolic 3,5,3'-triiodo-L-thyronine (T3)-binding protein (CTBP) in rat kidney. Specialized functions of two CTBPs in intracellular T3 translocation. *J Biol Chem* 264, 4864-4871 (1989).

289 Mori, J. *et al.* Nicotinamide adenine dinucleotide phosphate-dependent cytosolic T(3) binding protein as a regulator for T(3)-mediated transactivation. *Endocrinology* 143, 1538-1544 (2002). https://doi.org:10.1210/endo.143.4.8736

290 Beslin, A., Vie, M. P., Blondeau, J. P. & Francon, J. Identification by photoaffinity labelling of a pyridine nucleotide-dependent tri-iodothyronine-binding protein in the cytosol of cultured astroglial cells. *Biochem J* 305 (Pt 3), 729-737 (1995). https://doi.org:10.1042/bj3050729

291 Oshima, A. *et al.* CRYM mutations cause deafness through thyroid hormone binding properties in the fibrocytes of the cochlea. *J Med Genet* 43, e25 (2006). https://doi.org:10.1136/jmg.2005.034397

292 Consortium, G. T. The Genotype-Tissue Expression (GTEx) project. *Nat Genet* 45, 580-585 (2013). https://doi.org:10.1038/ng.2653

293 Hallen, A., Cooper, A. J., Smith, J. R., Jamie, J. F. & Karuso, P. Ketimine reductase/CRYM catalyzes reductive alkylamination of alpha-keto acids, confirming its function as an imine reductase. *Amino Acids* 47, 2457-2461 (2015). https://doi.org:10.1007/s00726-015-2044-8

294 Leandro, J. & Houten, S. M. The lysine degradation pathway: Subcellular compartmentalization and enzyme deficiencies. *Mol Genet Metab* 131, 14-22 (2020). https://doi.org:10.1016/j.ymgme.2020.07.010

295 Matthews, D. E. Review of Lysine Metabolism with a Focus on Humans. *J Nutr* 150, 2548S-2555S (2020). https://doi.org:10.1093/jn/nxaa224

296 Arruda, P. & Barreto, P. Lysine Catabolism Through the Saccharopine Pathway: Enzymes and Intermediates Involved in Plant Responses to Abiotic and Biotic Stress. *Front Plant Sci* 11, 587 (2020). https://doi.org:10.3389/fpls.2020.00587

297 Mills, P. B. *et al.* Mutations in antiquitin in individuals with pyridoxine-dependent seizures. *Nat Med* 12, 307-309 (2006). https://doi.org:10.1038/nm1366

298 Almannai, M., Alfadhel, M. & El-Hattab, A. W. Carnitine Inborn Errors of Metabolism. *Molecules* 24 (2019). https://doi.org:10.3390/molecules24183251

299 Borum, P. R., Broquist, H. P. & Roelops, R. J. Muscle carnitine levels in neuromuscular disease. *J Neurol Sci* 34, 279-286 (1977). https://doi.org:10.1016/0022-510x(77)90075-2

300 Orngreen, M. C. Substrate kinetics in patients with disorders of skeletal muscle metabolism. *Dan Med J* 63 (2016).

301 Kobayashi, M., Hashizume, K., Suzuki, S., Ichikawa, K. & Takeda, T. A novel NADPH-dependent cytosolic 3,5,3'-triiodo-L-thyronine-binding protein (CTBP; 5.1S) in rat liver: a comparison with 4.7S NADPH-dependent CTBP. *Endocrinology* 129, 1701-1708 (1991). https://doi.org:10.1210/endo-129-4-1701

302 Kinney, C. J. *et al.* mu-Crystallin in Mouse Skeletal Muscle Promotes a Shift from Glycolytic toward Oxidative Metabolism. *Curr Res Physiol* 4, 47-59 (2021). https://doi.org:10.1016/j.crphys.2021.02.003

303 Suzuki, S. *et al.* micro-Crystallin as an intracellular 3,5,3'-triiodothyronine holder in vivo. *Mol Endocrinol* 21, 885-894 (2007). https://doi.org:10.1210/me.2006-0403

304 Lin, Y. T. *et al.* Hypothalamic NPFFR2 attenuates central insulin signaling and its knockout diminishes metabolic dysfunction in mouse models of diabetes mellitus. *Clin Nutr* 43, 603-619 (2024). https://doi.org:10.1016/j.clnu.2024.01.013

305 Zhang, Y., Tsai, T. H., Ezrokhi, M., Stoelzel, C. & Cincotta, A. H. Tyrosine Hydroxylase Knockdown at the Hypothalamic Supramammillary Nucleus Area Induces Obesity and Glucose Intolerance. *Neuroendocrinology* (2023). https://doi.org:10.1159/000535944

306 Sharma, M., Yadav, Y. & Dey, C. S. Neuronal insulin signaling and resistance: a balancing act of kinases and phosphatases. *J Endocrinol* 260 (2024). https://doi.org:10.1530/JOE-23-0151

307 Yadav, R. & Patel, B. Insights on effects of Wnt pathway modulation on insulin signaling and glucose homeostasis for the treatment of type 2 diabetes mellitus: Wnt activation or Wnt inhibition? *Int J Biol Macromol* 261, 129634 (2024). https://doi.org:10.1016/j.ijbiomac.2024.129634

308 Parra-Montes de Oca, M. A., Sotelo-Rivera, I., Gutierrez-Mata, A., Charli, J. L. & Joseph-Bravo, P. Sex Dimorphic Responses of the Hypothalamus-Pituitary-Thyroid Axis to Energy Demands and Stress. *Front Endocrinol (Lausanne)* 12, 746924 (2021). https://doi.org:10.3389/fendo.2021.746924

309 El Salam, M. A. A. Obesity, An Enemy of Male Fertility: A Mini Review. *Oman Med J* 33, 3-6 (2018). https://doi.org:10.5001/omj.2018.02

310 Panagiotidou, A., Chatzakis, C., Ververi, A., Eleftheriades, M. & Sotiriadis, A. The Effect of Maternal Diet and Physical Activity on the Epigenome of the Offspring. *Genes (Basel)* 15 (2024). https://doi.org:10.3390/genes15010076

311 Kweon, J. Y., Mun, H., Choi, M. R., Kim, H. S. & Ahn, Y. J. Maternal obesity induced metabolic disorders in offspring and myeloid reprogramming by epigenetic regulation. *Front Endocrinol (Lausanne)* 14, 1256075 (2023). https://doi.org:10.3389/fendo.2023.1256075

312 Suleiman, J. B., Mohamed, M. & Bakar, A. B. A. A systematic review on different models of inducing obesity in animals: Advantages and limitations. *J Adv Vet Anim Res* 7, 103-114 (2020). https://doi.org:10.5455/javar.2020.g399

313 Zhang, Y. *et al.* Positional cloning of the mouse obese gene and its human homologue. *Nature* 372, 425-432 (1994). https://doi.org:10.1038/372425a0

314 Giacomello, E. *et al.* Age Dependent Modification of the Metabolic Profile of the Tibialis Anterior Muscle Fibers in C57BL/6J Mice. *Int J Mol Sci* 21 (2020). https://doi.org:10.3390/ijms21113923

315 Valéria Augusto, C. R. P., Gerson Eduardo Rocha Campos. Skeletal Muscle Fiber Types In C57BL6J Mice. *Journal of Morphological Sciences* 21, 89-94 (2004).

316 Sher, J. & Cardasis, C. Skeletal muscle fiber types in the adult mouse. *Acta Neurol Scand* 54, 45-56 (1976). https://doi.org:10.1111/j.1600-0404.1976.tb07619.x

317 Collins, S., Martin, T. L., Surwit, R. S. & Robidoux, J. Genetic vulnerability to diet-induced obesity in the C57BL/6J mouse: physiological and molecular characteristics. *Physiol Behav* 81, 243-248 (2004). https://doi.org:10.1016/j.physbeh.2004.02.006

318 Giudicelli, R., Fuentes, P., Orfanos, J. & Reboud, E. [Diagnostic and therapeutic problems posed by iatrogenic perforations of the oesophagus. With reference to 18 cases (author's transl)]. *Ann Chir Thorac Cardiovasc* 30, 305-310 (1976).

319 Surwit, R. S., Kuhn, C. M., Cochrane, C., McCubbin, J. A. & Feinglos, M. N. Diet-induced type II diabetes in C57BL/6J mice. *Diabetes* 37, 1163-1167 (1988). https://doi.org:10.2337/diab.37.9.1163

320 Kaku, K., Fiedorek, F. T., Jr., Province, M. & Permutt, M. A. Genetic analysis of glucose tolerance in inbred mouse strains. Evidence for polygenic control. *Diabetes* 37, 707-713 (1988). https://doi.org:10.2337/diab.37.6.707

321 Kayo, T., Fujita, H., Nozaki, J., E, X. & Koizumi, A. Identification of two chromosomal loci determining glucose intolerance in a C57BL/6 mouse strain. *Comp Med* 50, 296-302 (2000).

322 Taylor, B. A. & Phillips, S. J. Obesity QTLs on mouse chromosomes 2 and 17. *Genomics* 43, 249-257 (1997). https://doi.org:10.1006/geno.1997.4835

323 Berglund, E. D. *et al.* Glucose metabolism in vivo in four commonly used inbred mouse strains. *Diabetes* 57, 1790-1799 (2008). https://doi.org:10.2337/db07-1615

324 Montgomery, M. K. *et al.* Mouse strain-dependent variation in obesity and glucose homeostasis in response to high-fat feeding. *Diabetologia* 56, 1129-1139 (2013). https://doi.org:10.1007/s00125-013-2846-8

325 Buckley, T. N. *et al.* High-fat feeding disrupts daily eating behavior rhythms in obesity-prone but not in obesity-resistant male inbred mouse strains. *Am J Physiol Regul Integr Comp Physiol* 320, R619-R629 (2021). https://doi.org:10.1152/ajpregu.00150.2020

326 Montgomery, M. K. *et al.* Association of muscle lipidomic profile with high-fat diet-induced insulin resistance across five mouse strains. *Sci Rep* 7, 13914 (2017). https://doi.org:10.1038/s41598-017-14214-1

327 Kutscher, C. L. & Miller, D. G. Age-dependent polydipsia in the SWR-J mouse. *Physiol Behav* 13, 71-79 (1974). https://doi.org:10.1016/0031-9384(74)90308-4

328 Eberhart, G. P., West, D. B., Boozer, C. N. & Atkinson, R. L. Insulin sensitivity of adipocytes from inbred mouse strains resistant or sensitive to diet-induced obesity. *Am J Physiol* 266, R1423-1428 (1994). https://doi.org:10.1152/ajpregu.1994.266.5.R1423

329 Kless, C., Rink, N., Rozman, J. & Klingenspor, M. Proximate causes for diet-induced obesity in laboratory mice: a case study. *Eur J Clin Nutr* 71, 306-317 (2017). https://doi.org:10.1038/ejcn.2016.243

330 Johnson, G. B., Riggs, B. L. & Platt, J. L. A genetic basis for the "Adonis" phenotype of low adiposity and strong bones. *FASEB J* 18, 1282-1284 (2004). https://doi.org:10.1096/fj.04-1572fje

331 Alexander, J., Chang, G. Q., Dourmashkin, J. T. & Leibowitz, S. F. Distinct phenotypes of obesity-prone AKR/J, DBA2J and C57BL/6J mice compared to control strains. *Int J Obes (Lond)* 30, 50-59 (2006). https://doi.org:10.1038/sj.ijo.0803110

332 Aga, H. *et al.* Identification of Novel Potential Type 2 Diabetes Genes Mediating beta-Cell Loss and Hyperglycemia Using Positional Cloning. *Front Genet* 11, 567191 (2020). https://doi.org:10.3389/fgene.2020.567191

333 Boudina, S. *et al.* Early mitochondrial adaptations in skeletal muscle to diet-induced obesity are strain dependent and determine oxidative stress and energy expenditure but not insulin sensitivity. *Endocrinology* 153, 2677-2688 (2012). https://doi.org:10.1210/en.2011-2147

334 Wu, Y. *et al.* Increased Variation in Body Weight and Food Intake Is Related to Increased Dietary Fat but Not Increased Carbohydrate or Protein in Mice. *Front Nutr* 9, 835536 (2022). https://doi.org:10.3389/fnut.2022.835536

335 Vafiadaki, E. *et al.* Cloning of the mouse dysferlin gene and genomic characterization of the SJL-Dysf mutation. *Neuroreport* 12, 625-629 (2001). https://doi.org:10.1097/00001756-200103050-00039

336 Weller, A. H., Magliato, S. A., Bell, K. P. & Rosenberg, N. L. Spontaneous myopathy in the SJL/J mouse: pathology and strength loss. *Muscle Nerve* 20, 72-82 (1997). https://doi.org:10.1002/(sici)1097-4598(199701)20:1<72::aid-mus10>3.0.co;2-3

337 McGeachie, J. K. & Grounds, M. D. Retarded myogenic cell replication in regenerating skeletal muscles of old mice: an autoradiographic study in young and old BALBc and SJL/J mice. *Cell Tissue Res* 280, 277-282 (1995). https://doi.org:10.1007/BF00307799

338 Mitchell, C. A., McGeachie, J. K. & Grounds, M. D. Cellular differences in the regeneration of murine skeletal muscle: a quantitative histological study in SJL/J

and BALB/c mice. *Cell Tissue Res* 269, 159-166 (1992). https://doi.org:10.1007/BF00384736

339 McLennan, I. S. Neurogenic and myogenic regulation of skeletal muscle formation: a critical re-evaluation. *Prog Neurobiol* 44, 119-140 (1994). https://doi.org:10.1016/0301-0082(94)90035-3

340 Schiaffino, S., Serrano, A. L., Jerkovic, R., Di Lisi, R. & Murgia, M. Neural regulation of myosin gene expression in regenerating skeletal muscle. *Acta Physiol Scand* 163, S11-15 (1998). https://doi.org:10.1046/j.1365-201X.1998.1630s3S11.x

341 Swoap, S. J. *et al.* Interaction of thyroid hormone and functional overload on skeletal muscle isomyosin expression. *J Appl Physiol (1985)* 77, 621-629 (1994). https://doi.org:10.1152/jappl.1994.77.2.621

342 Diffee, G. M., Haddad, F., Herrick, R. E. & Baldwin, K. M. Control of myosin heavy chain expression: interaction of hypothyroidism and hindlimb suspension. *Am J Physiol* 261, C1099-1106 (1991). https://doi.org:10.1152/ajpcell.1991.261.6.C1099

343 Deane, C. S. *et al.* Impaired hypertrophy in myoblasts is improved with testosterone administration. *J Steroid Biochem Mol Biol* 138, 152-161 (2013). https://doi.org:10.1016/j.jsbmb.2013.05.005

344 Staron, R. S. *et al.* Fiber type composition of the vastus lateralis muscle of young men and women. *J Histochem Cytochem* 48, 623-629 (2000). https://doi.org:10.1177/002215540004800506

345 Larsson, L. & Yu, F. Gender-related differences in the regulatory influence of thyroid hormone on the expression of myosin isoforms in young and old rats. *Acta Physiol Scand* 159, 81-89 (1997). https://doi.org:10.1046/j.1365-201X.1997.559328000.x

346 Yu, F. *et al.* Effects of thyroid hormone receptor gene disruption on myosin isoform expression in mouse skeletal muscles. *Am J Physiol Regul Integr Comp Physiol* 278, R1545-1554 (2000). https://doi.org:10.1152/ajpregu.2000.278.6.R1545

347 Soukup, T. & Jirmanova, I. Regulation of myosin expression in developing and regenerating extrafusal and intrafusal muscle fibers with special emphasis on the role of thyroid hormones. *Physiol Res* 49, 617-633 (2000).

348 Maia, A. L., Kim, B. W., Huang, S. A., Harney, J. W. & Larsen, P. R. Type 2 iodothyronine deiodinase is the major source of plasma T3 in euthyroid humans. *J Clin Invest* 115, 2524-2533 (2005). https://doi.org:10.1172/JCI25083

349 Minchew, E. C., Williamson, N. C., Readyoff, A. T., McClung, J. M. & Spangenburg, E. E. Isometric skeletal muscle contractile properties in common strains of male laboratory mice. *Front Physiol* 13, 937132 (2022). https://doi.org:10.3389/fphys.2022.937132

350 Marsili, A. *et al.* Mice with a targeted deletion of the type 2 deiodinase are insulin resistant and susceptible to diet induced obesity. *PLoS One* 6, e20832 (2011). https://doi.org:10.1371/journal.pone.0020832

351 Laarse, W. J. V. D. Genetic Architecture of Numbers of Fast and Slow Muscle Fibers in the Mouse Soleus Muscle. *Heredity* 53, 643-647 (1984).

352 Shimi, G., Sohouli, M. H., Ghorbani, A., Shakery, A. & Zand, H. The interplay between obesity, immunosenescence, and insulin resistance. *Immun Ageing* 21, 13 (2024). https://doi.org:10.1186/s12979-024-00414-7

353 Okamura, T. *et al.* Ectopic fat obesity presents the greatest risk for incident type 2 diabetes: a population-based longitudinal study. *Int J Obes (Lond)* 43, 139-148 (2019). https://doi.org:10.1038/s41366-018-0076-3

354 Chandrasekaran, P. & Weiskirchen, R. The Role of Obesity in Type 2 Diabetes Mellitus-An Overview. *Int J Mol Sci* 25 (2024). https://doi.org:10.3390/ijms25031882

355 Paternoster, S. & Falasca, M. The intricate relationship between diabetes, obesity and pancreatic cancer. *Biochim Biophys Acta Rev Cancer* 1873, 188326 (2020). https://doi.org:10.1016/j.bbcan.2019.188326

356 Pavli, P., Triantafyllidou, O., Kapantais, E., Vlahos, N. F. & Valsamakis, G. Infertility Improvement after Medical Weight Loss in Women and Men: A Review of the Literature. *Int J Mol Sci* 25 (2024). https://doi.org:10.3390/ijms25031909

357 Zheng, L. *et al.* Obesity and its impact on female reproductive health: unraveling the connections. *Front Endocrinol (Lausanne)* 14, 1326546 (2023). https://doi.org:10.3389/fendo.2023.1326546

358 De Pergola, G. & Silvestris, F. Obesity as a major risk factor for cancer. *J Obes* 2013, 291546 (2013). https://doi.org:10.1155/2013/291546

359 Liu, X. Z., Pedersen, L. & Halberg, N. Cellular mechanisms linking cancers to obesity. *Cell Stress* 5, 55-72 (2021). https://doi.org:10.15698/cst2021.05.248

360 Kantowski, T., Schulze Zur Wiesch, C., Aberle, J. & Lautenbach, A. Obesity management: sex-specific considerations. *Arch Gynecol Obstet* (2024). https://doi.org:10.1007/s00404-023-07367-0

361 Tak, Y. J. & Lee, S. Y. Anti-Obesity Drugs: Long-Term Efficacy and Safety: An Updated Review. *World J Mens Health* 39, 208-221 (2021). https://doi.org:10.5534/wjmh.200010

362 Grandl, G., Novikoff, A., DiMarchi, R., Tschop, M. H. & Muller, T. D. Gut Peptide Agonism in the Treatment of Obesity and Diabetes. *Compr Physiol* 10, 99-124 (2019). https://doi.org:10.1002/cphy.c180044

363 Patil, M., Casari, I., Warne, L. N. & Falasca, M. G protein-coupled receptors driven intestinal glucagon-like peptide-1 reprogramming for obesity: Hope or hype? *Biomed Pharmacother* 172, 116245 (2024). https://doi.org:10.1016/j.biopha.2024.116245

364 Hope, D. C. D. *et al.* Hypoaminoacidemia underpins glucagon-mediated energy expenditure and weight loss. *Cell Rep Med* 3, 100810 (2022). https://doi.org:10.1016/j.xcrm.2022.100810

365 Muller, T. D. *et al.* Glucagon-like peptide 1 (GLP-1). *Mol Metab* 30, 72-130 (2019). https://doi.org:10.1016/j.molmet.2019.09.010

366 Chanoine, J. P., Hampl, S., Jensen, C., Boldrin, M. & Hauptman, J. Effect of orlistat on weight and body composition in obese adolescents: a randomized controlled trial. *JAMA* 293, 2873-2883 (2005). https://doi.org:10.1001/jama.293.23.2873

367 Liu, T. T., Liu, X. T., Chen, Q. X. & Shi, Y. Lipase Inhibitors for Obesity: A Review. *Biomed Pharmacother* 128, 110314 (2020). https://doi.org:10.1016/j.biopha.2020.110314

368 Trapp, C. M. & Censani, M. Setmelanotide: a promising advancement for pediatric patients with rare forms of genetic obesity. *Curr Opin Endocrinol Diabetes Obes* 30, 136-140 (2023). https://doi.org:10.1097/MED.0000000000000798

369 Brent, G. A. Mechanisms of thyroid hormone action. *J Clin Invest* 122, 3035-3043 (2012). https://doi.org:10.1172/JCI60047

370 Sinha, R. & Yen, P. M. in *Endotext* (eds K. R. Feingold *et al.*) (2000).

371 Kuna, S. T. *et al.* Long-term effect of weight loss on obstructive sleep apnea severity in obese patients with type 2 diabetes. *Sleep* 36, 641-649A (2013). https://doi.org:10.5665/sleep.2618

372 Miller, M. A. & Howarth, N. E. Sleep and cardiovascular disease. *Emerg Top Life Sci* 7, 457-466 (2023). https://doi.org:10.1042/ETLS20230111

373 Al Zweihary, A. M. Safety and Effectiveness of Tirzepatide Use in Obesity Without Type 2 Diabetes Mellitus. *Cureus* 16, e51788 (2024). https://doi.org:10.7759/cureus.51788

374 Kelly, A. S. *et al.* The effect of glucagon-like peptide-1 receptor agonist therapy on body mass index in adolescents with severe obesity: a randomized, placebo-controlled, clinical trial. *JAMA Pediatr* 167, 355-360 (2013). https://doi.org:10.1001/jamapediatrics.2013.1045

375 Weghuber, D. *et al.* A 6-month randomized, double-blind, placebo-controlled trial of weekly exenatide in adolescents with obesity. *Pediatr Obes* 15, e12624 (2020). https://doi.org:10.1111/ijpo.12624

376 Kelly, A. S. *et al.* A Randomized, Controlled Trial of Liraglutide for Adolescents with Obesity. *N Engl J Med* 382, 2117-2128 (2020). https://doi.org:10.1056/NEJMoa1916038

377 Bensignor, M. O. *et al.* Evaluating potential predictors of weight loss response to liraglutide in adolescents with obesity: A post hoc analysis of the randomized,

placebo-controlled SCALE Teens trial. *Pediatr Obes* 18, e13061 (2023). https://doi.org:10.1111/ijpo.13061

378 Weghuber, D. *et al.* Once-Weekly Semaglutide in Adolescents with Obesity. *N Engl J Med* 387, 2245-2257 (2022). https://doi.org:10.1056/NEJMoa2208601

379 Samms, R. J., Coghlan, M. P. & Sloop, K. W. How May GIP Enhance the Therapeutic Efficacy of GLP-1? *Trends Endocrinol Metab* 31, 410-421 (2020). https://doi.org:10.1016/j.tem.2020.02.006

380 Miga, K. H., Eisenhart, C. & Kent, W. J. Utilizing mapping targets of sequences underrepresented in the reference assembly to reduce false positive alignments. *Nucleic Acids Res* 43, e133 (2015). https://doi.org:10.1093/nar/gkv671

381 Lushchak, O. V., Piroddi, M., Galli, F. & Lushchak, V. I. Aconitase post-translational modification as a key in linkage between Krebs cycle, iron homeostasis, redox signaling, and metabolism of reactive oxygen species. *Redox Rep* 19, 8-15 (2014). https://doi.org:10.1179/1351000213Y.0000000073